UNIVERSITA' DEGLI STUDI DI NAPOLI FEDERICO II

DIPARTIMENTO DI INGEGNERIA CHIMICA

Dottorato di Ricerca in Ingegneria Chimica

(XXII Ciclo)

Advanced Catalytic Systems For The Partial Oxidation of Hydrocarbons: Improving Sulphur Tolerance of Rh Based Catalysts

Scientific Committee:

Prof. Gennaro Russo
Prof. Paolo Ciambelli
Dr. Luciana Lisi
Dr. Stefano Cimino

Candidate:

Reza Torbati

November 2009

Abstract

The catalytic partial oxidation (CPO) of methane over precious metal catalyst has been shown to be an attractive way to obtain syngas (CO and H_2) or H_2 which can be converted to clean fuels by Fischer–Tropsch synthesis or employed in fuel cells. However, the presence of sulphur bearing compounds naturally occurring in the fuel, or added as odorants to pipe-line natural gas (approximately up to 10 ppm), can have a detrimental effect on the CPO activity.

In this work the effect of sulphur addition on the catalytic partial oxidation (CPO) of methane in the low to moderate temperature regime (300-800 °C) and under self-sustained high temperature (>800 °C) condition was investigated on Rh-based catalysts supported on either La_2O_3 or SiO_2 stabilised γ-Al_2O_3. Based on the results of catalytic activity measurements and in-situ FT-IR/DRIFT spectroscopic characterisation, as well as TPR/TPD studies, it has been shown that the presence of sulphur can severely suppress the formation of synthesis gas by inhibiting the steam reforming (SR) reactions during the CPO of methane. It was demonstrated that the support material plays a crucial role in the CPO of methane in the low to moderate temperature regime. In the presence of a sulphating support such as La_2O_3-Al_2O_3 the partial oxidation reaction was much less inhibited than a less sulphating support such as SiO_2-Al_2O_3. The sulphating support acts as a sulphur storage reservoir, which minimises the poison from adsorbing on or near the active Rh sites where reactions take place. However under the typical operating conditions of methane CPO i.e. at high temperatures and short contact times over structured reactors, sulphur in the feed inhibits the SR reaction by directly poisoning the active Rh sites thus preventing the sulphur storage capacity of the support from showing any beneficial effect on the S-tolerance.

Both steady state and transient operation of the CPO reactor were investigated particularly with regards to poisoning/regeneration cycles and low temperature light-off phase. The analysis of products distribution in the effluent and heat balance demonstrated that sulphur reversibly adsorbed on Rh selectively inhibits the SR reaction path to syn-gas production. The extent of SR inhibition is greater when operating in air and diminishes at lower CH_4/O_2 feed ratios. The poisoning effect was also shown to be independent from the type of sulphur bearing compound and only indirectly affected by the type of catalyst support (La_2O_3 or SiO_2 stabilised alumina) through the value of Rh dispersion. In fact by using in situ DRIFTS

experiments of adsorbed CO at room temperature it was found that sulphur acts as a selective poison by preferentially adsorbing on smaller well dispersed Rh crystallites whilst larger metallic Rh sites are mostly unaffected. The adsorption of CO at room temperature before and after S poisoning is schematically represented below.

Partial substitution of Rh/La-Al_2O_3 monolith catalysts with either Pt or Pd did not influence the way S adsorbs on highly dispersed Rh sites. Pd was found to have a detrimental effect on the overall catalytic activity and to be ineffective at improving the S-tolerance. On the other hand the partial substitution of Rh with Pt reduced the detrimental impact of S, which strongly inhibits the SR reaction on dispersed Rh sites but has a much smaller impact on Pt active sites. The improved tolerance of the bimetallic Rh-Pt catalyst against sulphur is due to its higher operating temperature related to the high oxidation activity of Pt which facilitates sulphur desorption from the catalyst and reduces its accumulation.

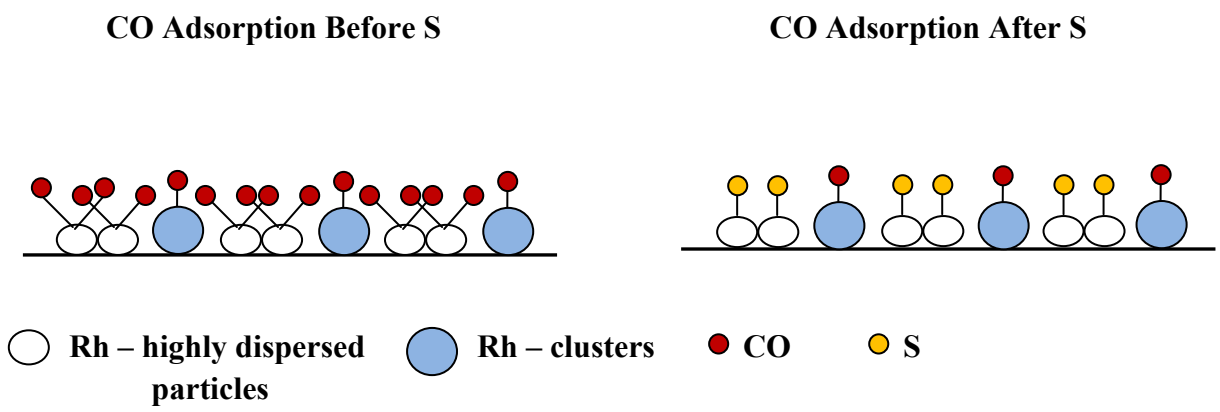

Schematic representation of CO adsorption at room temperature before and after sulphur poisoning

Contents

Chapter 1: Introduction

1. Introduction 1
1.1. Steam Reforming vs Partial Oxidation 3
1.2. Methane Partial Oxidation Mechanism 4
1.3. Catalysts for POM to Synthesis Gas 5
1.4. Major Issues for the CPO Process 5
1.5. Aim of The Work 7
1.6. Literature Review on Sulphur Poisoning 7
1.6.1. Poisoning by Sulphur Compounds 8
1.6.2. Pd Catalysts 9
1.6.3. Pt Catalysts 14
1.6.4. Rh Catalysts 15
1.6.5. Regeneration of Sulphur Poisoned Precious Metal Catalysts 20
1.7. Outline of the Thesis 21
References 23

Chapter 2: Experimental and Characterisation Techniques

2.1. Catalyst Preparation 26
2.1.1. Powder Catalysts 26
2.1.2. Monolith Catalysts 26
2.2. Catalyst Testing 27
2.2.1. Powder Catalysts 27
2.2.2. Monolith Catalysts 28
2.3. Catalyst Characterisation Techniques 30
2.3.1. Measurement of Surface Area 30
2.3.1.1 Total Surface Area 30
2.3.1.2 Metal Surface Area 31
2.3.2. Temperature Programmed Techniques 32
2.3.2.1 Temperature Programmed Reduction (TPR) 32

2.3.2.2 Temperature Programmed Desorption (TPD) 33
2.3.3. Infrared Spectroscopy (IR) 33
2.3.3.1 Fourier Transform IR (FTIR) Spectroscopy 33
2.3.3.2 Diffuse Reflectance IR Fourier Transform Spectroscopy 35
References 40

Chapter 3: The Effect of Support on Sulphur Tolerance of Rh Based Catalysts for Methane Partial Oxidation

3.1. Introduction 41
3.2. Experimental Procedure 41
3.3. Results and Discussion 41
3.3.1. Characterisation 41
3.3.2 Activity Measurement 50
3.4. Conclusions 60
References 61

Chapter 4: Sulphur Inhibition on the Catalytic Partial Oxidation of Methane Over Rh Based Monolith Catalysts

4.1. Introduction 62
4.2. Experimental Procedure 62
4.3. Results and Discussion 62
4.3.1 Pseudo-adiabatic Catalytic Tests 63
4.3.2. CPO Light-Off 72
4.4. Conclusions 75
References 76

Chapter 5: Effect of Partial Substitution of Rh Catalysts with Pt or Pd During the Catalytic Partial Oxidation of Methane in the Presence of Sulphur

5.1. Introduction 77
5.2. Experimental Procedure 77

5.3. Results and Discussion 77
5.3.1. Characterisation 77
5.3.2. CPO Light-Off 85
5.3.3. CPO Activity Measurement 87
5.4. Conclusions 95
References 96

Chapter 6: Overall Conclusions

6.1. Overall Conclusions 98

1. Introduction

Due to the dependency of the world economy on oil as an energy source for transportation, the scarcity of oil resources and an increasing need for sustainable energy have led to a sharp increase in oil price. This has resulted in an increased interest in the use of natural gas to meet the world's energy demand. The world has large deposits of natural gas and estimates of its size continue to grow as a result of innovations in exploration and extraction techniques. Natural gas resources are widely and plentifully distributed around the globe. Global reserves have more than doubled in the last twenty years and it is estimated that a significant amount of natural gas remains are to be discovered. The proven natural gas reserves i.e. those that could be economically produced with the current technology would be sufficient for nearly 70 years at current consumption rates. The largest volumes of natural gas are present in the Middle East and in the former Soviet Union and they account for almost three-quarters of world natural gas reserves (Figure 1.1), indicating that a considerable unbalance exists in the geographical distribution of reserves and consumption [1]. Indeed, most natural gas reserves are located in remote areas and consequently it must be transported across vast distances to reach its market. Hence, industry is currently facing the challenge of reducing this geographical imbalance by developing technologies and processes to market remote natural gas reserves.

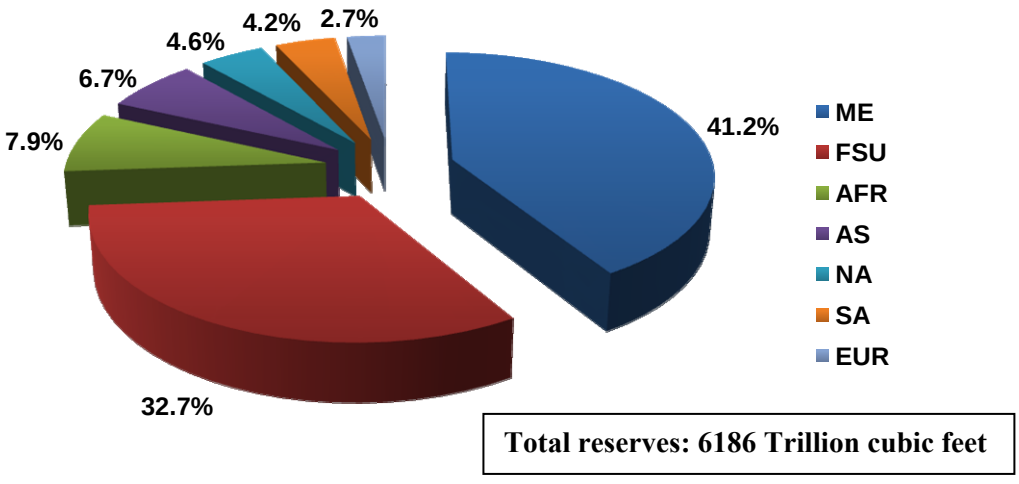

Figure 1.1: *World natural gas reserves by geographic region at the end of 2008 [1]. ME = Middle East, FSU = Former Soviet Union, AFR = Africa, AS = Asia, NA = North America, SA = South America, EUR = Europe.*

Conversion of methane to more useful and easily transportable liquid fuels is therefore of high interest. Since natural gas, mostly methane, is difficult to convert directly to liquid fuels,

the preferred route is first to produce syngas (CO and H_2), and then convert this to methanol or to higher alkanes by Fischer–Tropsch synthesis [2]. Syngas can also be used directly in conjunction with fuel cells after water gas shift (WGS) and CO removal for use in hydrogen powered vehicles or small scale domestic energy supply. Current use of natural gas is mostly based on exhaustible resources, but methane is also a product from the decay or fermentation of organic material [3]. Conversion of methane to synthesis gas is therefore a technology capable of contributing to a carbon-neutral energy chain sometime in the future. The catalytic partial oxidation (CPO) of methane over precious metal catalyst has been shown to be an attractive way to obtain syngas [4]. One advantage is that the process is slightly exothermic, whereas steam reforming (SR) is endothermic. The kinetics of SR is substantially slower than that of CPO which allows for more compact systems. This in turn makes the systems interesting for remote gas fields. An additional advantage of CPO is that it produces a H_2/CO-ratio of 2, which is needed for the downstream processing to liquid fuels [5].

Furthermore, the CPO of methane has been recently proposed as a preliminary conversion stage for hybrid gas turbine catalytic burners. In this case a fuel-rich/air mixture is first catalytically converted to both partial and total oxidation products which are subsequently oxidized with excess air to complete the combustion in a homogeneous flame. The syngas, produced under fuel-rich conditions improves the flame stability, allowing lower combustion temperatures and consequently strong reduction of NOx emissions [6]. The H_2-assisted combustion concept has also been proposed for conventional internal combustion engine (ICE), drastically reducing both NO_x and smoke engine emissions [7]. A schematic of the most important methane applications via syngas as an intermediate is reported in Figure 1.2.

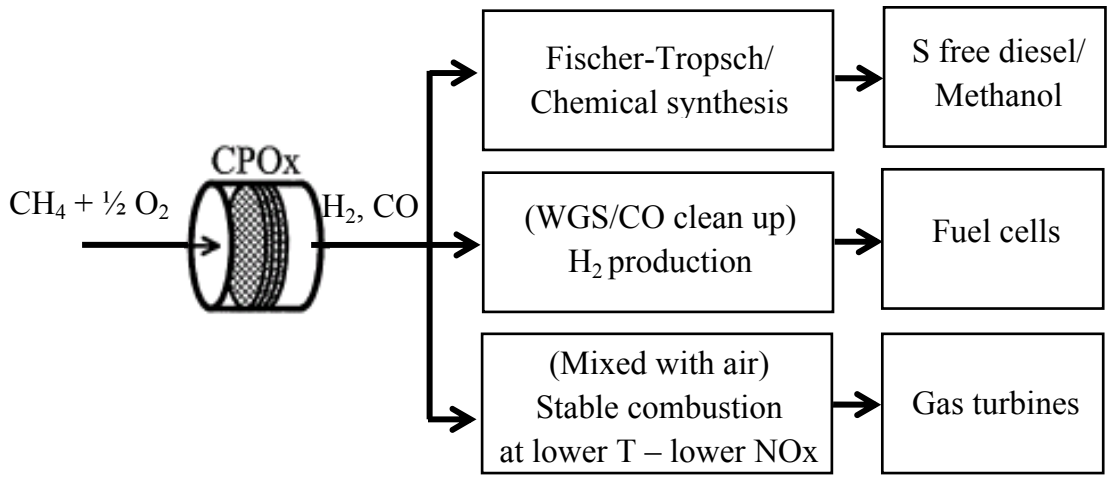

Figure 1.2: *Schematic of the most important methane applications via syngas as an intermediate.*

1.1. Steam Reforming vs Partial Oxidation

The steam reforming of methane (SRM) is currently the principal commercial process used to produce syngas:

$$CH_4 + H_2O \longrightarrow CO + 3H_2 \qquad \Delta H_r^{25°C} = +206 \text{ kJ/m} \qquad (1.1)$$

This reaction is highly endothermic, so it is performed in large furnaces to supply the necessary energy. Although, SR is a mature technology, it requires large heat exchange reactors, demanding large initial investment [8]. Furthermore, the product H_2/CO ratio of methane steam reforming is too high for many downstream processes. A promising alternative technology that has received much attention during the last decade is CPO of methane at high temperature and short contact time conditions [9]. In this process, methane is converted with oxygen or air over noble metal catalysts to yield syngas with a H_2/CO ratio that is ideal for FT syntheses:

$$CH_4 + ½O_2 \longrightarrow CO + 2H_2 \qquad \Delta H_r^{25°C} = -36 \text{ kJ/mol} \qquad (1.2)$$

The mild exothermicity of the reaction allows autothermal reactor operation at high temperatures exceeding 1000°C, which result in very high reaction rates at very short contact times (SCT). The CPO process can handle a large volume of the feed gas with only a small amount of the catalyst, leading to a dramatic reduction in a reactor size and complexity, as compared to the existing SR technologies. Thus, the process is becoming a preferred

technology for the small-scale production of syngas in both stationary and mobile fuel processing systems [10].

1.2. Methane Partial Oxidation Mechanism

The reaction pathway for partial oxidation of methane to syngas has been debated widely in the literature and so far there has been no final agreement on the reaction mechanism. The two possible reaction pathways that have been proposed in the literature are shown in Figure 1.3. One is the direct partial oxidation mechanism [4] where the direct production of synthesis gas involves initial formation of CO and H_2, which preferentially desorb from the catalyst surface before being converted towards the total oxidation products CO_2 and H_2O. The other is the indirect partial oxidation mechanism [11] also known as the combustion-reforming mechanism involving total oxidation of a portion of the CH_4 followed by the endothermic reforming reactions of the unconverted CH_4 with H_2O and CO_2 formed in the previous step and the water gas shift reaction.

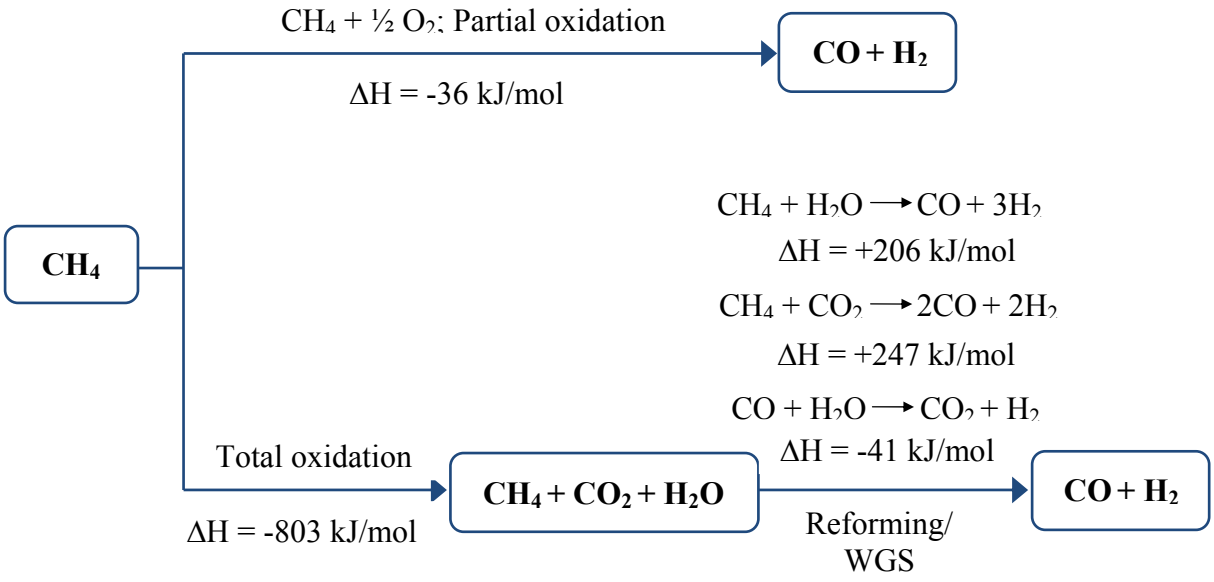

Figure 1.3: *Proposed mechanisms of catalytic partial oxidation of methane to syngas.*

The direct mechanism has been proposed mainly based on results from methane catalytic partial oxidation reaction at short contact time on rhodium and platinum coated monolith catalysts [4,12,13]. The indirect mechanism, however, was proposed mostly due to the observations of the temperature profile of catalysts bed. It was found that the catalyst temperature was significantly higher in the front of catalyst bed than the latter part of catalyst

bed, caused by the initial exothermic combustion reactions followed by the endothermic reforming reactions [14,15]. This phenomenon was present on different catalyst and under different reaction conditions [16].

1.3. Catalysts for POM to Synthesis Gas

Many catalysts have been investigated for the CPO of methane to syngas, such as Rh, Pt, Pd, Ir, Ni, Fe, Co, Re, and Ru (group VIII metals). Comparative studies on the activity of various supported group VIII metals can be found in Torniainen et al. [13] and Enger et al. [16]. At present, both Ni and Rh-based catalysts have been identified to be the most promising CPO catalysts. In contrast to supported Ni catalysts, however, Rh-based catalysts display both high activity and stability during the catalytic partial oxidation of methane to synthesis gas. Rh catalysts also show higher resistance to carbon deposition and to sulphur poisoning [9,17]. A comparison in CPO activity for various metal coated monoliths was investigated by Torniainen et al. [13]. They demonstrated that Ni catalysts deactivate due to metal evaporation and formation of NiO and $NiAl_2O_4$, whilst Rh coated monoliths showed stable performance for several hours. Pt and Ir also showed high stability, but significantly lower conversions and selectivities compared to Rh catalysts. Rapid deactivation was also observed in case of Pd coated monoliths as a result of coke deposition. Finally, Fe, Re, and Ru catalysts could not sustain the CPO reaction at the applied conditions. The authors thus concluded that Rh-based catalysts are the most suitable for synthesis gas production [13]. However, due to the high cost of Rh, its use for commercial application is one of the key issues – Figure 1.4.

1.4. Major Issues for the CPO Process

In addition to the high cost of rhodium another major concern is the presence of sulphur containing compounds naturally occurring in natural gas or added as odorants necessary for safety reasons can result in a sulphur concentration totaling approximately 10 ppm, which can adversely affect the catalytic performance. Sulphur chemisorbs onto and reacts with the active catalytic sites, thus preventing reactant access [18]. In addition sulphation of the support component can also occur, which consequently will have an impact on the metal-support interaction and hence results in catalyst deactivation. Although desulphurisation units can be used to significantly reduce the sulphur content in the feed, its inclusion increases the

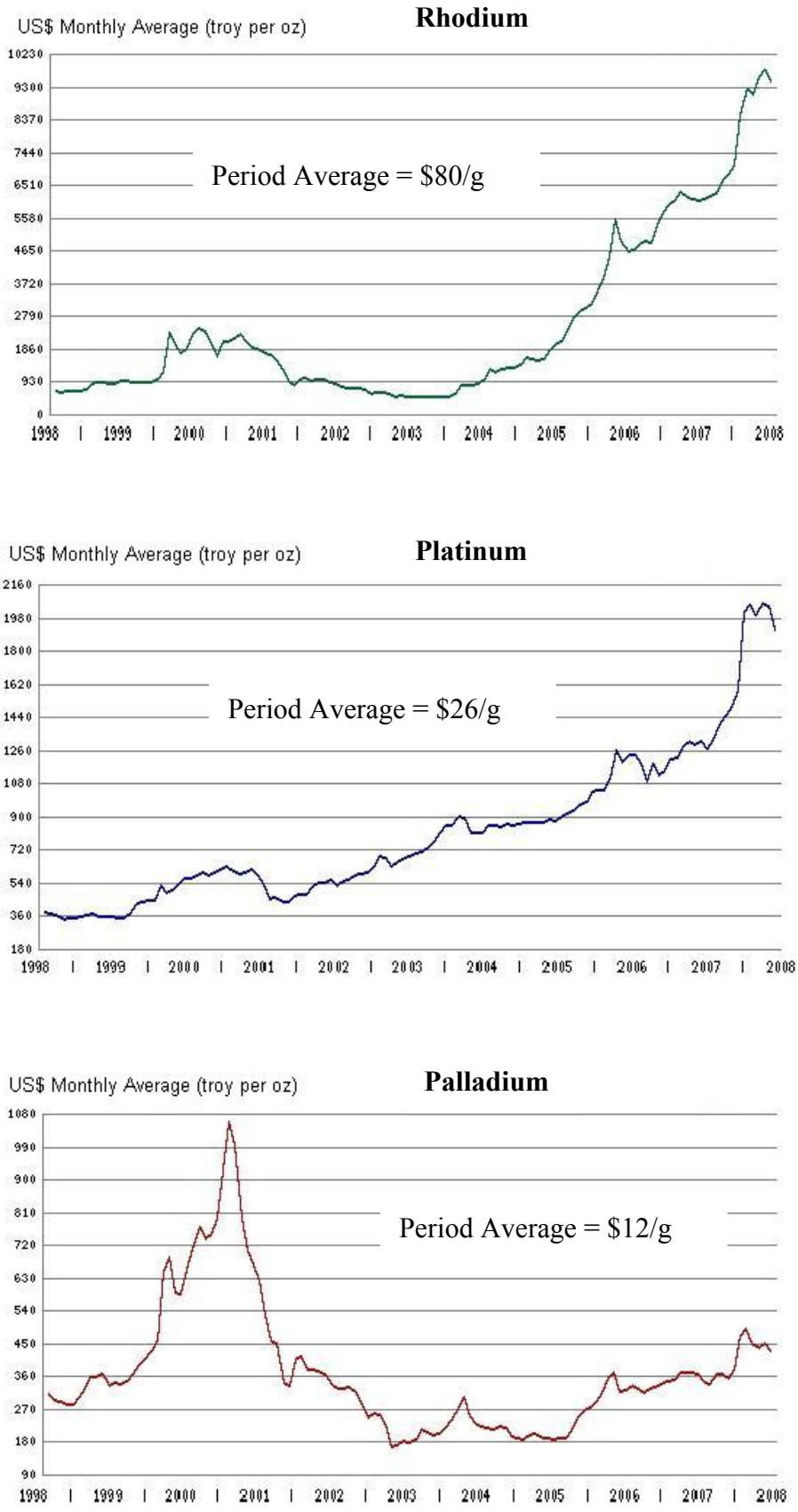

Figure 1.4: *Johnson Matthey base prices (monthly average) for Rh, Pt and Pd from July 1998 to July 2008 [19].*

complexity, size and cost of the fuel processing system. Moreover, the present catalytic hydrodesulphurisation (HDS) technology can not completely remove all the sulphur from the fuel. Thus, "sulphur-free" fuels in fact still contain up to 10 ppm of S after HDS treatment which can significantly reduce the catalytic activity. Therefore it will be more desirable to develop catalysts that are intrinsically sulphur tolerant and are not readily poisoned by the amounts of sulphur commonly found in fuels such as natural gas and commercial low sulphur fuels.

1.5. Aim of The Work

The objective of this thesis is to study the effect of sulphur poisoning during the catalytic partial oxidation of natural gas at high temperatures and short contact times. The work will focus specifically on understanding the mechanism by which S poisons the CPO of methane with particular emphasis on the effects of temperature and reaction environment. The effect of addition of different sulphur compounds (SO_2/H_2S) into the reaction feed on the catalytic performance will also be investigated, in order to observe if the extent of catalyst poisoning is affected by different S species. Special attention will also be given to the rate at which the catalysts regenerate following exposure to sulphur.

The final aim of the present study is to develop low cost sulphur tolerant rhodium based catalysts with high catalytic activity and good thermal durability for the partial oxidation of methane to syngas.

1.6. Literature Review on Sulphur Poisoning

In order to be able to design active and more sulphur tolerant catalysts, a good understanding of deactivation mechanisms by which sulphur poisons the catalytic activity will be essential. Although there have been many studies examining the effect of sulphur on methane conversion under combustion conditions, studies on the effect of sulphur on the CPO of methane over Rh based catalysts have so far remained scarce and only very recently papers have started being published addressing the issue. Therefore, this review gives a brief summary on the interaction of sulphur with precious metals followed by a status of knowledge and a summary of open literature examining the effect of sulphur in the reaction mixture on the catalytic activity of Pd

and Pt catalysts in the oxidation of methane and on the catalytic activity of Rh based catalysts for the partial oxidation of methane and hydrocarbons. With respect to the total oxidation of methane, special attention will be given to Pd rather than Pt, due to its very high activity for methane combustion. The influence of the reaction conditions (sulphur concentration, temperature), or the nature of the support on the poisoning will also be examined.

1.6.1. Poisoning by Sulphur Compounds

The presence of organo-sulphur compounds naturally occurring in natural gas or added as odorants necessary for safety reasons can severely affect the catalytic performance. Sulphur can readily get oxidised or reduced over a catalyst, depending on the gas composition (lean and rich conditions). Under oxygen deficient condition H_2S is formed, which is a strong poison for metal surfaces. It binds very strongly to the active metal sites on the catalyst, forming stable surface metal sulphides (Me-S) and thereby prevents the reactants from adsorbing at the surface. However, under oxygen rich conditions, SO_3 is produced over the precious metal containing catalyst and this will cause the sulphation of the support material (e.g. sulphation of CeO_2, Al_2O_3), which can affect the metal-support interaction. The order of S-poisoning for sulphur containing species can be given as: $H_2S>SO_2>SO_4^{2-}$.

Precious metals are well-known oxidation catalysts with high activities, and are widely used for controlling exhaust gas emissions such as hydrocarbons and carbon monoxide. Apart from the higher specific activities, precious metals are preferred because they are less liable to sulphur poisoning than base metal catalysts which are severely deactivated by the formation of stable surface sulphates resulting in the elimination of base metals as viable candidates for automotive emission control [20].

Under stoichiometric and rich conditions, SO_2 formed during combustion is dissociatively adsorbed on platinum group metal (PGM) surfaces to form strongly bound adsorbed sulphur $(S)_{ad}$ species. Sulphur inhibition results from both physical blockage and electronic effects of $(S)_{ad}$, such that low coverage of $(S)_{ad}$ results in disproportionately higher levels of reaction site blockage. This is responsible for the nonlinear effects observed with increasing fuel sulphur level. Migration of sulphur into bulk Pd accounts for its greater sensitivity to, and irreversibility of, sulphur inhibition. Weaker interaction with SO_2 and easier removal of adsorbed sulphur

result in better sulphur tolerance for Rh. Overall, the order of sulphur sensitivity is Pd>Pt>>Rh [21].

1.6.2. Pd Catalysts

Sulphur containing compounds can react with a catalyst in a variety of ways. In an oxidizing environment SO_2 and SO_3 are formed, whereas under reducing conditions H_2S is formed. Considering a Pd/alumina catalyst, SO_2 formed in the combustion chamber, reacts with the catalyst in different ways: Sulphur dioxide is oxidized over palladium oxide to form sulphur trioxide, which can then either react with the Pd/PdO to form less active $PdSO_4$ or can spill-over to the carrier and further react with alumina to form aluminium sulphate species which is stable to temperatures of approximately 700 °C. Thus, the nature of the support can have a significant influence on catalyst sulphation.

The influence of the nature of the support on the poisoning of Pd catalysts by the addition of H_2S was examined by Hoyos et al. [22]. Alumina and silica supported Pd catalysts were tested at 350 °C in the oxidation of methane under oxidising conditions in the absence and in the presence of H_2S. It was shown that the presence of sulphur strongly deactivates the catalyst and the extent of deactivation is independent of the support. However, the regeneration of the catalysts at 600 °C under a S free mixture improved the activity of the alumina supported catalyst, whereas the activation was instantaneous for silica supported sample. The chemical analysis of the samples confirmed the storage of sulphur species by alumina. H_2S is oxidized at temperatures above 300 °C over noble metals [23] to SO_2/SO_3, which reacts with the active components of the carrier. IR studies have also revealed the presence of $PdSO_4$ species. The sulphate formed is thermally stable at temperatures up to 400 °C and is totally decomposed upon heating in flowing nitrogen at 600 °C over silica supported catalysts [22]. Although the extent of deactivation was the same for both catalysts, the rate of deactivation was slower in the case of alumina supported Pd-catalyst. This property was attributed to temporary shielding of palladium by alumina support, which acts as a scavenger for SO_2/SO_3 and this slows down the Pd poisoning. Silica, being a non-sulphating carrier, has no SO_2-trapping ability and the deactivation is faster. On the other hand regeneration of Pd/SiO_2 catalyst is much faster since only the decomposition of $PdSO_4$

is required, whereas the removal of sulphur from the support ($Al_2(SO_4)_3$) requires higher temperature.

Lampert et al. [24] studied the effect of SOx on the activity of platinum and palladium catalysts. As little as 1 ppm SO_2 was shown to be sufficient to inhibit the oxidation of methane over palladium catalyst, whereas as C_2H_6, C_3H_8 and CO oxidations were inhibited to a lesser extent. A mechanism was proposed as a 1:1 selective adsorption of SOx on a PdO on non-sulphating support such as SiO_2, where the deactivation is rapid. When alumina is used, the catalyst can tolerate more SOx since the alumina support acts as a scavenger of SOx. In order to have a better understanding of the role of the carrier in SOx poisoning, it is useful to study the adsorption/desorption behaviour of different carriers. The adsorption of SOx at 320 °C and its desorption at 650 °C (in air) are given in Table 1.1. As can be seen alumina reacts strongly and retains SO_2, with the amount retained depending on the surface area and alumina phase composition (α, θ or γ). A lower support surface area, either having the same phase (α) or different phases (α, θ), results in less SO_2 uptake. The silica based supports do not react with SO_2 and complete desorption of SO_2 at 650 °C is taking place from the active metal (Table 1.1). Hence the trapping ability of the carrier can increase the SOx tolerance and at the same time 'delay' the regeneration of the catalyst. An example of catalyst deactivation and regeneration for Pd supported on alumina (sulphating support) and ZrO_2–SiO_2 (non-sulphating support) is given in Figure 1.5. As expected, the deactivation, due to the presence of sulphur, is higher for the non-sulphating carrier (curve 2, Figure 1.5a). When SO_2 is removed from the gas stream (curve 3, Figure 1.5a and b) the higher activity of the Pd/ alumina, compared to Pd/ZrO_2–SiO_2 catalyst, is due to a decrease in sulphur on the catalytic

Pd catalyst support	Surface area (m^2/g)	SO_2 adsorbed at 320 °C (wt%)	SO_2 retained at 650 °C (wt%)
γ-Alumina	375	6.7	5.8
γ-Alumina	150	5.3	3.9
θ + α-Alumina	50	0.9	0.2
ZrO_2–SiO_2	240	0.7	0.0
SiO_2	300	0.2	0.0

Table 1.1: *Adsorption of sulphur oxides at 320 °C for 6 wt% Pd on different supports [24].*

sites as the support adsorbs more of the SO_2 spilling-over from Pd. After the catalyst is treated at 650 °C, the sulphur from sulphated alumina support continues to spill 'onto' the palladium surface, preventing the complete decontamination of the Pd/alumina catalyst (curve 4, Figure 1.5b). On the other hand, for the non-sulphating carrier, the sulphates decompose and the activity is recovered (curve 4, Figure 1.5a).

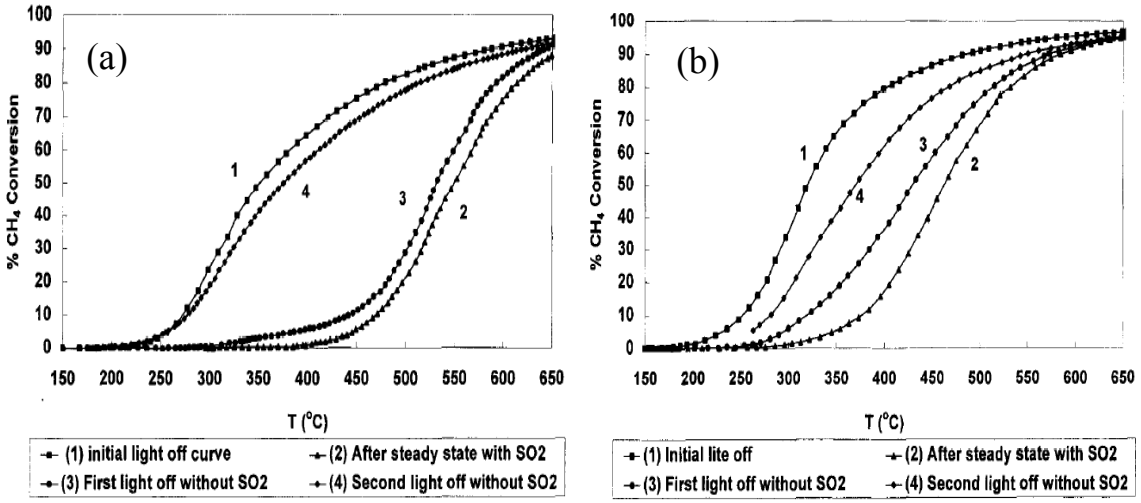

Figure 1.5: *(a) The deactivation and decontamination of Pd-supported on ZrO_2–SiO_2 following steady state exposure to SO_2 and reactivation at 650 °C in the sulphur free process gas, Curve 1: the initial methane light-off curve for the catalyst without SO_2 in the process gas (800 ppm CH_4, 8%O_2, 0.9 ppm SO_2, balance N_2). Curve 2: After 11 h at 320 °C in the process gas with 0.9 ppm SO_2. Curve 3: Light-off curve in sulphur free process gas. Curve 4: The second light-off curve in the sulphur-free mixture. Thermal decontamination of the catalyst is due to desorption of SO_2 at 650 °C in the sulphur free mixture, corresponding to the maximum temperature for light-off curve 3. Monolith supported catalysts, 400 cpsi catalyst [24]. (b) The deactivation and decontamination of Pd-supported on γ-alumina. Conditions are the same as in (a).*

Yu and Shaw [25], however, proposed an alternative explanation to the deactivation by sulphur by formation of palladium sulphate. The catalyst (4 wt.% PdO supported on γ-Al_2O_3, 67m^2/g) was prepared from the nitrate salt and calcined in air at 500 °C before testing in 1 vol.% methane in air. The progressive inhibition of the conversion versus time by adding H_2S (80 ppm) to the feed at 400 °C was again shown. Suppressing H_2S allowed the activity to be only slightly recovered. Pre-exposure of the catalyst to H_2S in air (24 h) at increasing temperatures (100 – 400 °C) caused an increasing inhibiting effect on the activity. FT-IR data indicated the formation of aluminium sulphate (1145 cm^{-1}). On the basis of the decrease of the BET area, due to aluminium sulphate formation, the PdO occlusion was proposed to

explain the decrease of the activity instead of the formation of palladium sulphate. Hydrogen treatment at 600 °C was shown to remove most of the sulphate species from the catalyst surface thus regenerating most of the initial activity for methane oxidation. This interpretation of the poisoning of palladium catalysts by sulphur was not further considered by other groups.

The mechanism of the deactivation of PdO/Al_2O_3 catalysts by SO_2 was re-examined by Mowery et al. [26,27] focusing on the deactivation in the presence of both water and SO_2. Sulphur dioxide was shown to cause both inhibition and deactivation for methane oxidation. This deactivation was partly reversible at 460 °C and completely reversible at 520 °C. Water caused both inhibition and irreversible deactivation at either temperature. However, the presence of both water and SO_2 in the feed caused the catalyst to deactivate more rapidly and the recovery of the activity was more difficult than when either poison was added separately. On the basis of TPD and FT-IR experiments, the authors proposed the following mechanism- Figure 1.6. Under dry conditions SO_2 can adsorb onto either alumina or PdO, and migrates via surface diffusion between the supported phase and the support. On PdO some SO_2 is oxidized to SO_3, which can form $PdSO_4$ or spillover onto the support leading to sulphation. Because of this scavenging effect of the support for both SO_2 and SO_3, the rate of sulphation and hence deactivation of PdO is relatively low. Water inhibits the scavenging of SO_2 by

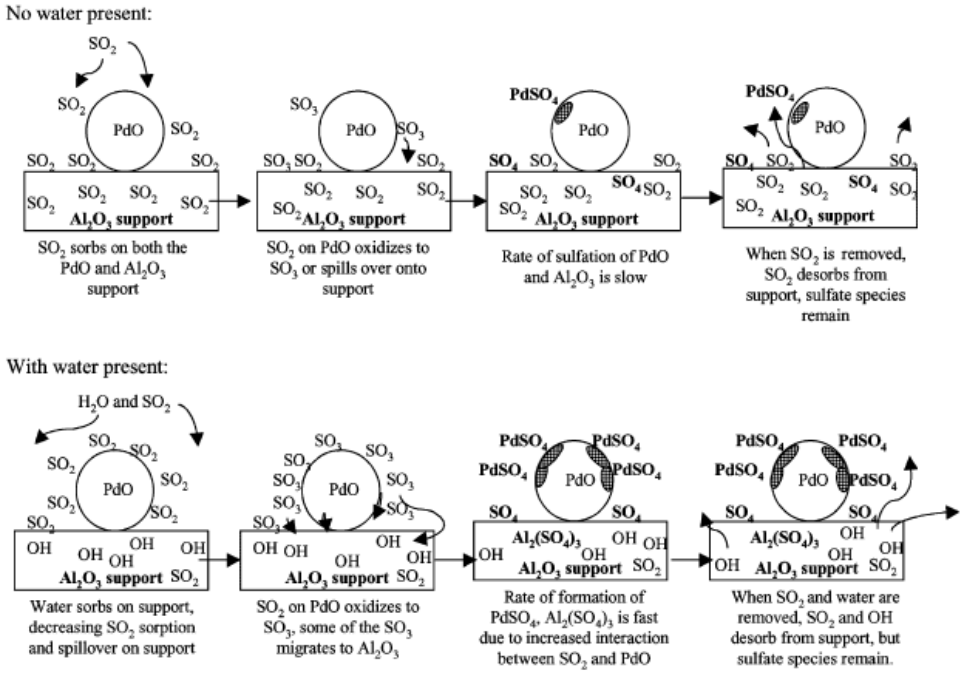

Figure 1.6: *Schematic of possible mechanisms of the effect of water on sulphation of Pd/Al_2O_3 [27].*

Al_2O_3 by decreasing the number of sites available for SO_2 adsorption. Thus, SO_2 adsorbed on the supported PdO particles cannot spillover onto the alumina surface, but is oxidized to SO_3 increasing the formation rate of $PdSO_4$. Increased formation of $Al_2(SO_4)_3$ may occur because of the increased rate of SO_3 formation and SO_3 migration to Al_2O_3 even in the presence of water.

Gélin et al. [28] investigated the effect of H_2S poisoning and regeneration under oxidizing conditions of alumina supported Pd catalyst for complete oxidation of methane. Exposure to H_2S induced a strong and irreversible deactivation of the catalyst. A poisoning mechanism of Pd/Al_2O_3 by progressive formation of inactive $PdSO_4$ species was suggested (Figure 1.7). Although palladium sulphate species are known to fully decompose below 600 °C, sulphate species present on the H_2S-poisoned Pd/Al_2O_3 catalyst were shown to decompose in O_2/He only above 600 °C. It was deduced that below 600 °C and above ca. 400 °C, sulphate species are re-distributed at the surface of the catalyst. Accordingly, active PdO sites are partly regenerated and the extent of the catalytic recovery increases with the increase of temperature of the treatment in O_2/He. However, although sulphate species were partly removed from the catalyst, a treatment in O_2 at temperatures as high as 650 °C did not allow the complete regeneration of the catalytic activity of the H_2S-poisoned Pd/Al_2O_3. The authors suggested that, while being not completely removed from the catalyst, sulphate species can migrate back and forth between PdO and basic alumina sites, depending on the temperature, therefore preventing the complete regeneration of the catalyst with respect to methane oxidation.

The regeneration of a S poisoned Pd/Al_2O_3 catalyst for methane combustion was also investigated by Arosio et al. [29], in order to determine the temperature threshold to achieve catalyst reactivation under different CH_4 containing atmospheres. Under lean combustion conditions in the presence of excess O_2, partial regeneration took place only above 750 °C after decomposition of stable sulphate species adsorbed on the support. Short CH_4-reducing, O_2-free pulses led to partial catalyst reactivation at temperatures as low as 550 °C and to practically complete regeneration at 600 °C. Also in this case reactivation was associated with SO_2 release due to the decomposition of stable support sulphates likely promoted by CH_4 activation onto the reduced metallic Pd surface. Rich combustion pulses with $CH_4/O_2 = 2$ were also found to be effective to CH_4 reducing pulses in catalyst regeneration. The authors also proposed that the reductive regeneration of S poisoned catalyst with CH_4 containing

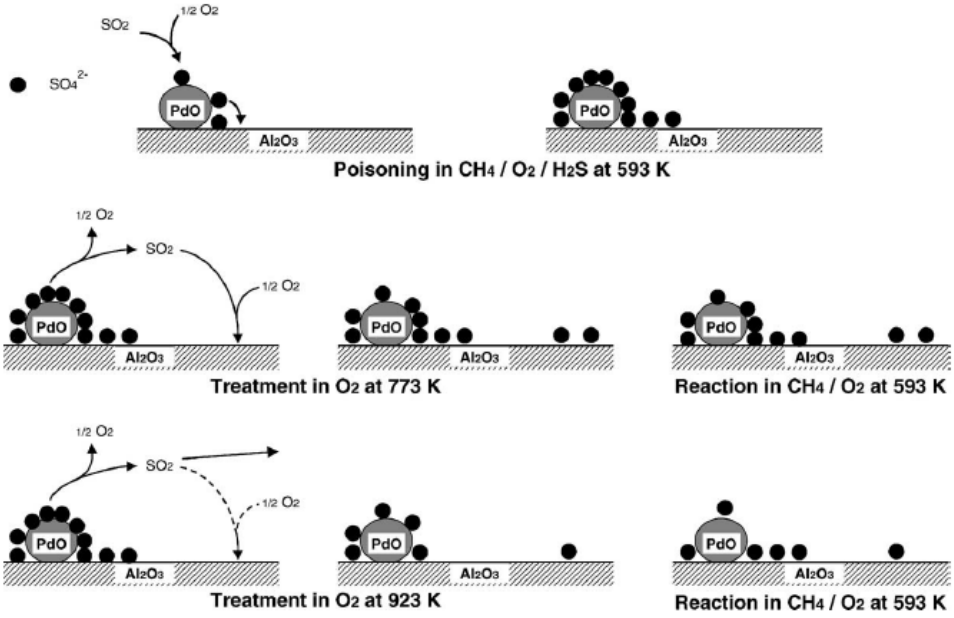

Figure 1.7: *Scheme of H_2S poisoning and regeneration mechanisms for Pd/Al_2O_3 catalysts. H_2S easily converts to SO_2. PdO oxidises SO_2 to SO_3. SO_3 is trapped by PdO and spills to Al_2O_3 sites surrounding the PdO particles by surface diffusion. At saturation of these sites, SO_3 poisons PdO by palladium sulphate formation. Under O_2 at 500 °C, $PdSO_4$ slowly decomposes to PdO and $SO_2/(1/2)O_2$. SO_3 around PdO spills back to PdO. SO_2 can re-oxidise to SO_3 on basic alumina sites away from PdO particles and cannot evolve from the catalyst. SO_3 is re-distributed on the catalyst surface by gas diffusion. Under O_2 at 650 °C, sulphate at alumina sites slowly decomposes into SO_2. SO_2 is slowly removed from the catalyst. The decomposition is catalysed by PdO and the concentration in SO_3 on Al_2O_3 around PdO decreases. On quenching, PdO surface is still partially covered by SO_3. Under reaction, SO_3 spills to Al_2O_3 sites around PdO. The activity increases until saturation of alumina sites by surface diffusion. The activity is not fully restored [28].*

atmosphere was more effective than analogous treatment with H_2 containing streams, possibly due to the milder reduction action resulting in minor formation of surface sulphides.

1.6.3. Pt Catalysts

Unlike Pd, Pt possesses greater resistance to S-poisoning [24,30] but is less active in methane oxidation (although very active in saturated HC oxidation). Even though Pt is very active for oxidation of SO_2 to SO_3, platinum does not adsorb SO_3 and its deactivation can be minimized using a non-sulphating support. Exposure of Pt/alumina catalyst to SO_2 has been shown to increase the catalytic activity for combustion of propane and other normal alkanes [31,32]. This observation is explained as catalyst sulphation results in reduction of small PtO_2 particles and sintering of these particles to a more active state [33]. Type of hydrocarbon and

the catalyst support influence the activity of HC oxidation over Pt. SO_2 inhibits the oxidation of reactive hydrocarbons such as ethylene and other olefins as well as CO, but enhances the oxidation of saturated hydrocarbons [30] over Pt/γ-alumina. Addition of 20 ppm SO_2 to the synthetic gas mixture under oxidizing conditions has been shown to increase the light-off temperature of propylene and CO by 40 and 45 °C, respectively [34]. The light-off temperature in propane is decreased by 15 °C over ZrO_2 and SiO_2 carriers, compared to 150 °C over γ-alumina [32].

1.6.4. Rh Catalysts

A number of catalysts have been tested for the CPO of hydrocarbons from methane up to diesel and jet-fuels and Rh-based catalysts have shown the highest activity and selectivity to syngas. However, the presence of sulphur compounds in the fuel can have a detrimental effect on the catalytic activity of Rh catalysts for the partial oxidation reactions. So far, studies on the effect of S compounds on the catalytic partial oxidation of hydrocarbons over Rh based catalysts remain scarce and only very recently papers have been published addressing the issue.

In the partial oxidation of tar derived from the pyrolysis of wood biomass (cedar wood), Tomishige et al. [35,36] investigated the effect of H_2S addition over steam reforming Ni catalyst and $Rh/CeO_2/SiO_2$ using a fluidized bed reactor. Steam reforming Ni catalyst was effective for the tar removal without H_2S addition, however, the addition of H_2S (168 ppm) drastically deactivated the catalyst. In contrast, Rh/CeO_2-SiO_2 exhibited higher and more stable activity than the Ni catalyst even under the presence of high concentration of H_2S (280 ppm). The surface sulphur content over the Rh/CeO_2-SiO_2 catalyst after the reaction with the addition of H_2S was determined to be very low (i.e. below the detection limit of XPS), where as on the Ni catalyst the adsorption of sulphur was observed by XPS. This was related to the self-cleaning of catalyst surface during the circulation in the fluidized bed reactor. The authors suggested that although sulphur can adsorb on the Rh/CeO_2-SiO_2 catalyst, it can be removed by the oxidation to SO_2 in the oxidising atmosphere, in the lower part of the catalyst bed and by the reduction to H_2S in the reducing atmosphere, in the upper part of the bed i.e. in the absence of oxygen and the presence of synthesis gas.

Recently, a few special sulphur tolerant reforming catalysts have been mentioned in the open literature, albeit with confidential formulations [37-39]. A specific supported precious metal catalyst with a proprietary formulation, able to cope with 100 ppm sulfur, has been developed by Johnson Matthey for steam reforming of higher hydrocarbons [37]. A proprietary catalyst of bimetallic compound supported on high-surface area Al_2O_3 treated with an oxide with oxygen ion-conducting properties and sulfur resistance comparable to that of the Johnson Matthey catalyst has been developed by InnovaTek [38]. The U.S. Department of Energy's Argonne National Laboratory has developed a highly sulfur-tolerant Pt/dope-ceria autothermal reforming catalyst with proprietary formulations, but only initial reaction results in the presence of sulfur have been reported [39].

Furthermore, Strohm and co-workers [40] investigated the catalytic effectiveness and deactivation behaviour of Rh/CeO_2-Al_2O_3 catalysts for low-temperature steam reforming of liquid fuels using model and real jet fuel as the feedstock in the absence and presence of different amounts of organic sulphur. The effect of addition of Ni, to retard the sulphur poisoning of Rh was also investigated. The authors observed that although, the monometallic Rh/CeO_2-Al_2O_3 catalyst was active for reforming of sulphur free jet fuel at temperatures less than 520 °C with high conversion to syngas, the catalyst deactivated rapidly during the reforming of liquid fuel with more than 10 ppm S. The addition of Ni (5 wt%-10 wt%) by co-impregnation in to the Rh/CeO_2-Al_2O_3 catalyst lead to much higher sulphur tolerance. The bimetallic Rh-Ni/CeO_2-Al_2O_3 catalyst allowed for successful low-temperature reforming of a JP-8 jet fuel containing 22 ppm sulphur for 72 h with >95% conversion. It was proposed that the Ni closely interacts with Rh metal and protects Rh from sulphur poisoning through two possible mechanisms. First, Rh species are surrounded by Ni species in close vicinity (when prepared by co-impregnation onto CeO_2–Al_2O_3), and Ni reacts preferentially with sulphur, thus protecting the Rh active sites from sulphur adsorption. Secondly, when some Rh atoms do react with sulphur, such sulphur in RhSx can transfer to Ni present in the close vicinity of Rh. S in RhSx may be transferred to the Ni metal through sulphur spillover with or without the aid of gas phase hydrogen. In either case, a close interaction between the added Ni and Rh was necessary. Evidence of Rh and Ni interactions was obtained by TPR and XPS analysis which supported the hypothesis that Ni protects Rh through a close Rh–Ni interaction. However, the authors failed to mention the effect of saturation of Ni sites by sulphur on the reaction and more importantly how the catalyst could be regenerated once Ni saturation had occurred.

The autothermal reforming (ATR) of commercial gasoline and its surrogates (*n*-octane with or without the addition of thiophene) on Rh-based monolithic catalysts was studied by Qi et al. [41]. The optimal catalyst composition was found to be around 0.3wt%Rh/ 3wt%MgO/ 20wt%CeO_2–ZrO_2 (3:1) supported on cordierite monolith, which enabled octane to be fully converted into reformate with minor amount of residual CH_4 when temperatures were higher than 670 °C. The catalyst also converted aromatics such as toluene into CH_4-free reformate at only a relatively higher temperature, accounting for the high hydrogen selectivity for gasoline at the similar operation conditions. The catalyst also showed resilient response to sulphur poisoning, although the presence of sulphur in the fuel significantly affected the hydrogen selectivity. The sulphur poisoning effect was found to be reversible to some extent with the catalyst activity almost completely recovering after the pure octane was fed into the system again. The researchers suggested that the role of MgO in Mg-Ce-Zr oxide compared to CeO_2-ZrO_2 was to enhance the redox properties, which were favourable for ATR reaction. It was also suggested that sulphation of ceria could act as a potential sink for sulphur during the ATR reaction.

However, sulphation of the support is implicated as the main cause of deactivation during hydrogen generation over supported rhodium catalysts [42]. Based on the kinetic model for steam reforming over rhodium catalysts, it has been demonstrated that the turnover frequency is proportional to the specific perimeter of the metal particles, i.e. the total length of the metal-support interface per unit surface area. The kinetics can be explained by a bi-functional reaction mechanism [42] in which the hydrocarbon is activated by the rhodium, while water adsorbs on the support to form surface hydroxyl species. Sulphation of the support inhibits steam reforming by preventing (i) the formation of hydroxyl species adjacent to the metal-support interface and (ii) migration of more remote hydroxyl species to the interface where they can interact with adsorbed hydrocarbon. Similar mechanism has also been proposed for the partial oxidation of methane over alumina supported Rh catalyst where hydroxyl groups on the support are involved in methane conversion [43,44].

It is also reported that the catalytic activity of Rh catalyst is significantly affected by the presence of sulphur impurities either in feed or in the support and the small amount of sulphur can deactivate Rh via coordination to active metal centres [45]. It was shown that sulphate impurity in Al_2O_3 support had a negative effect on the performance of Rh/γ-Al_2O_3 during dry

reforming of methane. However, the catalytic activity was significantly improved by removing sulphate from the support.

Recently Bitsch-Larsen and co-workers [46] reported results on the effect of sulphur addition on the CPO methane over Rh-Ce coated foam monoliths. The authors found that upon the addition of small amounts of sulphur, the CH_4 conversion and selectivity to H_2 decreased along with a sharp increase in the operating temperature. This observation was explained by sulphur poisoning of the active sites for steam reforming. Additionally, the poisoning effect was found to be almost independent of the sulphur level. A doubling of the sulphur level from 14 to 28 ppm did not result in significant changes, showing that the effect saturates at a few ppm. Furthermore, it was observed that the effect was reversible and the catalyst slowly regained its initial activity when the sulphur was removed from the feed. A faster regeneration of the catalyst was also possible by reduction in hydrogen or a decrease in the C/O ratio which allowed the sulphur to burn off.

The effect of temperature, steam-to-carbon ratio, and the addition of K on the sulphur tolerance of Rh supported on a lanthanum-modified alumina catalyst for reforming low-sulphur (34 ppm S) gasoline was investigated by Ferrandon et al. [47]. The presence of sulphur in gasoline poisoned the Rh/La–Al_2O_3 catalyst, with the effect of sulphur being more pronounced at 700 °C than at 800 °C. At 700 °C, only 50% of the catalyst performance could be recovered when the feed was switched back from the low sulphur to sulphur-free gasoline. The performance loss was attributed to excessive coking that occurred while reforming the 34 ppm S gasoline. At 800 °C, sulphur poisoning appeared to be reversible, with nearly 100% recovery of the catalyst performance when the feed was switched back from low-sulphur to sulphur-free gasoline. Increasing the H_2O:C ratio from 2.0 to 3.0 led to a significant improvement in the performance of the catalyst at 700 °C due to lower coke formation. An increase in the bed temperature was observed when reforming gasoline-containing sulphur due to a stronger inhibition of the endothermic steam reforming reaction than of the exothermic oxidation reaction, thereby resulting in an increased sintering of Rh. The addition of K to Rh was also found to enhance the sulphur tolerance of the catalyst by increasing the reaction temperature and by blockage of Rh sites preventing H_2S adsorption and coke formation.

The addition of Pd to Rh has also been shown to improve the sulphur tolerance and hydrogen yield during the steam reforming of sulphur containing fuels [48]. The enhancement observed by the bimetallic Rh-Pd was explained by the strong metal-metal interaction between rhodium and palladium which would allow it to pass on the sulphur to Pd forming palladium sulphide.

The improvement in sulphur tolerance and hydrogen yield by the addition of Pd to Rh supported on ceria based catalysts for the steam reforming of simulated jet fuel was also observed by McCoy and co-workers [49]. In the absence of sulphur the Pd-Rh catalyst gave the highest hydrogen yield of approximately 45% after 2 h and did not demonstrate any noticeable level of deactivation at longer time on stream. Moreover, in the presence of 50 ppm sulphur the bimetallic Pd-Rh catalyst, showed better resistance to deactivation compared to those containing either of the two single metals.

The autothermal reforming of simulated and commercial low-sulphur diesel fuel (10 ppm S) on zirconia-supported Rh, Pt and bimetallic Rh-Pt catalysts has very recently been investigated for obtaining fuel gas suitable for solid oxide fuel cell applications [50]. Comparison of the mono- and bimetallic catalysts showed the amount of deposited sulphur to be highest on the monometallic Rh catalyst and lowest on the bimetallic Rh-Pt catalyst. Bitter et al. [51] proposed that the activity of a Pt/ZrO_2 catalyst in CO_2/CH_4 reforming is proportional to the concentration of the $Pt–ZrO_2$ interface, whereas the activity of a Rh/ZrO_2 catalyst is directly proportional to the availability of Rh sites. For the bimetallic $Rh-Pt/ZrO_2$ catalyst it was observed that the metal clusters consist of a $Rh_xPt_{1\_x}$ alloy subsurface and an active Rh_2O_3 overlayer [49]. It was proposed that the close interaction between Rh and Pt, similar to the interaction between Ni and Rh observed in the steam reforming of jet fuel [40], reduced the binding of the noble metal with the sulphur.

Very recently Shamsi [53] reported results on the CPO of methane into syngas over fresh and sulphided alumina supported Rh and Ru-Pd catalysts as well as NiMgO supported on gadolinium-doped cerium oxide material at the temperature range of 450-750 ºC. Rh catalyst was shown to have the best overall activity, less carbon deposition, both fresh and after exposure to hydrogen sulphide at 850 ºC. Although the catalyst activity and selectivity was greatly affected by exposure to H_2S, the catalyst could be fully regenerated following reduction with hydrogen at high temperatures. The extent of catalyst regeneration was also found to be highly dependent on temperature at which the catalyst was reduced.

Ruthenium catalysts prepared by a sol-gel method were also found in a very recent study to exhibit a promising sulphur resistance at low thiophene concentration (10 ppm) during for low temperature CPO of methane (at 550 ºC). However, at higher thiophene concentrations the catalyst deactivated due to the build-up of sulphur on the active sites [54].

1.6.5. Regeneration of Sulphur Poisoned Precious Metal Catalysts

Although the development of a sulphur tolerant catalyst is very important for many industrial applications, the ease at which the catalyst can regenerate following sulphur poisoning is also very crucial. Most of the current studies have examined the influence of SO_2 or H_2S on catalyst performance, but very few have actually examined the effectiveness of catalyst regeneration.

Deng and Nevell studied the sulphur poisoning and recovery of supported Pd, Rh, and Ir catalysts for methane oxidation. They reported that all of these catalysts were significantly affected by sulphur poisoning [55]. By using XPS they confirmed the formation of sulphate species and found that its concentrations decreased with increasing temperature.

The influence of sulphur poisoning (H_2S) and regeneration in reducing conditions on the activity for methane oxidation of Pt, Pd or Rh on alumina was examined by Nasri et al. [56]. The catalysts were either reduced in H_2 at 400 °C (fresh) or exposed to 100 ppm H_2S/900 ppm H_2 at 100 °C and regenerated in H_2 at 400 °C (regenerated). The reaction feed consisted of 4 vol.% CH_4 in air. For Pt and Rh catalysts, regenerated samples were found to be slightly more active than the fresh ones, while the reverse was observed for alumina supported palladium catalyst. The reaction studies showed the order of the activity for the freshly reduced catalysts to be Pd>Rh>Pt whilst the success of regeneration of the active catalyst by reduction followed the order Rh>Pt>Pd. However, in a separate study when the same authors investigated the ease of regeneration of the poisoned catalysts, following combustion of methane in the presence of 10 ppm S (as a synthetic odorant mixture) as a function of temperature over alumina supported precious metal catalysts, they observed a different behaviour [57]. Upon regeneration by reduction in hydrogen at 400 °C for 30 min all the catalysts recovered some activity, but in the case of platinum this was very slight. In contrast, the rhodium catalyst was regenerated beyond the activity observed in its freshly reduced state. Thus, the activity of the regenerated catalysts followed the order Rh>Pd>>Pt. This order is different from that observed in their initial study [56] where the success of catalyst

regeneration followed the order Rh>Pt>Pd. The difference in the order of regeneration is due to the different sulphation conditions adopted in the two studies, although there was no comment by the researchers regarding the discrepancy in the order of catalyst regeneration.

In the first study [56] the alumina supported precious metal catalysts were exposed to 100 ppm H_2S in a reducing atmosphere at only 100 °C, whilst in the second study [57], sulphur was added into a 4% CH_4/air mixture and the catalytic combustion of methane was measured as a function of temperature, starting from 230 °C up to about 600 °C. Under such conditions, the organo-sulphur compounds used in this study such as ethyl mercaptan, methyl mercaptan, as well as hydrogen sulphide, would be present as SO_2, which would then get oxidised over the precious metal to form the stable sulphate species on the catalyst. Since Pt has the highest activity for the oxidation of SO_2 to SO_3, this would lead to a greater sulphation of the alumina support with respect to Pd and Rh and, consequently, the catalyst would become more difficult to regenerate.

Increasing the reaction temperature has been shown to have a beneficial effect on the performance and recovery of catalysts when steam reforming sulphur-containing fuels [58,59]. Koningen and Sjostrom [58] observed no loss in catalyst performance with H_2S at concentrations as high as 2000 ppm when steam reforming gasified biomass at 800 °C using a nickel-based catalyst. Zheng et al. reported no loss in performance with a 2 wt% Rh/CeO_2–Al_2O_3 when reforming JP-8 containing 33 ppm of S at 800 °C [59]. Since H_2S was detected in the product stream, they attributed the observed sulphur tolerance to low adsorption of sulphur.

Ferrandon et al. [47] also observed a significant improvement in the sulphur tolerance of the catalyst with increasing reaction temperature during the steam reforming of sulphur containing fuels [47] as the stable S species decompose more readily at higher reaction temperatures, thus reducing the sulphur coverage on the catalyst surface.

1.7. Outline of the Thesis

The main objective of this work is to develop low cost rhodium based catalysts with high catalytic activity, good thermal durability and sulphur tolerance for the partial oxidation of

methane to syngas. From the above literature review it is clear that the choice of the support and active metal(s) is of great importance to the improvement of the sulphur-resistance of the catalyst. As a result, this work will focus on improving the sulphur tolerance of the Rh catalyst by: (i) modifying the structure of the carrier support and (ii) adding a second metal (bimetallic systems) without compromising the overall catalytic activity. This thesis can be divided into three main sections, as detailed below.

The first part (Chapter 3) deals with the nature of the support material by investigating the effect of SO_2 addition on the CPO of methane in the low to moderate temperature regime (300 to 800°C) over Rh catalysts supported on two different commercially available γ-Al_2O_3 supports stabilised either with SiO_2 or La_2O_3.

In the second part (Chapter 4) the effect of sulphur addition during the CPO of methane at high temperatures (>800ºC) and short contact times was investigated over Rh catalysts supported on either La_2O_3-Al_2O_3 or SiO_2-Al_2O_3 coated monolith samples. The effects of feed ratio, nitrogen dilution and sulphur precursors such as SO_2 and H_2S were also examined as well as the rate at which the catalysts regenerate following exposure to sulphur.

In the final part (Chapter 5), the CPO of methane at high temperatures was investigated over monometallic Rh and bimetallic Rh-Pt and Rh-Pd catalysts supported on La stabilised γ-Al_2O_3 coated monoliths with the aim of improving the sulphur tolerance of the catalyst whilst reducing its cost by decreasing the Rh content. Special attention was also given to identifying sites responsible for the loss in the catalytic activity in the presence of sulphur.

Finally, the overall conclusions are presented in Chapter 6.

References

[1] "Worldwide look at reserves and production", Oil & Gas Journal, 106 (December 22, 2008).

[2] J.R. Rostrup-Nielsen, Catal. Rev. 46 (2004) 247.

[3] X. Tong, L.H. Smith, P.L. McCarty, Biomass 21 (1990) 239.

[4] D.A. Hickman, L.D. Schmidt, Science 259 (1993) 343.

[5] M.C.J. Bradford, M.A. Vannice, Catal. Rev. Sci. Eng. 41 (1999) 1.

[6] S. Cimino, G. Landi, L. Lisi, G. Russo, Catal. Today 117 (2006) 454.

[7] A. Tsolakis, A. Megaritis, S.E. Golunski, Energy & Fuels 19 (2005) 744.

[8] A.M. Adris, B.B. Pruden, C.J. Lim, J.R. Grace. Can. J. Chem. Eng. 74 (1996) 177.

[9] D.A. Hickman, E. A. Haupfear, L. D. Schmidt, Catal. Lett. 17 (1993) 223.

[10] J.R. Salge, G.A. Deluga, L.D. Schmidt, J. Catal. 235 (2005) 69.

[11] O.V. Buyevskaya, D. Wolf, M. Baerns, Catal. Lett. 29 (1994) 249.

[12] D.A. Hickman, L. D. Schmidt, J. Catal. 138 (1992) 267.

[13] P.M. Torniainen, X. Chu, L. D. Schmidt, J. Catal. 146 (1994) 1.

[14] M. Prettre, Ch. Eichner, M. Perrin, Trans. Faraday Soc. 42 (1946) 335.

[15] W.J.M. Vermeiren, E. Blomsma, P.A. Jacobs, Catal. Today, 13 (1992) 427.

[16] B.C. Enger, R. Lodeng, A. Holmen, Appl. Catal. A: General 346 (2008) 1.

[17] K. Heitnes, J. Hofstad, B. Hoebink, A. Holmen and G. Marin, Catal. Today 40 (1998) 157.

[18] D.E. Grove, Platinum Metals Rev. 47 (1) (2003) 44.

[19] www.platinum.matthey.com/prices

[20] M. Shelef, K. Otto, N. C. Otto., Poisoning of Automotive Catalysts, Adv. Catal. 27 (1978) 311.

[21] T.J. Truex, Interaction of Sulfur with Automotive Catalysts and the Impact on Vehicle Emissions, SAE paper 011543 (1999).

[22] L.J. Hoyos, H. Praliaud, M. Primet, Appl. Catal. A: General 98 (1993) 125.

[23] M.V. Mathieu, M. Primet, Appl. Catal. 9 (1984) 361.

[24] K. Lampert, M. Shahjahan Kazi, RJ. Farrauto, Appl Catal B: Environ. 14 (1997) 211.

[25] T.C. Yu, H. Shaw, Appl. Catal. B: Environ. 18 (1998) 105.

[26] D.L. Mowery, M.S. Graboski, T.R. Ohno, R.L. McCormick, Appl. Catal. B: Environ. 21 (1999) 157.

[27] D.L. Mowery, R.L. McCormick, Appl. Catal. B: Environ. 34 (2001) 287.

[28] P. Gélin, L. Urfels, M. Primet, E. Tena, Catal. Today 83 (2003) 45.

[29] F. Arosio, S. Colussi, G. Groppi, A. Trovarelli, Catal. Today 117 (2006) 569.

[30] H.S. Gandhi, M. Shelef, Appl Catal. 77 (1991) 175.

[31] H.C, Yao, H.K. Stepien, H.S. Gandhi, J Catal. 67 (1981) 237.

[32] C.P. Hubbard, K. Otto, H.S. Gandhi, J Catal. 144 (1993) 484.

[33] A.F. Lee, K. Wilson, R.M. Lambert, C.P. Hubbard, R.G. Hurley, H.S. Gandhi, J. Catal. 184 (1999) 491.

[34] H.C, Yao, H.K. Stepien, H.S. Gandhi, J. Catal. 67 (1979) 231.

[35] K. Tomishige, T. Miyazawa, T. Kimura, K. Kunimori, N. Koizumi, M. Yamada, Appl. Catal. B. Environ. 60 (2005) 299.

[36] K. Tomishige, T. Miyazawa, T. Kimura, K. Kunimori, Catal. Communications, 6 (2005) 37.

[37] S.B. Brady, P.W. Farnell, M. Fowles, Johnson Matthey patent WO 2006/109095 A1.

[38] Q. Ming, P.M. Irving, Innovatek Canadian patent CA 2593413 A1 (2008).

[39] M. Krumpelt, S. Ahmed, R. Kumar, R. Doshi, U.S. Patent 6,110,861 (2000).

[40] J.J. Strohm, J. Zheng, C Song, J. Catal. 238 (2006) 309.

[41] A. Qi, S. Wang, C. Ni, D. Wu, International J. of Hydrogen Energy, 32 (2007) 981.

[42] J. Barbier, D. Duprez, Appl. Catal. B: Environ. 4 (1994) 105.

[43] K. Walter, O.V. Buyevskaya, D. Wolf, M. Baerns, Catal. Lett. 29 (1994) 261.

[44] D. Wang, O. Dewaele, A.M. Groote, G.F. Froment, J. Catal. 159 (1996) 418.

[45] S. Yokota, K. Okumura, M. Niwa, Appl. Catal. A: General 310 (2006) 122.

[46] A. Bitsch-Larsen, N.J. Degenstein, L.D. Schmidt, Appl. Catal. B: Environ. 78 (2008) 364.

[47] M. Ferrandon, J. Mawdsley and T. Krause, Appl. Catal. A: General 342 (2008) 69.

[48] A.M. Azad and M.J. Duran, Appl. Catal. A: General 330 (2007) 77.

[49] A.C. McCoy, M.J. Duran, A.M. Azad, S. Chattopadhyay and M.A. Abraham, Energy and Fuels, 21 (2007) 3513.

[50] R.K. Kaila, A. Gutiérrez, A.O.I. Krause, Appl. Catal. B: Environ. 84 (2008) 324.

[51] J.H. Bitter, K. Seshan, J.A. Lercher, J. Catal. 176 (1998) 93.

[52] R.K. Kaila, A. Gutierrez, R. Slioor, M. Kemell, M. Leskela, A.O.I. Krause, Appl. Catal. B: Environ. 84 (2008) 223.

[53] A. Shamsi, Catal. Today 139 (2009) 268.

[54] J. Requies,S. Rabe, F. Vogel, T.B. Truong, K. Filonova, V.L. Barrio, J.F. Cambra, M.B. Guemez, P.L. Arias, Catal. Today 143 (2009) 9.

[55] Y. Deng, T.G. Nevell, R.J. Ewen, C.L. Honeybourne, Appl. Catal. A: Gen. 102 (1993) 51.

[56] N.S. Nasri, J.M. Jones, A. Williams, Energy & Fuels, 12 (1998) 1130.

[57] J.M. Jones, V.A. Dupont, R. Brydson, D.J. Fullerton, N.S. Nasri, A.B. Ross, A.V.K. Westwood, Catal. Today, 81 (2003) 589.

[58] J. Koningen, K. Sjostrom, Ind. Eng. Chem. Res. 37 (1998) 341.

[59] J. Zheng, J.J. Strohm, C Song, X. Ma, L. Sun, Prep. Pap. Am. Chem. Soc. Div. Fuel Chem. 48 (2003) 750.

2. Experimental and Characterisation Techniques

2.1 Catalyst Preparation

2.1.1 Powder Catalysts

The incipient wetness impregnation method is the simplest and most direct method of deposition of the active components and was used to prepare all the powder catalysts. The object is to fill the pores with a solution of metal salt of sufficient concentration to give the correct metal loading. Because the amount of solution containing the precursor does not exceed the pore volume of the support, this method is also known as dry impregnation. The sample is then dried and calcined at a certain temperature. Drying is necessary to crystallize the salt on the pore surface. If not performed properly, this step can result in irregular and uneven concentration distributions. Calcination converts the salt to an oxide or metal.

Rhodium (1wt.%) catalysts supported on 3% La_2O_3-stabilised γ-Al_2O_3 and 10% SiO_2-Al_2O_3 materials (respectively type SCFa140-L3 and type Siralox 10-360 from Sasol) were prepared by the incipient wetness impregnation method using an aqueous solution of $Rh(NO_3)_3$ (Aldrich). The samples (hereafter labelled as R-LA and R-SA) were dried at 120 °C for 8 h and calcined in air at 550 °C for 2 h (referred to as fresh); part of the samples was further calcined in air at 800 °C for 4 h to investigate the effect of thermal ageing. A 1.0 wt.% Rh supported on α-Al_2O_3 powder (Sasol) was also prepared by the same procedure.

2.1.2 Monolith Catalysts

Commercial cordierite monoliths (Corning) with a cell density of 600 cpsi were cut in the shape of disks (L=10 mm, D=17mm) and washcoated with either La_2O_3-stabilised γ-Al_2O_3 or SiO_2-stabilised γ-Al_2O_3 using a modified dip-coating procedure [1]. The samples were dipped in a slurry (20 wt.% solid) of finely grounded La_2O_3 or SiO_2 stabilised γ-Al_2O_3 powder, diluted nitric acid solution and Disperal (Condea). Following each coating the excess slurry was removed by blowing air through the channels, after which the samples were dried at 120 °C and then calcined in air at 550 °C for 2 h. The process was repeated four times in order to achieve a washcoat loading of approximately 30% (w/w) with respect to the initial weight of the monolith sample, after which the samples were finally calcined in air at 800 °C for 3 h. Rhodium with a target loading of ~0.75 (w/w) with respect to the active washcoat layer was dispersed onto the

coated monoliths by repeated impregnation cycles using an aqueous solution of $Rh(NO_3)_3$. After each cycle the excess solution was removed by gently blowing with compressed air, the monolith samples were dried at 120 °C and then calcined in air at 550 °C for 2 h.

Bimetallic Rh-Pt and Rh-Pd catalysts were prepared by sequentially impregnating calcined Rh (loading 0.5%) monolith samples with a solution of H_2PtCl_6 or $Pd(NO_3)_2$. The target Rh/Pt and Rh/Pd weight ratio was 1 with a total metal loading of 1.0 wt%. Reference powder catalysts with same composition were prepared by incipient wetness impregnations of the γ-Al_2O_3 powders used as washcoat for the monoliths. All the catalysts were calcined in air at 550 °C for 3h.

2.2 Catalyst Testing

2.2.1 Powder Catalysts

For powder samples (250-300 μm) catalytic tests were carried out in a fixed bed quartz flow reactor using a standard feed of composition $CH_4/O_2/N_2$ = 1/0.6/98.4, at GHSV = 7.5 x 10^4 h^{-1} and total P = 1.2 atm. During temperature programmed experiments, the reactor was externally heated under feed mixture from 300°C to 800°C at 10°C min^{-1}. The sample temperature was measured using a K-type thermocouple inserted in the catalytic bed. The activity measurements over fresh samples were repeated twice in order to allow for catalyst activation under reaction at high temperature. Exit gases passed through a $CaCl_2$ water trap and analyzed continuously for H_2, CO, CO_2, CH_4 concentrations by a Hartmann & Braun Advance Optima analyser. Carbon balance was always closed within ±4%; O_2 conversion was estimated by closing mass balances for H and O. To examine the effects of sulphur in the reaction mixture, 20 ppm or 100 ppm SO_2 was added to the reactor feed at 500°C for 1 h. In fact it has been recently reported that S-poisoning impact on CPO performance of Rh-based catalysts is not dependent on the type of sulphur species introduced (i.e. thiophene, sulphur dioxide, benzothiophene, dibenzothiophene) but only on their quantity [27]. Before adding the SO_2, the partial oxidation reactions were allowed to stabilise 15 min at 500°C. Following sulphation at 500°C under reaction mixture, the sample was cooled down on bypass and the light-off ramp was repeated in order to determine the extent of catalyst deactivation. The sample was then cooled and the temperature programmed activity measurement was repeated in order to determine the extent of catalyst recovery from sulphur poisoning.

2.2.2 Monolith Catalysts

Methane CPO experiments were performed under autothermal conditions at high temperatures and short contact times in order to reproduce conditions of practical interest for self-sustained high temperature operation, using 600 cpsi cordierite monoliths in the shape of disks (L=10 mm, D=17mm). The catalytic monoliths were stacked between two inert radiation shields (mullite foams, 45 ppi) to reduce radiative heat losses from the glowing catalyst. An uncoated foam monolith (SiC foam, 10 ppi) was also located in the upstream of the front radiation shield to ensure complete mixing of the reactants. The catalytic monoliths were placed in a quartz reactor and tightly sealed in an alumino-silicate mat to prevent reactants from bypassing the catalyst and to reduce heat loss by conduction. The quartz reactor itself was wrapped with thick layer of ceramic wool and placed in an electric furnace, used only to light-off the reacting mixture.

Three K-type thermocouples (d = 0.5 mm), entering from the top of the reactor, were placed in the middle of the SiC foam used for distribution of reactants (T_1), middle of the front radiation shield (T_2) and in the middle of the central channel of the catalyst in close contact with its surface (T_{cat}). A fourth thermocouple (T_4, K-type with d = 1 mm) was used to measure the gas exit temperature downstream of the rear heat shield (Figure 2.1). High-purity gases (CH_4, O_2, N_2, H_2S 206 ppm in N_2 and SO_2 185 ppm in N_2) calibrated via 5 Brooks 5850-series mass-flow controllers were pre-mixed and fed to the reactor with total flow rates in the range of 85 to 135 l/h corresponding to a gas hourly space velocity (GHSV) between 5 and 8 x 10^4 h^{-1} (on the basis of honeycomb volume). Methane CPO Experiments were carried out under self-sustained pseudo-adiabatic conditions at fixed preheating temperature of 250°C and an overall reactor pressure of P=1.2 bar, at various CH_4/O_2 ratios (1.6 – 2) with either using simulated air as oxidant or oxygen with N_2 added to obtain a fixed dilution level (10 to 20% vol.%) of the feed. The catalytic monoliths were tested after stabilisation upon exposure to standard reacting conditions.

The impact of sulphur addition on the catalytic performance was investigated at CH_4/O_2 feed ratios in the range 1.6 – 2 under both transient and steady state conditions. The sulphur level was varied between 2 and 58 ppm on a molar basis with respect to the total flow of gases by partially substituting the N_2 flow in the feed with an equal flow of H_2S or SO_2 in N_2 mixtures. Catalytic light-off temperatures were determined by ramping-up the external furnace from

200°C under flow conditions at CH_4/O_2=1.8 with air, at different sulphur levels (H_2S from 0 to 20ppm vol.) over fresh, S-poisoned and regenerated (under reaction) catalysts.

For both powder and monolith samples methane conversion, yields and selectivities to CO and H_2 were calculated according to the definitions:

$$x_{CH_4} = 100 \cdot \left(1 - \frac{CH_4{}^{OUT}}{CH_4^{OUT} + CO_2^{OUT} + CO^{OUT}} \right)$$

$$Y_{CO} = 100 \cdot \left(\frac{CO^{OUT}}{CH_4^{OUT} + CO_2^{OUT} + CO^{OUT}} \right) \qquad S_{CO} = 100 \cdot \left(\frac{Y_{CO}}{x_{CH_4}} \right)$$

$$Y_{H_2} = \frac{100}{2} \cdot \left(\frac{H_2{}^{OUT}}{CH_4^{OUT} + CO_2^{OUT} + CO^{OUT}} \right) \qquad S_{H_2} = 100 \cdot 2 \cdot \left(\frac{Y_{H2}}{x_{CH_4}} \right)$$

based on the exit dry-gas mol fractions of CO, CO_2, CH_4 and H_2 independently measured by a continuous analyser with cross sensitivity correction (ABB Advance Optima). No other hydrocarbons except from methane were detected in the products, whereas O_2 was always completely converted (TCD-GC analysis). Carbon and hydrogen balances were always closed within ±1.5% and ±3.5 respectively. Sulphur species were not directly measured but preliminary TGA analysis excluded any significant sulphur capture effect by materials placed in the reactor before the catalyst (i.e. mullite and SiC foams) under representative operating conditions. Thermodynamic equilibrium calculations were performed using CHEMKIN 4.1.1 software [2] excluding carbon formation on the catalysts.

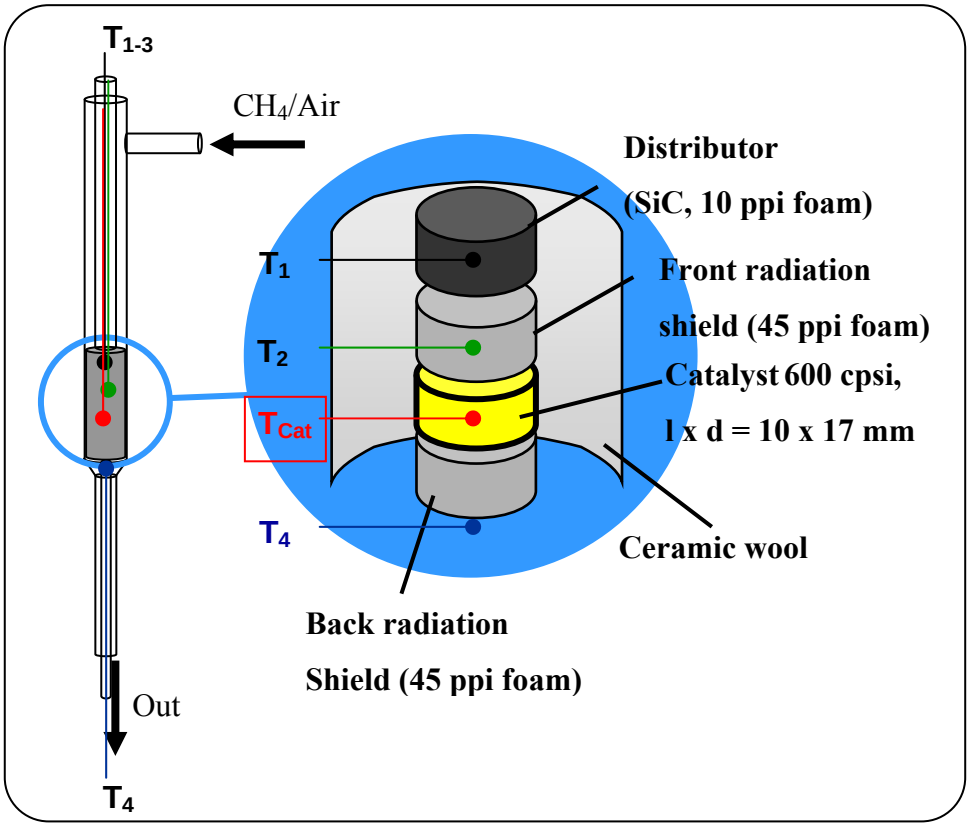

Figure 2.1*: Schematic representation of the positioning of the thermocouples inside the quartz reactor.*

2.3 Catalyst Characterisation Techniques

A variety of characterisation techniques were used to investigate the effect of sulphur poisoning over Rh-based catalysts. A brief description of the characterisation techniques utilised in this thesis is presented in the preceding sections.

2.3.1 Measurement of Surface Area

2.3.1.1 Total Surface Area

In order to measure the surface area of any porous material a reliable, non-specific method is needed. Physisorption is fairly material-independent in the sense that N_2 molecules at low temperature tend to form a monolayer which depends only on the size of the N_2 molecule, which is a known standard (16.2×10^{-20} m^2); the molecules pack together as closely as they can, independent of the substrate atomic structure. The BET stands for Brunauer, Emmett, and Teller, the three scientists who optimized the theory for measuring surface area.

In this thesis, physisorption measurements were carried out to characterize catalysts before and after thermal ageing at 800 ºC. Specific surface areas (m^2/g) and pore volumes were measured according to the standard BET method, as described above, by using a Quantachrome Autosorb 1-C. The sample of approximately 0.2 grams was first loaded into a round bottom sample tube, dried and degassed at 150 ºC under vacuum for about 3 hours and then cooled to liquid nitrogen temperature (-196 ºC) by immersing the sample tube into liquid nitrogen. Desorption followed adsorption in pore distribution measurements. The equipment automatically measured, recorded and calculated nitrogen adsorption at various pressures.

Actual metal content was quantitatively determined on selected fresh and used catalysts by inductively coupled plasma spectrometry (ICP) on an Agilent 7500 ICP-MS instrument, after microwave-assisted digestion of samples in nitric/hydrochloric acid solution.

2.3.1.2 Metal Surface Area

The active metal surface area and metal dispersion (i.e. fraction of active metal atoms on the catalyst surface) of the catalysts were determined by H_2 and CO-pulse chemisorption measurements using a Quantachrome Autosorb 1-C equipment. An exact amount of sample (ca. 0.1 grams) was weighed and placed into a round bottom sample tube stacked between two pieces of quartz wool. Prior to H_2 adsorption measurement, the sample was heated under He at 120 °C for 30 minutes and then reduced at 800°C under a flow of pure H_2. After 2 h at this temperature, the sample was evacuated and cooled under vacuum to 40 °C where H_2 or CO adsorption was performed. The gas irreversibly (strongly) adsorbed onto the active surface area was obtained by subtracting the total amount of hydrogen adsorbed (physical and chemical adsorption) and the amount of hydrogen that did not react with the active sites of the sample. The chemically adsorbed hydrogen was evaluated by carrying out a new series of H_2 injections following evacuation of the sample which removes physically adsorbed H_2. The whole operations were controlled automatically by a personal computer. The sequences of experiments were programmed in the provided program editor. Once a sample was loaded in the sample tube and all required gas cylinders were ready, the next step involved running the programme.

Similar procedures were also used for the CO chemisorption measurements. However, in the case of metal oxides (such as CeO_2, SiO_2 and Ce-Zr-mixed oxides) in contact with active

metals, adsorbed H_2-molecules can also diffuse from the active metal particles to the washcoat [3,4]. In fact in this study the use of H_2 chemisorption to determine metal dispersion was found not to be suitable, particularly in the case of R-SA sample: due to the occurrence of spillover phenomena, the experimental H/Rh values are much larger than those expected for true H_2 adsorption on the metal. The active metal particle size and dispersions were calculated by assuming the stoichiometric factor between a chemisorbed gas molecule and metal atoms to be 1:1. However, the stoichiometric ratio may depend on the precious metal particle size, a reason why caution should be exercised when comparing the dispersion values of different catalysts.

2.3.2 Temperature Programmed Techniques

Transient techniques such as temperature-programmed reduction and temperature-programmed desorption are most commonly used techniques for catalyst characterization and catalyst activity studies. These techniques can provide useful information on solid surfaces, their interactions with adsorbed gas molecules, and thermal stability of surface desorption states [5,6]. In these methods the catalyst is heated at a specific rate whilst monitoring the evolution of species from the surface back into the gas phase using a gas chromatography (GC) or mass spectroscopy (MS).

2.3.2.1 Temperature Programmed Reduction (TPR)

TPR gives information on the reducibility of metal oxides. Catalysts that are easier to reduce, i.e., in which metal oxides are bound less strongly to the support, show reduction peaks at lower temperatures. The reduction of a metal oxide MO_n by hydrogen to its metallic form is described by equation (2.1).

$$MO_n + nH_2 \longrightarrow M + nH_2O \qquad (2.1)$$

In this research, TPR experiments were carried out with Micrometrics TPD/TPR 2900 apparatus equipped with a TCD detector on both fresh and sulphur poisoned catalysts. The sample (100 mg), was heated at 10 °C min^{-1} between room temperature and 900 °C in flowing 2% H_2/Ar mixture (25 cm^3 min^{-1}). The exit gas from the reactor was passed through cold basic KOH trap to remove any water, CO_2 and acidic sulphur compounds such as H_2S or SO_2.

2.3.2.2 Temperature Programmed Desorption (TPD)

TPD is a method by which molecules are first adsorbed onto a surface at a fixed temperature. The temperature is then ramped up at a fixed rate and the desorption kinetics of the molecules from the surface are monitored by a mass spectrometer. The general technique of thermally desorbing adsorbates and measuring the change in partial pressure in the spectrometer is one of the most widely used experimental tools in surface science. The technique provides important information such as number of molecules adsorbed, number of different adsorption states, reaction order, activation energy for desorption and hence a measure of the adsorption strength. In this work, TPD experiments were performed using 200 mg of sulphated catalyst. The sample was heated from ambient to 1000°C under a He stream (25 cm^3 min^{-1}) at 10°C min^{-1}. The reaction products were monitored with a quadrupole mass spectrometer (QMS 200 - Pfeiffer).

2.3.3 Infrared Spectroscopy (IR)

Infrared spectroscopy (IR) undoubtedly represents one of the most important tools in catalysis research and has been a workhorse technique for materials analysis in the laboratory for many decades. An infrared spectrum represents a fingerprint of a sample with absorption peaks which correspond to the frequencies of vibrations between the bonds of the atoms making up the material. Because each different material is a unique combination of atoms, no two compounds produce the exact same infrared spectrum. Therefore, infrared spectroscopy can result in a positive identification (qualitative analysis) of every different kind of material. In addition, the size of the peaks in the spectrum can give an indication of the amount of material present. The two most frequently used IR techniques for catalyst characterization are transmission infrared and diffuse reflectance spectroscopy [7].

2.3.3.1 Fourier Transform IR (FTIR) Spectroscopy

Fourier transform IR (FTIR) spectroscopy has been the most commonly used method of IR spectroscopy, until recently. In this mode a small continuous reactor (i.e., IR cell) contains a very thin, pressed wafer of the catalyst (10-50 mg) through which IR radiation is directed. Some of the infrared radiation is absorbed by the sample and some of it is passed through (transmitted). The resulting spectrum represents the molecular absorption and transmission, creating a molecular fingerprint of the sample. This configuration, however, often leads to

internal and external transport limitations and completely uncharacterised gas mixing. In addition the technique is limited to the analysis of samples transparent to IR radiation and formed into the shape of a self-supported pellet which can prevent interacting of reactants with the catalysts. Some samples cannot be analyzed due to the lack of mechanical strength and/or transmission. This applies in particular to hydrated samples or certain catalysts used to combat automotive pollution. In order to ensure a deeper penetration of the incident beam and less specular reflection of the sample surface due to sample's strong absorption, the sample is usually diluted with a non absorbing material such as KBr before being pressed into a disk of a few tenths of a millimeter in thickness. However, due to its low melting point KBr diluted disks can not be used if the in-situ measurements are carried out at high temperatures (>400°C).

In this study FTIR measurements were carried out using a Perkin-Elmer Spectrum GX spectrometer in the transmission mode with a spectral resolution of 4 cm^{-1}. The stainless steel IR cell (Graseby Specac) is placed inside the sample compartment of a Perkin-Elmer infrared spectrometer equipped with a MIR-TGS detector where sample temperatures of up to 800 °C can be achieved. The IR cell reactor (Figure 2.2) is equipped with an internal cooling system, which prevents excessive heating of the FTIR sample compartment. Further heat shields on either side of the cell have been provided to avoid any heat radiation reaching the detector. The cell windows (ZnSe) and body are heated and controlled up to 200 °C. This prevents condensation of evolved materials and also allows the unit to be used as a high pressure heated gas cell when necessary. The cell temperature is controlled from a dedicated electronics unit where both sample and cell body temperature can be set using a simple controller with digital display of the temperature. Due to the minimum reactor internal volume, the absorbance of gas phase species is reduced. The IR cell is connected to a vacuum and high purity gases, controlled with Brooks 5850-MFC system where pre-mixed gases could be introduced into the reactor. A PC with a Perkin-Elmer's IR (PE-IR) spectroscopy software was used to record the FT-IR spectra collected by the spectrometer.

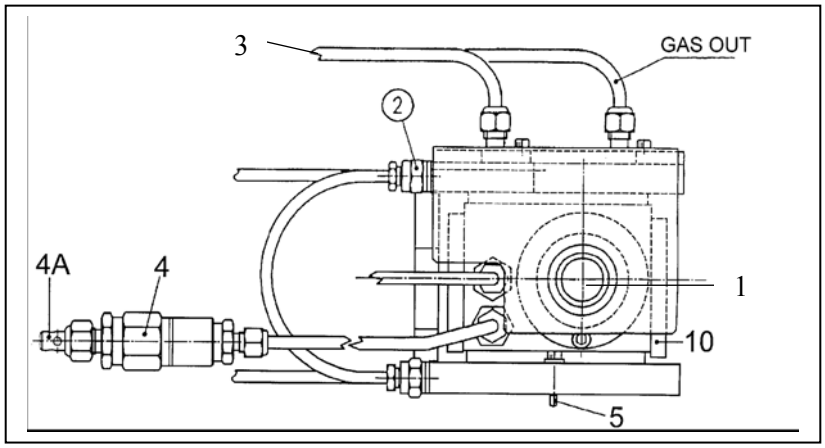

Figure 2.2: *Assembly of cell reactor in transmission mode: 1) ZnSe window; 2) water cooling connectors; 3) inlet gas; 4) pressure burst disc attachment; 5) cooling plates.*

For FT-IR measurements a 15-30 mg amount of sieved catalyst, <100 mesh, was pressed into self-supporting disk and placed in the holder in the IR cell. The disk was treated in the following way: (i) it was outgassed at 300 °C for 2 h and then cooled to room temperature where a background spectra of the sample was recorded; (ii) it was reduced at 300 °C with a 2% H_2/N_2 mixture for 2 hrs, after which time the cell was cooled down to room temperature and evacuated; (iii) CO was adsorbed at room temperature (2%CO/N_2 mixture, 100cm^3 min^{-1}) for 30 minutes and any excess CO removed by evacuation prior to recording the IR spectra. Spectra were also recorded under reaction conditions by dosing 100cm^3 min^{-1} of a CH_4/O_2/Ar mixture (2/1/97) at 300, 400 and 500 °C, respectively. To examine the effects of sulphur in the reaction mixture, 40 ppm SO_2 was added to the reactor feed. Before the SO_2 was added, the partial oxidation reactions were allowed to (30 min.) stabilise at 500 °C.

2.3.3.2 Diffuse Reflectance Infrared Fourier Transform Spectroscopy (DRIFTS)

Many of the problems associated with the transmission arrangement can be avoided by employing DRIFTS which was introduced by Hamadeh et a1. [8] for catalytic studies. Diffuse reflection (reflectance) is, by definition, that process in which the angle of reflection is different from the angle of incidence. In the diffuse reflectance mode, samples can be measured as loose powders, which can avoid the diffusion limitation associated with tightly pressed samples. DRIFTS is a common technique that collects and analyzes scattered IR energy. When a beam of infrared radiation impinges onto a fine particulate material it

essentially undergoes reflection in one of several ways. It can undergo reflection, refraction, scattering absorption to a varying degree, before re-emerging as diffuse reflectance (Figure 2.3).

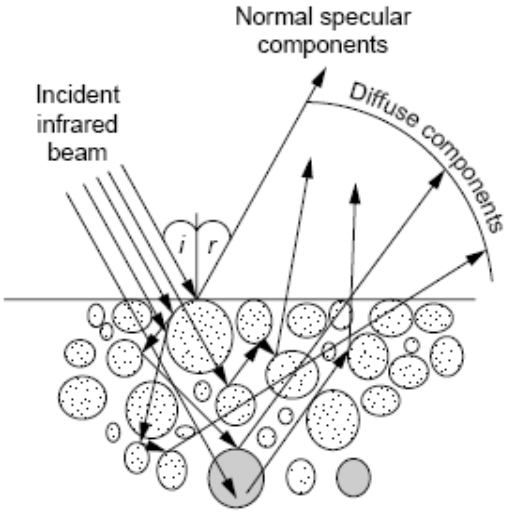

Figure 2.3: *Interaction of IR beam on a powdered sample [9]*.

First, the radiation can be reflected off the top surface of the particles, at the angle of incidence, without penetrating the particles. This top surface reflection represents the true specular reflection and is a function of the refractive index and the absorptivity of the sample. Second, the beam can undergo multiple reflections off particle surfaces, all without penetrating into the particle. After these multiple reflections, the resulting beam emerges from the sample at a random angle relative to the incident beam. This reflection mode is known as diffuse specular reflectance and is a complex of the refractive index of the sample. The third mode of interaction, true diffuse reflectance, results from the incident radiation penetrating the surface of the sample and reflecting off the particles in the material. Due to its interaction with the surface, the beam contains information about the absorption characteristics of the sample material. However, this diffuse reflection is optically indistinguishable from diffuse specular reflection. Factors affecting whether reflectance is either diffuse or specular are dependent on the nature of the material and the orientation of the particles in the powdered sample. Most materials reflect both diffusely and specularly which is known as a mixed reflection. The back reflected, diffusely scattered light (some of which is absorbed by the sample) is then collected by a large aperture optic

and then directed on to the detector. Only the part of the beam that is scattered within a sample and returned to the surface is considered to be diffuse reflection.

Important factors which exert significant influence on the spectral quality for diffuse reflectance are particle size and packing. Reducing the size of the sample particles reduces the contribution of reflection from the surface resulting in an improvement in the quality of spectra (narrow bandwidths and better relative intensity). The sample should also be loosely but evenly packed in the cup to maximize IR beam penetration and minimize spectral distortions. DRIFTS offers a number of advantages over transmission, including: very high sensitivity (down to low ppm levels), ability to analyse most non-reflective materials including highly opaque or weakly absorbing materials and most importantly minimal or no sample preparation is required. For strongly scattering or absorbing particles, DRIFTS has fewer limitations than transmission mode. Thus dilution is not required. This is a huge advantage when trying to analyze samples under reaction conditions, where undiluted samples are preferred. Furthermore, spectra can be recorded and changes can be analyzed at elevated temperature and/or under pressure which makes it an ideal choice for studying catalytic partial oxidation on supported catalysts.

In this work the DRIFTS study were carried out in the unit shown in Figure 2.4, using a PIKE Diffuse-IR cell equipped with a heat chamber which allows the sample to be heated from room temperature up to 900°C within the chamber. Any temperature can be set between this range and can be controlled automatically with the controller. The environment within the chamber can be inert gas, vacuum, reaction mixture etc. in order to create various measurement conditions. Inserting and changing samples is easily accomplished by opening and closing the screw cap which holds the ZnSe window. The cell is also equipped with an internal cooling system, which prevents excessive heating of the sample compartment. Samples can be loaded into either a ceramic or stainless steel sample cup. Reactants are introduced in the cell through a 1-mm (i.d.) pipeline and released close to the sample.

The accessory's optical design is optimized to efficiently collect diffuse radiation generated by the sample and minimize the effects of the specular radiation component. The heart of the Diffuse reflectance is a large, monolithic ellipsoidal reflector (**E**) which permits elimination

of most of the specular component. The initial planar mirror, (**1**) redirects the IR beam in the plane of incidence. The second planar mirror, (**2**) directs the beam to an optimal focusing location on a fixed off-axis ellipsoidal mirror, (**E1**), which focuses the incident beam on to the sample, while the second (fixed) ellipsoidal mirror, (**E2**), collects the radiation diffusely reflected by the sample and focuses it upon the third planar mirror, (**3**)**,** where upon it is redirected to a fourth planar mirror (**4**), which directs the radiation to the detector. Furthermore, the height of the planar mirrors may be adjusted using an alignment screw to maximize the through-put energy.

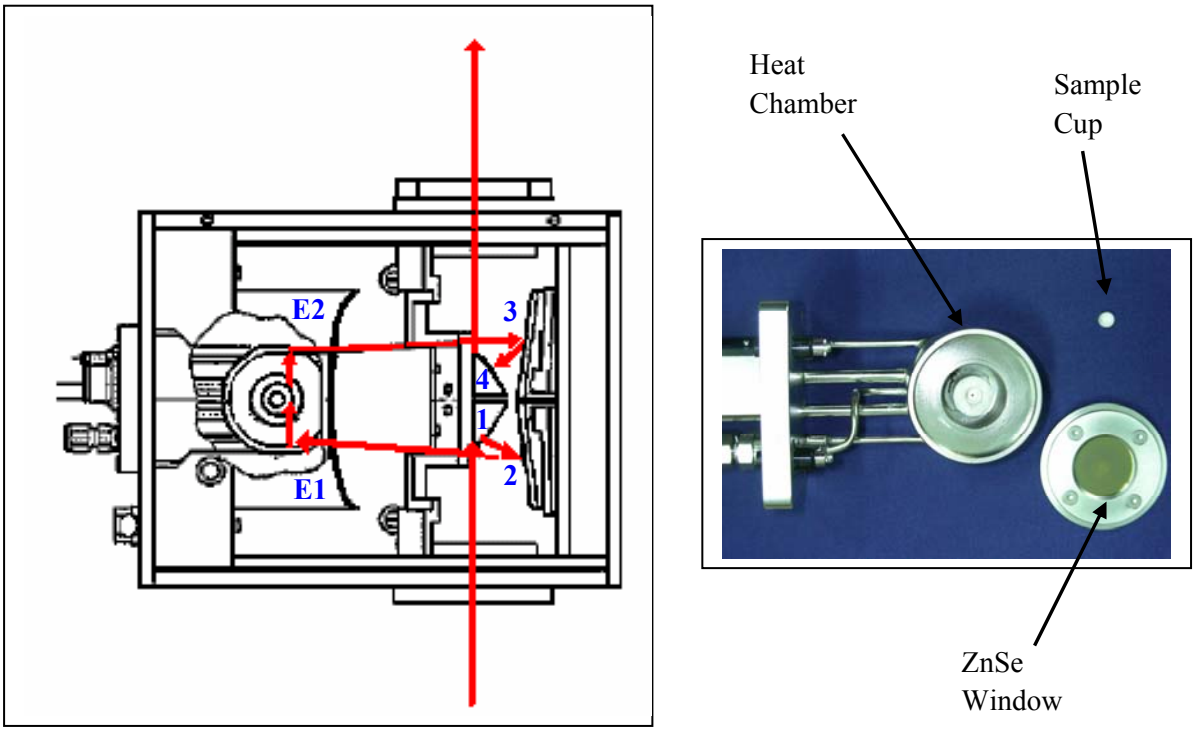

Figure 2.4: *Schematic representation of the Diffuse Reflectance attachment and the heat chamber.*

The nature of metal species was investigated by diffuse reflectance infrared Fourier transform spectroscopy (DRIFTS) using CO as a probe molecule. DRIFTS experiments were performed on a Perkin Elmer Spectrum GX spectrometer with a spectral resolution of 4 cm^{-1} and averaged over 50 scans. For each experiment approximately 0.03g of finely ground powder sample was placed into the ceramic cup of a commercial high-temperature Pike DRIFT cell equipped with a ZnSe window and connected to mass flow controlled gas lines. The sample was then treated in the following way: (i) prior to the experiments the sample was reduced with a 2% H_2/N_2 mixture for 1 hour at 800 °C and then cooled down to room temperature under the same mixture. The sample was purged with Ar for about 15 min before a

background spectrum was recorded; (ii) CO was adsorbed at room temperature (2%CO/N_2 mixture, 100 cm^3 min^{-1}) for 30 minutes and any excess CO was removed by flushing with Ar (100cm^3 min^{-1}) prior to recording the IR spectra (iii) the sample was then flushed with Ar at 800 °C for 15 min followed by exposure to 20ppm H_2S/2%H_2-N_2 (100 cm^3 min^{-1}) reaction mixture for 30 min; (iv) after sulphation at 800 °C, the sample was cooled down to room temperature under reaction mixture followed by purging with Ar for approximately 15 min before CO adsorption. All spectra were ratioed against the background spectra collected on the adsorbate-free sample at room temperature. The effect of regeneration of S poisoned catalyst by reduction under a mixture of 2%H_2/N_2 at high temperatures was also investigated.

References

[1] S. Cimino, G. Landi, L. Lisi, G. Russo, Catal. Today 117 (2006) 454-461.

[2] R.J Kee, F.M. Rupley, J.A. Miller, M.E. Coltrin, J.F. Grcar, E. Meeks, H.K. Moffat, A.E. Lutz, G. Dixon-Lewis, M.D. Smooke, J. Warnatz, G.H. Evans, R.S. Larson, R.E. Mitchell, L.R. Petzold, W.C Reynolds, M. Caracotsios, W.E. Stewart, P. Glarborg, C. Wang, O. Adigun, Chemkin Collection, Release 4.0, Reaction Design, Inc, San Diego, CA, (2004).

[3] S. Bernal, J.J. Calvino, G.A. Cifredo, J.M Gatica, J.A. Perez, J. Chem. Soc. Faraday Trans. 89 (1993) 3499.

[4] P. Fornasiero, R. Di Monte, G.R. Rao, J. Kašpar, S. Trovarelli, J. Catal. 151 (1995) 168.

[5] J.L. Falconer, J.A. Schwarz, Catal. Rev.Sci. Eng. 25 (1983) 141.

[6] F. Salvador, M.D. Merchán, Journal of Thermal Analysis and Calorimetry 51 (1998) 383.

[7] J.A. Lercher, C. Grundling, G. Eder-Mirth, Catal. Today 27 (1996) 353.

[8] I. M. Hamadeh, D. King, P.R. Griffiths, J. Catal. 88 (1984) 264.

[9] T. Armaroli, T. Bécuel, S. Gautier, Oil & Gas Science and Technology – Rev. 59 (2004) 215.

3. The Effect of Support on Sulphur Tolerance of Rh Based Catalysts for Methane Partial Oxidation

3.1 Introduction

The presence of sulphur containing compounds, naturally occurring in natural gas or added as odorants, can adversely affect the performance of noble metals based catalysts for the partial oxidation of methane to syngas. The aim of this chapter is to investigate the influence of the support material on the sulphur poisoning tolerance of rhodium catalysts for the partial oxidation of methane in the low to moderate temperature regime (300 to 800 °C). The effect of SO_2 addition on the CPO of methane has been investigated on Rh catalysts supported on two different commercially available γ-alumina materials stabilized either with 3% La_2O_3 or 10% SiO_2. The latter is an amorphous silica-doped alumina, the surface of which is enriched with silica.

3.2 Experimental Procedure

The Rh/La_2O_3-Al_2O_3 (R-LA) and Rh/SiO_2-Al_2O_3 (R-SA) were prepared by the incipient wetness impregnation method as describe in Chapter 2.1.1. The catalytic tests were carried out on powder samples as described in Chapter 2.2.1. Catalysts were characterised by techniques described in Chapter 2.3.

3.3 Results and Discussion

3.3.1 Characterisation

Table 3.1 illustrates catalysts denomination, metal loading, total surface areas and their dispersions measured by H_2 chemisorption, after calcination at 550 °C.

Name	Commercial Support	Stabilizer (w./w.%)	Rh loading (w./w.%)		Surface area (m^2/g)		Dispersion (%)
	Sasol		nominal	ICP	550°C	800°C	Fresh
R-LA	SCFa140-L3	3% La_2O_3	1.0	0.96	150	133	61
R-SA	Siralox 10-360	10% SiO_2	1.0	1.05	312	259	118

Table 3.1: *Characteristics of La_2O_3 and SiO_2 stabilised alumina supported Rh catalysts.*

The actual noble metal loading is close to the nominal one for both catalysts. Reduction of surface area is observed upon calcinations at 800 °C for both samples although it is proportionally less pronounced for R-LA due to the stronger inhibiting effect of surface lanthanum oxide towards γ-alumina phase transition. Nevertheless the R-SA catalyst still retained a specific surface area which was almost twice that of R-LA sample following thermal ageing at 800 °C. The high metal dispersion values obtained (>100%) for R-SA sample is related to the spillover phenomenon, as discussed in Chapter 2.3.

Due to the spillover effect of H_2, Rh dispersions were measured by using CO chemisorption method. However, the use of carbon monoxide adsorption for the metal surface area estimation over Rh based catalysts should also be approached with caution, as the chemisorption stoichiometry for CO varies due to multiple types of chemisorption (i.e., linear, bridged or dicarbonyl). In this study a ratio of one CO per Rh was assumed to be acceptable for calculating the Rh dispersion, since the CO uptake per Rh for both fresh samples was observed to be approximately 1, unlike the H_2 chemisorption experiments. Table 3.2 lists the metal dispersions of Rh catalysts measured by both CO and H_2 chemisorption methods. Comparing the two supports, for the thermally aged samples, the Rh dispersion was significantly higher on La-Al_2O_3 than on SiO_2- Al_2O_3, which is consistent with other studies that have reported that the addition of lanthanum to alumina increases the dispersion of metals [1].

Catalyst	Ageing in air	CO Chemisorption			H_2 Chemisorp. Dispersion (%)
		Particle size (nm)	CO Ads. (μmol/g)	Dispersion (%)	
R-LA	550°C	1.05	102	105	61
	800°C	2.6	41	42	-
R-SA	550°C	1.03	103	106	118
	800°C	5.1	21	22	-

Table 3.2: *Comparison of the Rh dispersion measured by CO and H_2 chemisorption methods. The metal dispersions were calculated by assuming a Rh/H = 1 and Rh/CO = 1 stoichiometry.*

TPR experiments were conducted to investigate the reducibility of rhodium oxide supported on La_2O_3 or SiO_2 stabilised aluminas. Figure 3.1 illustrates the reduction profiles of the fresh and thermally aged catalysts while the corresponding amount of hydrogen taken up by the sample is reported in Table 3.3.

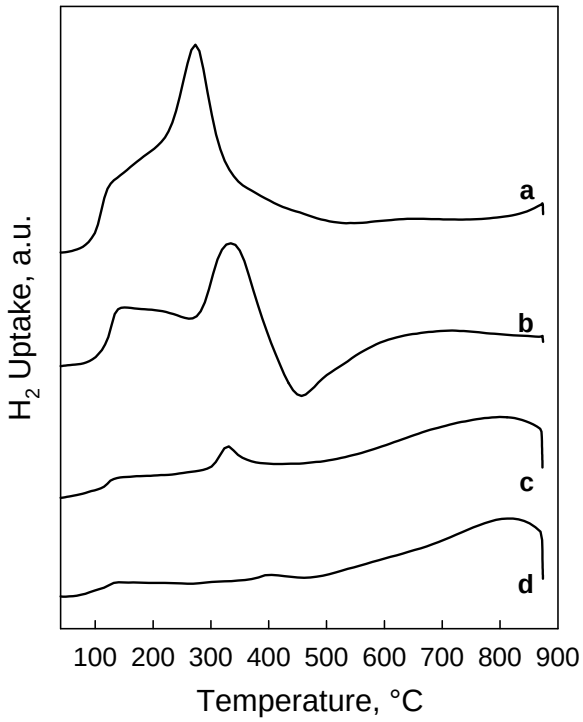

Figure 3.1: *H_2-TPR traces of R-LA (a,c) and R-SA (b, d) catalysts after calcination in air at 550 °C (a, b) and thermal ageing in air at 800 °C (c, d).*

Fresh catalysts calcined at 550 °C show a shoulder and a peak maximum at 125 °C and 270 °C for R-LA and 130 °C and 335 °C for R-SA, which would indicate the existence of two different states of oxidised rhodium on the sample. The lower temperature TPR peak (125 °C) has previously been attributed [1,2] to the reduction of rhodium oxide particles having no interaction with the support, while the higher temperature peak, accounting for significantly more hydrogen uptake, could be related to the reduction of Rh which has interacted strongly with the alumina.

The hydrogen consumption for the R-LA catalyst corresponds to the full reduction of Rh^{3+} to Rh^0. Interestingly the TPR profile of the fresh R-SA catalyst passes through a negative between 400 and 500 °C, probably caused by some H_2 desorption. The experiment was repeated twice and the same profile was obtained. The desorption of hydrogen from the sample could explain the very high H/Rh ratio obtained for the R-SA catalyst during H_2 chemisorption experiments. This finding agrees fairly well with the results obtained from the study of H_2 chemisorption on a ceria-supported rhodium catalyst [3] where it was shown that at room temperature, in the presence of highly dispersed Rh, ceria chemisorbs large amounts of hydrogen by the spillover

process. At higher temperature the reverse reaction i.e., the so-called back-spillover process can occur.

Thermal aging at 800 °C for 4 h in air produces Rh species which are more difficult to reduce, thereby causing a broadening of the reduction peak and a shift in the peak maximum to much higher temperature (around 800 °C for both samples). The increase in the reduction temperature is possibly caused by the formation of surface spinel type $Rh(AlO_2)y$ species, which are reduced at high temperatures [4]. A large decrease in the amount of surface rhodium in Rh/Al_2O_3 catalyst has been reported after high temperature ageing in an oxidising atmosphere due to a strong interaction between Rh_2O_3 and the support that can lead to severe catalyst deactivation [1,2]. However, the integration of the TPR profile of the thermally aged catalysts reveals only a limited decrease of accessible Rh_2O_3 in the sample (Table 3.3). This would then argue against any significant deep penetration of Rh into the alumina under the conditions of this study. In particular for the R-LA catalyst this could be due to the presence of La^{3+} in the γ-Al_2O_3 which can block the defect sites in the surface of the alumina thus reducing the interaction of Rh with the support [2,5]. The aged R-SA catalyst showed a very similar TPR trace, indicating comparable metal interaction with the support, which also led to the disappearance of the spillover effect. In addition the aged R-SA sample showed a slightly more pronounced decrease in the amount of hydrogen uptake with respect to the fresh catalyst.

Figure 3.2 shows a comparison of the H_2 uptake profiles for the fresh and sulphated catalysts and Table 3.3 illustrates a summary of the amount of hydrogen consumed before and after S ageing. For sulphated R-LA sample it can be seen that the initial part of the reduction profile closely follows the trace of the fresh oxidised sample up to approximately 300 °C, indicating that Rh_2O_3 species are largely unaffected. Indeed integration of the H_2 uptake profile up to this temperature accounts for the total reduction of Rh^{+3} to Rh^0 (Table 3.3). The remaining H_2 consumption is characterized by an intense peak centered at 535 °C with a shoulder at 400 °C, which can be attributed to the reduction of bulk $Al_2(SO_4)_3$ species which is completed by 800 °C. H_2-TPR of sulphated Rh supported on pure γ-alumina displayed a similar profile. In fact the reduction of lanthanum sulphates/oxysulphates which may be formed during sulphation would occur in the same temperature range [6], and could be therefore masked by the larger contribution of the $Al_2(SO_4)_3$ reduction.

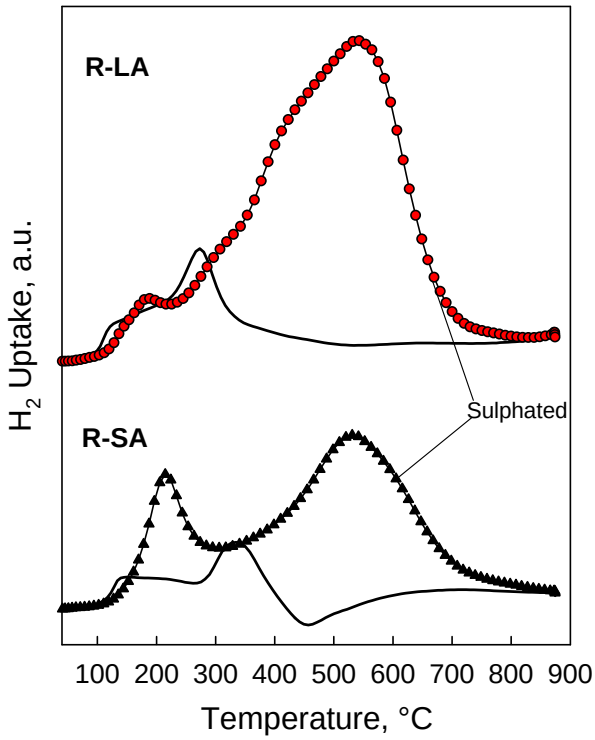

Figure 3.2: *H_2-TPR profiles of S aged Rh catalysts compared with TPR profiles of the corresponding fresh samples.*

Catalyst	H_2 Uptake mmoles H_2/g		H_2 Uptake - S aged mmoles H_2/g	
	550°C	800°C	Up to 310°C	Total
R-LA	0.16	0.15	0.15	1.0
R-SA	0.13	0.11	0.15	0.6

Table 3.3: *TPR analysis of the R-LA and R-SA samples before and after S ageing (100 ppm SO_2 in air at 300 °C for 2 h).*

The TPR profile of the S aged R-SA catalyst shows two distinct peaks of comparable maximum values respectively centered at 220 °C and 535 °C. The first peak can be assigned to the reduction of Rh^{+3} species since H_2 uptake up to 300 °C accounts once again for the total reduction of Rh^{+3} to metallic Rh^0 (Table 33.). However the presence of a single and well defined peak centered at 220 °C instead of a more complex profile with a maximum at 330 °C recorded on the fresh oxidized catalyst, suggests the presence of Rh^{+3} sulphated species rather than only Rh_2O_3. The formation of $Rh_2(SO_4)_3$ species has been reported for the SiO_2 supported Rh sample treated in SO_2/air mixtures [7].

With regards to the second peak at 535 °C ascribed to the reduction of bulk $Al_2(SO_4)_3$, the R-SA catalyst stores approximately half as much S than the corresponding R-LA sample (Table 3.3). The Siralox material used as a support in this study is an amorphous silica-doped alumina, the surface of which is enriched with silica [8], hence reducing the amount of surface alumina which is susceptible to sulphation. Under oxidizing conditions sulphur dioxide is readily oxidized over the noble metal to form sulphur trioxide, which can then spill-over to the carrier and further react with alumina to form aluminum sulphate species, thus restoring the Rh_2O_3 sites [7]. However in the case of pure silica or silica type materials the extent of sulphur storage is significantly reduced [7].

He-TPD experiments were also carried out to compare desorption temperature for the S aged R-LA and R-SA catalysts: the corresponding Mass Spectrometry (MS) signals are shown in Figure 3.3. The only detected MS-signal which was directly attributed to desorption of sulphur compounds was that of SO_2 (ms 64), whereas no signal for H_2S (ms 34) or SO_3 (ms 80) was detected. The same mass of catalyst was used in all experiments so the larger peak areas indicate larger amount of desorbing species per unit mass. On the R-LA catalyst SO_2 evolution profile is characterized by a small peak at approximately 600 °C and a sharp peak at ca. 950 °C. It is of interest to note that the intense SO_2 peak at ca. 950 °C is accompanied by a simultaneous large desorption of O_2 which can be attributed to the decomposition of bulk $Al_2(SO_4)_3$. On the other hand, the SO_2 desorption peak at 600 °C, accompanied by a much lower O_2 desorption, can be assigned to the decomposition of sulphate species (SO_x) on the Rh surface or at the metal support interface which can result in the oxidation of Rh metal particles. Similar TPD profiles were also obtained on Rh/Al_2O_3 only catalyst, thus excluding any major contribution from the La_2O_3 stabilizer.

The R-SA catalyst stores significantly less sulphur than the corresponding R-LA sample: the two main SO_2 desorption peaks have similar areas and a further small peak appears around 400°C, implying that a significant reduction in the formation of bulk $Al_2(SO_4)_3$ due to the presence of surface SiO_2 is accompanied by a larger accumulation of SO_x species on or close to the noble metal, which is in good agreement with the results obtained in TPR experiments.

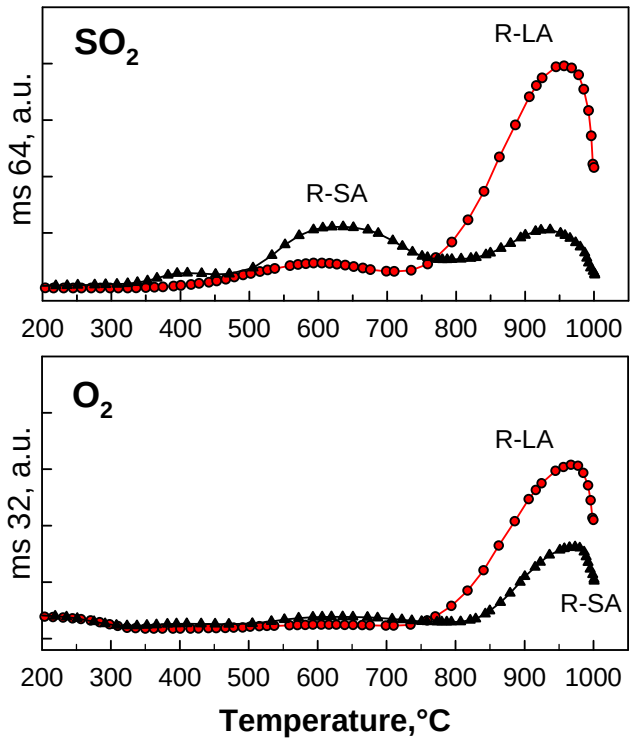

Figure 3.3: *Mass Spec. traces for SO_2 and O_2 during He-TPD on Rh catalysts following S ageing (100ppm SO_2 in air at 300 °C).*

FTIR experiments were also carried out to investigate the effect of SO_2 addition to the reaction mixture on Rh sites. The FT-IR spectrum of CO adsorbed at room temperature on a fresh R-LA catalyst pre-reduced in situ under H_2 at 300 °C is shown in Figure 3.4a. The dominant features of this spectrum are the doublet bands at 2089 and 2016 cm^{-1} corresponding to gem-dicarbonyl species on isolated Rh atoms [9] generated by the reaction of CO with Rh particles and hydroxyl groups of the support. The presence of these bands is related to highly dispersed Rh metal particles on the catalyst surface [9]. Similar bands were also observed for the R-SA sample, in agreement with other authors who did not detect any shift of gem-dicarbonyl bands for differently supported Rh samples [10].

Following CO evacuation at 300 °C, the sample was exposed to a flow of simulated CPO feed ($CH_4/O_2/Ar$ = 2/1/97, volume ratio) at 300, 400 and 500 °C, respectively. The reaction at each temperature was allowed to stabilize (30 min) prior to recording the IR spectra. The occurrence of the partial oxidation reaction at T≥400 °C was verified by the decrease in the intensity of the methyl band at 3016 cm^{-1} and a concomitant increase in the adsorbed CO band at 2017 cm^{-1}

assigned to carbonyl hydride on reduced Rh [11] (Figure 3.4 b-d). Similar results were also obtained for the R-SA catalyst.

The rate of deactivation of the catalysts in the presence of 40 ppm SO_2 in the feed stream was then measured at 500 °C as a function of time on stream (Figure 3.4 e,f). The detrimental effect of SO_2 in the reaction mixture on the catalytic activity of R-LA started to appear after approximately 50 min and was evident after 120 min as confirmed by the increase in the intensity of the methyl band at 3016 cm^{-1} and a simultaneous decrease in the adsorbed CO band at 2017 cm^{-1} with increasing exposure to gas phase SO_2. The rate of loss in the intensity of adsorbed CO band on the R-SA catalyst (not shown) was however much faster (started after about 30 min) indicating a lower tolerance of Rh to sulphur poisoning when supported on a less sulphating support. However, the presence of sulphate species, characterized by bands in the range 1045-1360 cm^{-1} [12] could not be detected, either due to low surface concentration and/or to limited sensitivity of the DTGS (Deuterated TriGlycerine Sulphate) detector used in this study.

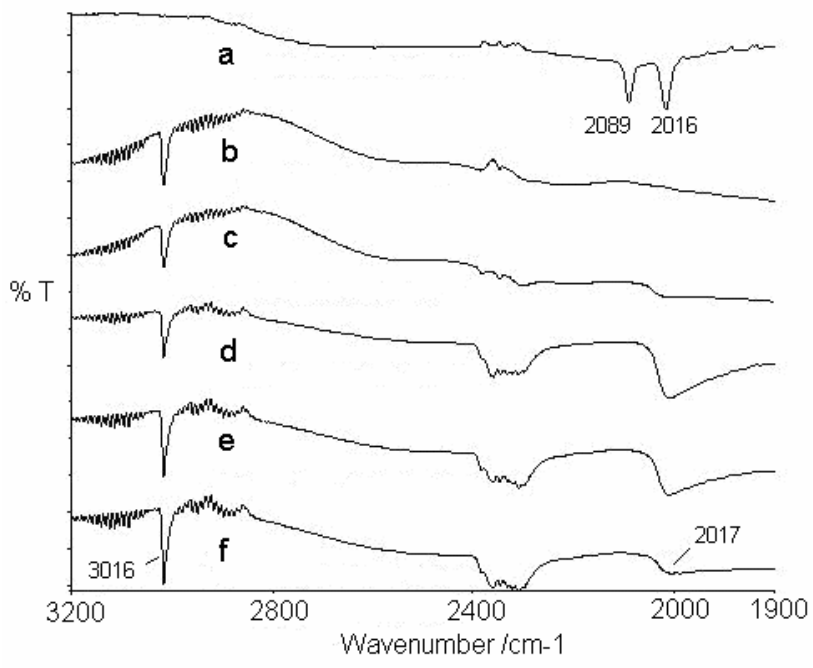

Figure 3.4: *FT-IR spectra of fresh R-LA: a) CO adsorption at room temperature after pre-reduction with H_2 at 300 °C. FT-IR spectra under CPO reaction ($CH_4/O_2/Ar=2/1/97$) at b) 300 °C, c) 400 °C, d) 500 °C and during progressive exposure to 40 ppm SO_2 under reaction at 500 °C: e) 60min, f) 120min.*

In conjunction with FTIR spectroscopy, CO adsorption at room temperature was used as a probe to investigate the nature of the metal species present on the catalyst. Figure 3.5 illustrates the CO spectra obtained at room temperature over a fresh R-LA catalyst following: a) reduction at 300 °C, b) partial oxidation test at 500 °C and c) partial oxidation test (for 2 h) at 500 °C in the presence of 40 ppm SO_2.

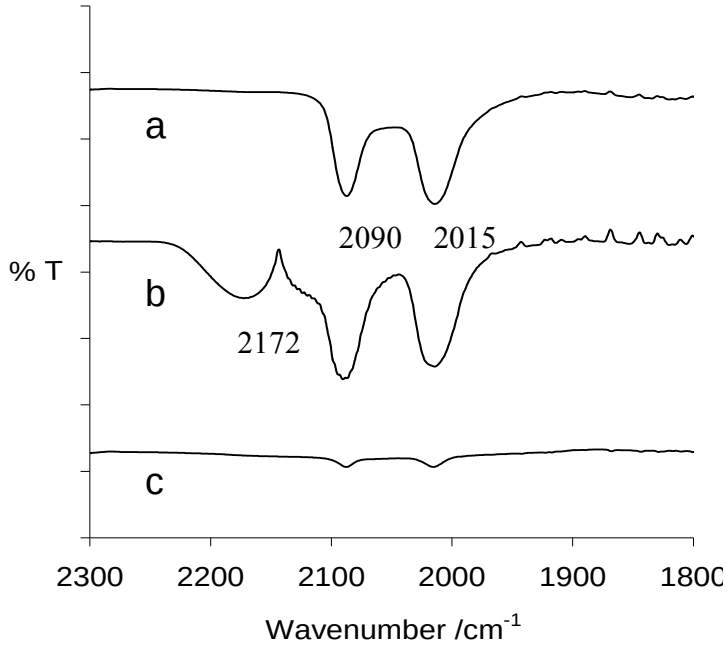

Figure 3.5: *FT-IR spectra of CO adsorption at room temperature over R-LA catalyst following: a) reduction of fresh catalyst at 300 °C, b) treatment with reaction mixture at 500 °C for 30 min ($CH_4/O_2/Ar=2/1/97$), c) partial oxidation test at 500 °C in the presence of 40 ppm SO_2 for 120 min.*

The CO spectrum obtained at room temperature, after exposure to the reaction mixture at 500 °C (Figure 3.5b), is quite similar to the freshly reduced sample (Figure 3.5a) showing the typical gem-dicarbonyl CO species associated with highly dispersed metallic Rh sites. The higher intensity of the gem-dicarbonyl bands is most probably caused by further reduction of Rh particles during the partial oxidation reaction at 500 °C, which agrees with the enhancement in activity reported on Rh catalysts after exposure to high temperature CPO reaction conditions, also observed on our catalysts following the first ramp during the temperature programmed reaction tests (see *activity measurements-3.3.2*). The band at 2172 cm^{-1} is assigned to the gas phase CO [13], which was already observed prior to evacuating the IR cell; this would imply an insufficient time of the evacuation process. However, exposure to the reaction mixture containing SO_2 at 500 °C, resulted in a significant decrease in the intensity of the doublet bands of adsorbed CO (Figure 3.5c). The decrease in intensity could either be due to the blockage or

the oxidation of Rh sites by sulphur. We tend to favour the latter, since during the activity measurement following sulphation the initial part of the catalytic activity was very similar to that of the fresh oxidised sample.

The spectra of CO adsorbed at room temperature over a R-SA catalyst (not shown) followed a similar behaviour to those obtained over the R-LA catalyst. Both catalysts showed some residual Rh^0 species on their surface which are responsible for the low CPO activity measured at the end of the sulphation period over both samples. The presence of metallic Rh species could be related to a partial regeneration of the catalyst during cool down in Ar from 500 °C to room temperature following exposure to the SO_2 reaction mixture.

3.3.2 Activity Measurement

Figure 3.6 and Figure 3.7 illustrate the methane conversion as a function of catalyst temperature over R-LA and R-SA catalysts, respectively. During the initial ramp over the fresh oxidised catalysts, methane conversion increased slowly with temperature up to about 400 °C where there was a sudden light-off, followed by a more steady increase in methane conversion (Ramp 1). The steep increase in conversion occurs when some of the metal oxide is reduced to metal allowing methane to dissociate more readily on the surface. Therefore, when the catalyst is exposed to the reaction condition at high temperatures (800 °C), reduced or partially reduced Rh sites were obtained which resulted in methane conversion at lower temperatures, as seen in Ramp 2.

In literature somewhat divergent results regarding the active state of rhodium for the partial oxidation of methane have been reported. While some researchers claim that metallic Rh sites are the most active [14,15], others propose a more complex structure with Rh being present on the surface at different oxidation states. Heitnes et al. [15] found that Rh_2O_3 shows low activity for syngas production and total oxidation products are mainly formed. The formation of syngas increased with time on stream since Rh reduction occurred under reaction conditions. The importance of partially oxidized Rh species for methane dissociation, which often is considered to be the rate-limiting step for methane oxidation reactions, has been recognized [16,17]. The increased methane dissociation over the partially oxidised rhodium state ($Rh^{\delta+}$) is related to its high ability to accept σ electrons of methane [17].

Following catalyst activation (Ramp 2) the samples were cooled down under reaction mixture to 500 °C where the effect of sulphur addition to the reaction mixture was investigated. Figure 3.8 illustrates the effect of addition of 20 ppm SO_2 at 500 °C for 1 h (exposures to *ca.* 4 mg S/g Cat.) in the reaction mixture on methane concentration as a function of time on stream over R-LA and R-SA catalysts. The partial oxidation reaction of methane was allowed to reach a steady state at 500 °C (15 min) before the addition of 20 ppm SO_2 into the feed stream. Before the addition of SO_2 both samples show similar methane (75-77%) and complete oxygen conversion levels; the corresponding measured selectivities to H_2 and CO are above 95% and 75% respectively, on both catalysts, with a H_2 to CO molar ratio of about 2.6. This ratio is lower than the equilibrium value at 500 °C (= 4.7), which indirectly indicates the absence of solid carbon formation predicted by thermodynamics up to 575 °C; moreover it suggests local hot spots formation in the catalyst bed caused by the exotherm of the reaction since the equilibrium value for H_2/CO is about 2.7 at 550 °C.

The addition of 20 ppm of SO_2 into the feed caused a small rise in measured bed temperature (*ca.* 10 °C) and after approximately 30 min (~2 mg S/g) in the presence of SO_2 the CH_4 conversion for the R-SA sample began to decrease indicating that the catalytic partial oxidation reaction was being inhibited by sulphur. On the contrary on R-LA catalyst there was no significant deactivation or change in syngas production during the 1 hr period in the presence of 20 ppm SO_2. This apparent support effect can be explained by the higher sulphur storage capacity of La_2O_3-Al_2O_3 support, which retains the sulphur thus delaying the poisoning of the Rh surface particles as confirmed by the TPR/TPD measurements.

With regards to R-SA catalyst, it is very interesting to note that the decrease in CH_4 conversion was not accompanied by a decline in oxygen conversion which, on the other hand, remained complete (Figure 3.8) during the entire experiment. In terms of products distribution this implies a progressive decline in H_2 and CO selectivities, as shown in Figure 3.9, in favour of total oxidation products (CO_2 and H_2O) which also explains the rise in temperature observed during the experiment. Furthermore, the simultaneous decrease in CO and H_2 selectivity is not consistent with water-gas shift being inhibited but indicates the following: the presence of sulphur species on R-SA would cause the oxidation of Rh active sites (Rh^{+3} possibly as sulphates or sulphites) thus preventing the formation of synthesis gas by most probably inhibiting the indirect reaction pathway which proceeds through the reforming of residual methane with water (and CO_2).

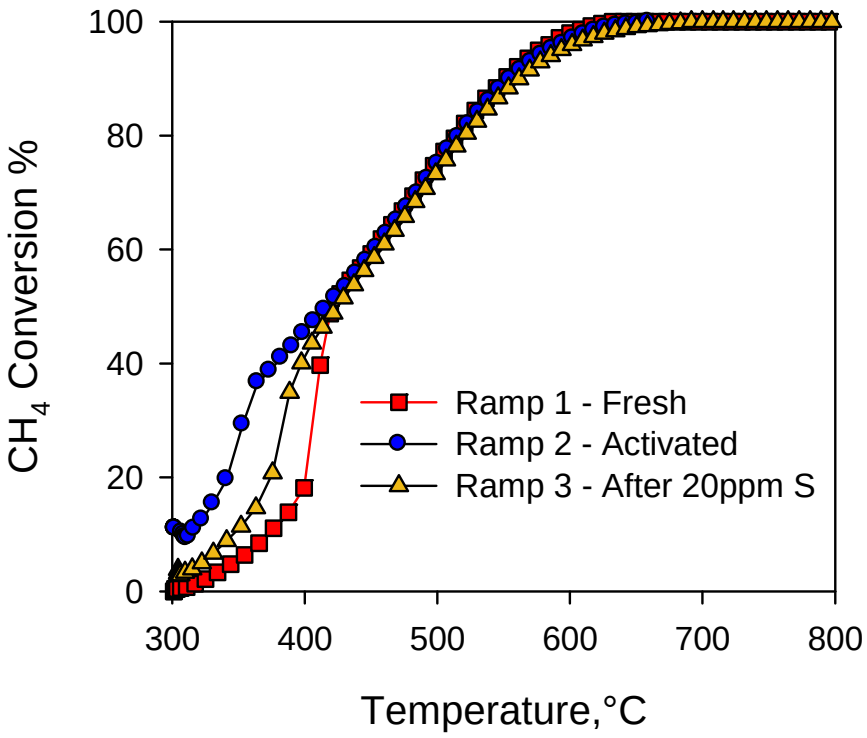

Figure 3.6: *Methane conversion as a function of temperature over R-LA catalyst: (1) fresh; (2) activated in ramp 1; (3) after sulphation in reaction at 500 °C for 1 h with 20 ppm SO_2.*

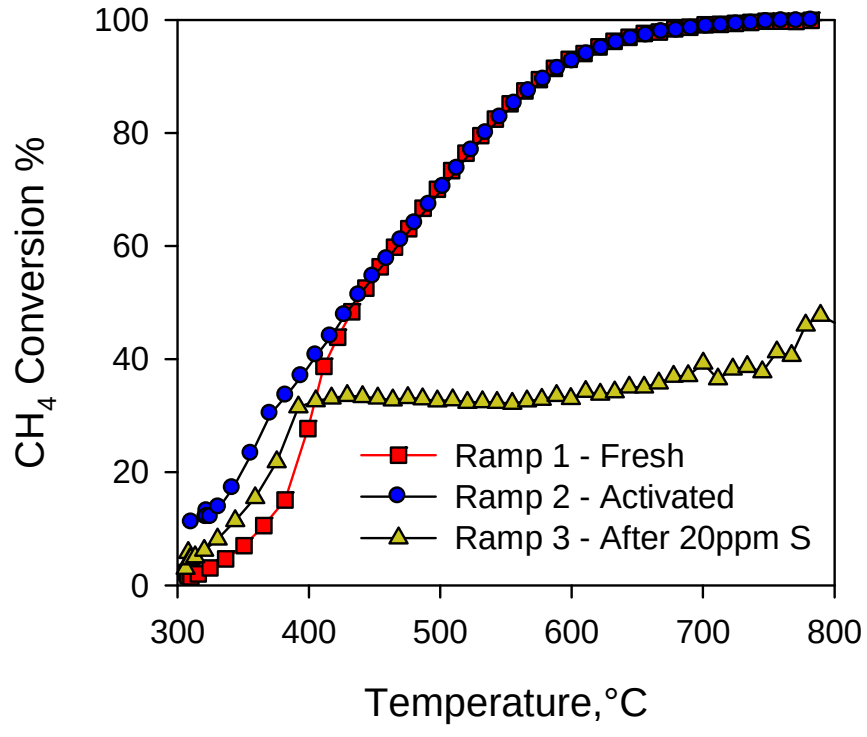

Figure 3.7: *Methane conversion as a function of temperature over R-SA catalyst: (1) fresh; (2) activated in ramp 1; (3) after sulphation in reaction at 500 °C for 1 h with 20 ppm SO_2.*

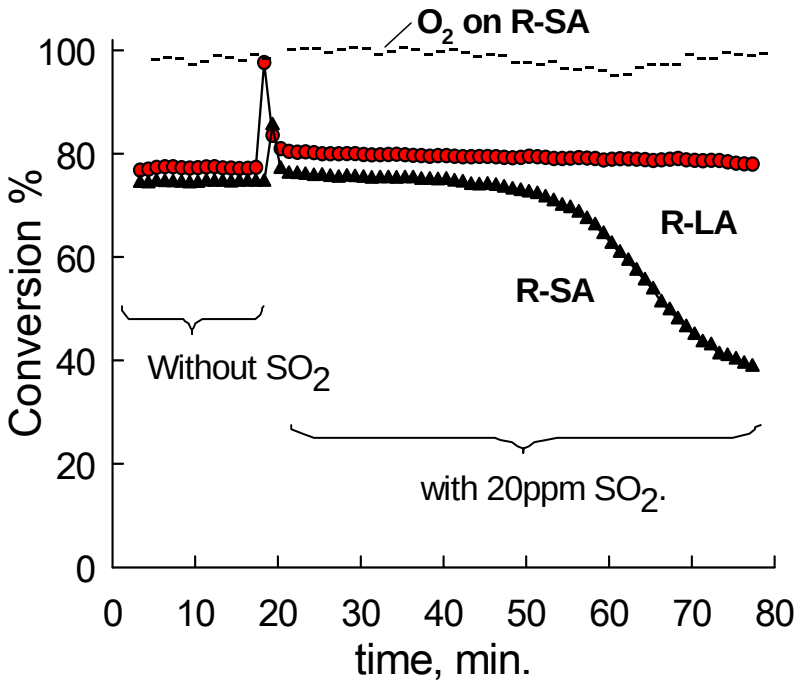

Figure 3.8: *Effect of addition of 20 ppm SO_2 in the reaction mixture at 500 °C on CH_4 conversion as a function of time on stream.*

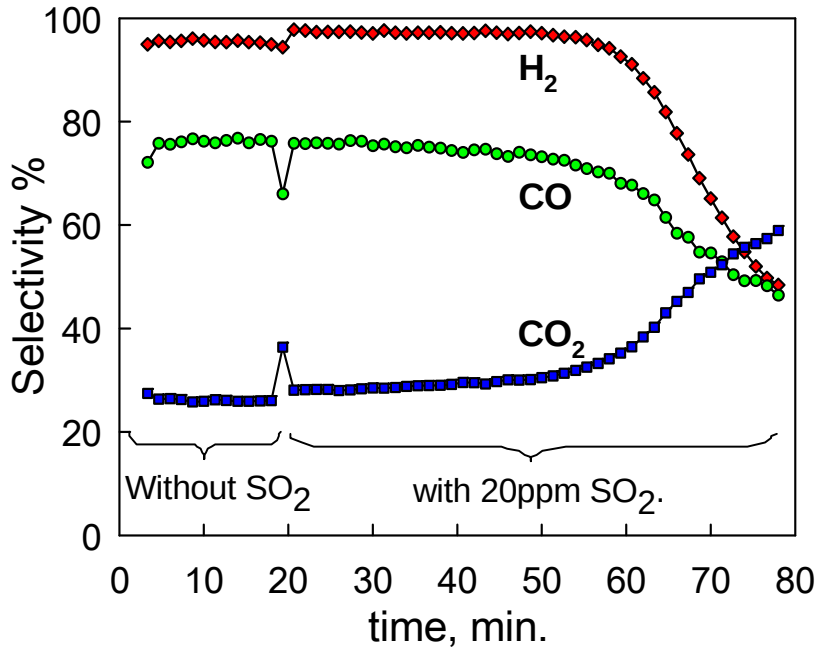

Figure 3.9: *Effect of SO_2 addition on the performance of R-SA during the addition of 20 ppm SO_2 at 500 °C as a function of time.*

Following sulphation at 500 °C under reaction mixture, the samples were cooled down on bypass and the light-off ramp was repeated in order to determine the extent of catalyst deactivation, Ramp 3 - Figures 3.6 and 3.7. With the exception of a slight shift in light-off towards higher temperature, compared to when activated under reaction mixture (Ramp 2), the R-LA sample did not show any significant deactivation by the sulphation process under the above condition and therefore it maintained its catalytic activity. The slight shift in light-off is most probably caused by the partial oxidation of the Rh active sites by SO_2 during the sulphation which retards the methane dissociation. The R-SA sample however was severely affected by the sulphation process as observed in Figure 3.7.

In order to investigate the extent of catalyst deactivation and regeneration following severe sulphur poisoning, the catalysts were subjected to temperature programmed reaction cycles from 300 °C up to 800 °C at 10 °C min^{-1} before and after exposures to 100 ppm SO_2 in the reaction mixture for 1 h at 500°C, where the catalysts were exposed to about 20 mg S/g Cat.

Figure 3.10a illustrates methane conversion as a function of catalyst temperature over R-LA catalyst. As discussed above, the methane conversion increased slowly with temperature over the fresh oxidised catalyst, before suddenly lighting-off at approximately 400 °C, and then increasing more steadily with temperature (Ramp 1). The corresponding selectivity plots for Ramp 1 in Figure 3.10 b-d clearly indicate that the first catalytic event at low temperature on the oxidized Rh (Rh_2O_3) catalyst was the total oxidation of methane, accompanied by an exotherm and high production of CO_2 (and water) at the beginning of the test. The steep increase in methane conversion occurs when some of the metal oxide is reduced to Rh metal thus allowing methane to dissociate more readily on the catalyst surface and to start forming partial oxidation products instead of combustion. Therefore, due to the reduction of Rh active sites which occur under reaction conditions, the rate of methane conversion increases at lower temperatures, Ramp 2 - Figure 3.10a. Indeed light-off was achieved as soon as the reaction mixture was dosed to the catalytic bed at 300 °C, with a relatively rapid transient formation of total combustion products (until molecular oxygen was completely consumed) and a progressive shift towards H_2 and CO products with increasing temperature, as predicted by equilibrium.

During sulphation at 500 °C under reaction mixture with 100 ppm SO_2 (not shown), also the R-LA sample underwent marked decrease in methane conversion as opposed to what was reported in Figure 3.8 during exposure to only 20 ppm SO_2. The activity began to drop after exposures to

approximately 6 mg S/g Cat. and this was accompanied by a shift in products towards CO_2 and H_2O at the expense of partial oxidation products. Following harsh sulphation at 500 °C the sample was cooled down and the light-off was repeated, Ramp 3 – Figure 3.10a. Even though the catalytic activity is severely affected, it is interesting to note that the initial part of the light-off curve is very similar to that obtained during the first ramp over the fresh oxidised sample (Ramp 1), showing a distinct ignition temperature at about 400 °C. This is likely to be due to the oxidation of metallic Rh particles by SO_2 during sulphation which delays the methane dissociation.

However, major differences between the fresh and sulphur poisoned catalyst arose following the light-off temperature where, unlike the fresh sample, the poisoned catalyst was no longer able to convert methane to partial oxidation products, even after all the molecular oxygen in the feed was consumed. During Ramp 3 methane conversion increased only marginally in the temperature range of up to 720 °C showing two distinct plateau regions: the first at approximately 430 °C extending up to approximately 530 °C, from where on methane conversion increases slowly, probably due to temperature activated desorption of S close to or directly bonded to Rh active sites; the second in the range between 570 °C-720 °C where a new poisoning effect appears which blocks CH_4 conversion at 35% irrespective of a temperature increase of up to 150 °C. Above this temperature methane conversion began to increase steadily but at 800 °C the catalyst only recovered 50% of its initial methane conversion, most likely caused by the slow decomposition of stable $Al_2(SO_4)_3$.

After Ramp 3 to 800 °C, the sample was cooled and the activity measurement repeated in order to determine the extent of catalyst recovery from sulphur poisoning – Ramp 4, Figure 3.10a. The catalyst almost completely regained all its initial low temperature activity (similar to Ramp 2) up to 530 °C, before showing a rapid decline in methane conversion, which reaches a plateau of 35% at approximately 600 °C up to 720 °C before increasing again at higher temperatures. Interestingly the corresponding selectivity profiles for CO and H_2 (Figure 3.10 b,c - Ramp 4) follow an identical pattern to that of methane conversion: at approximately 530 °C there is a sharp fall in the selectivity for H_2 and CO (mirrored by the CO_2 trace) before increasing again at higher temperatures (>700 °C). On the other hand the oxygen conversion was always complete and was not affected by sulphur poisoning (not shown).

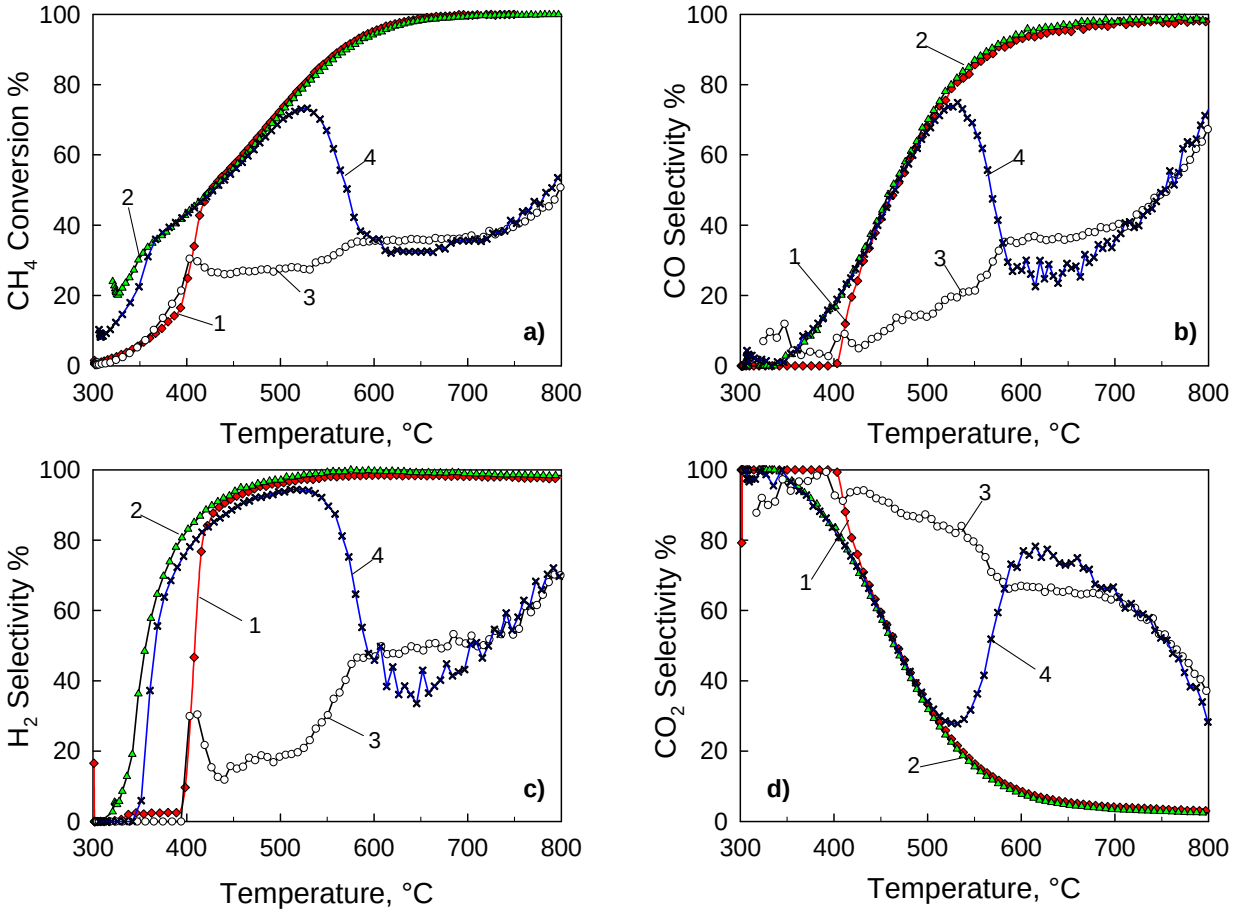

Figure 3.10: *Methane conversion and selectivities for CO, H_2 and CO_2 as a function of temperature over R-LA catalyst: (1) fresh; (2) activated in ramp 1; (3) after sulphation in reaction at 500 °C for 1 h with 100 ppm SO_2; (4) after regeneration in ramp 3.*

Since the catalyst recovered all its initial low temperature activity following regeneration (Ramp 3), this indicates that surface Rh sites regained their initial reduced active state and that they were free from any sulphur poisoning. Thus, the sudden decline in methane conversion at 530 °C, which is accompanied by a decrease in selectivity for both CO and H_2, must be caused by the presence of residual sulphur on the support which can migrate back onto the Rh metal sites and thereby poisoning the partial oxidation reaction. It is also worth noting that the above temperature (530 °C) corresponds to the peak maximum temperature obtained during the TPR profile of the SO_2 aged R-LA (and R-SA) catalyst which was assigned to the reduction of bulk $Al_2(SO_4)_3$. The changes in H_2 and CO formation over the catalyst are most likely to be due to poisoning of steam (and dry) reforming reaction which is known to occur on supported Rh catalysts [18]. Indeed even in the presence of unconverted methane, water and CO_2, no further syngas is produced regardless of any temperature increase. Similar results were also obtained on Rh/Al_2O_3 only sample (not shown), thus ruling out any major contribution from the La_2O_3

stabilizer. The above results are in agreement with the latest findings on Rh-Ce coated monoliths operated under self-sustained high temperature conditions [19].

Figure 3.11 a-d shows the methane conversion and the corresponding selectivities for CO, CO_2 and H_2 over R-SA catalyst before and after sulphur poisoning. Following catalyst conditioning (Ramp 2) methane conversion plots for R-LA and R-SA samples are superimposed. Furthermore after sulphation the methane conversion profile for the R-SA sample follows a very similar trend to that of R-LA sample with the exception that it has a slightly higher light-off temperature (Ramp 3). However, during Ramp 4 it appeared that the R-SA catalyst did not recover its low temperature activity as much as the R-LA sample, following the regeneration step. This is because the SiO_2-Al_2O_3 support can not act as an effective S trap, as confirmed by TPR/TPD. As a result, sites on Rh will become the major targets for selective chemisorption by sulphur species which will lead to higher concentrations of SO_x species on Rh as well as sites surrounding the precious metal: this results in a more rapid and severe deactivation in the low temperature region than for the La_2O_3-Al_2O_3 supported material. Nevertheless, above the temperature decomposition threshold of the rhodium sulphate species, which depends on the specific conditions, the situation is somehow reverted with the R-SA catalyst which is able to produce more syn-gas than the R-LA sample. This is shown in Figure 3.11 b,c by the higher values of CO and H_2 selectivities measured above 550 °C during both ramp 3 and ramp 4 on R-SA sample with respect to the corresponding values for R-LA (Figure 3.10 b,c). Moreover, the CO selectivity for R-SA sample >550 °C shows a further relative maximum centred at approximately 600 °C mirrored by the CO_2 trace (Figure 3.11d). On the whole, the lower amount of sulphur stored as $Al_2(SO_4)_3$ on R-SA seems to cause a slightly lower inhibition on the catalytic partial oxidation reaction at higher temperatures (500-700 °C).

Overall the results illustrate that on the less-sulphating support, S accumulates to a greater extent directly on and around the active Rh sites where reactions take place [15], whilst a sulphating support such as La_2O_3-Al_2O_3 can act (temporarily) as a sink for sulphur species thus limiting and delaying its accumulation on the Rh sites. Temperature programmed reaction cycles demonstrated that Rh sites can be almost completely regenerated at relatively low temperatures; however, as temperature increases above a threshold level, sulphur species stored on the support surrounding the Rh particles can spill back onto the metal thus re-oxidizing it and consequently inhibiting the catalytic partial oxidation reaction. Most affected appears to be the indirect reaction path to syngas involving steam reforming of residual methane.

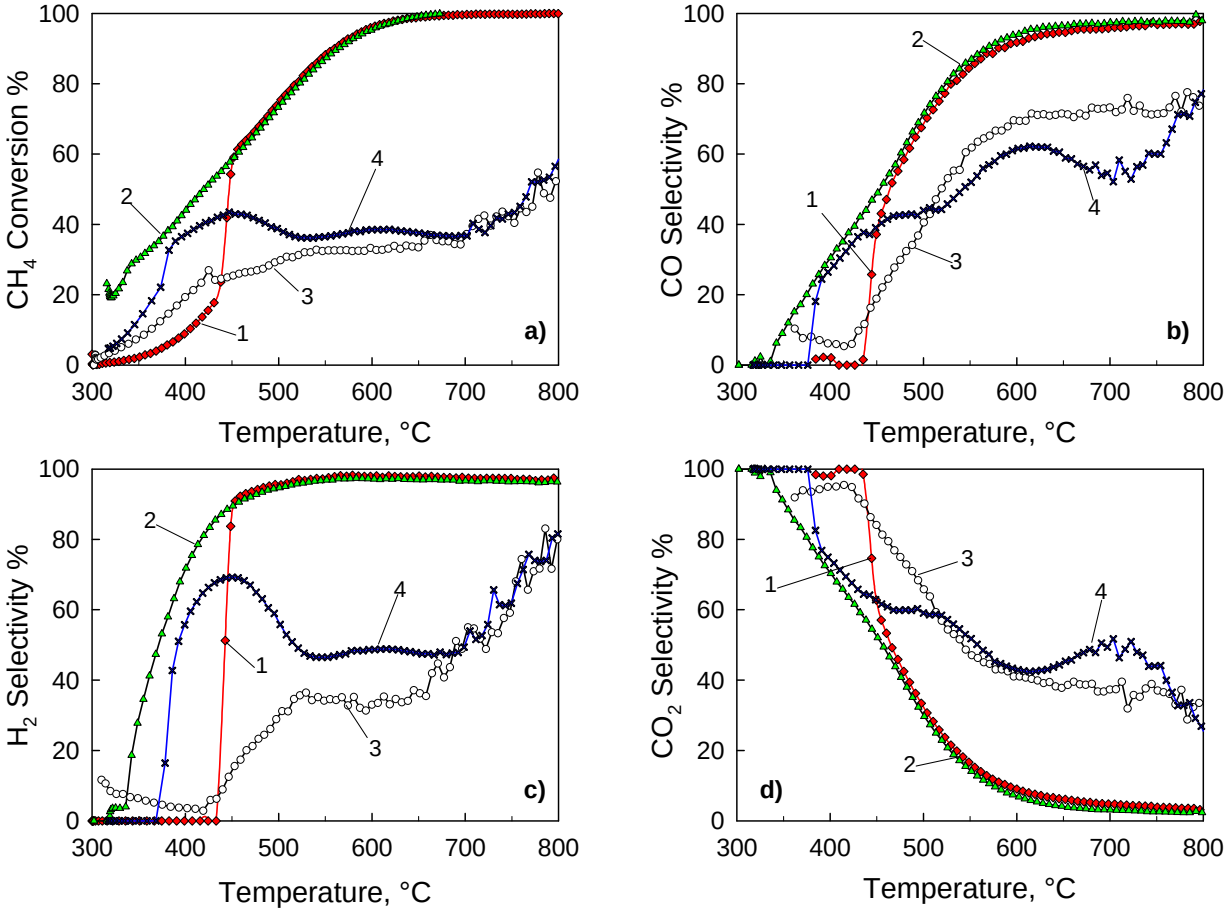

Figure 3.11: *Methane conversion and selectivities for CO, H_2 and CO_2 as a function of temperature over R-SA catalyst: (1) fresh, (2) activated in ramp 1; (3) after sulphation in reaction at 500 °C - 1 h with 100 ppm SO_2; (4) after regeneration in ramp 3.*

On the basis of catalytic activity measurements and in-situ FT-IR spectroscopic characterisation, as well as TPR/TPD studies the following mechanism is proposed – Figure 3.12. Under the reaction condition in the presence of SO_2, Rh oxidises SO_2 to SO_3 which then spills on to the support by surface diffusion causing the sulphation of the support material. During this process the Rh particles also get oxidised. The La-Al_2O_3 support can act as a sulphur getter and therefore at low concentrations of SO_2 (20 ppm) it is able to keep the sulphur away from the active metal sites and this minimises the build-up of S on or close to the active Rh sites where reactions take place (a). Under the reaction mixture at high temperatures (~530 °C), the sulphate at alumina sites slowly decomposes into SO_2 (and O_2) which is then removed from the catalyst (b). However, upon saturation of the alumina sites by sulphate species (100 ppm SO_2) the support can no longer act as a trap and thus results in the build-up of S on or close to the active Rh sites (c). At high temperatures, sulphur species stored on the support, surrounding the Rh sites, can spill back onto the metal, thus re-oxidising it and consequently

inhibiting the CPO reaction in favour of the total oxidation of methane (d). The SiO_2-Al_2O_3 support on the other hand stores significantly less sulphate species due to the presence of surface silica, as a result, regardless of the SO_2 concentration, the catalyst accumulates more sulphate species around the precious metal which can inhibit the CPO reaction at even low SO_2 concentrations (e-h).

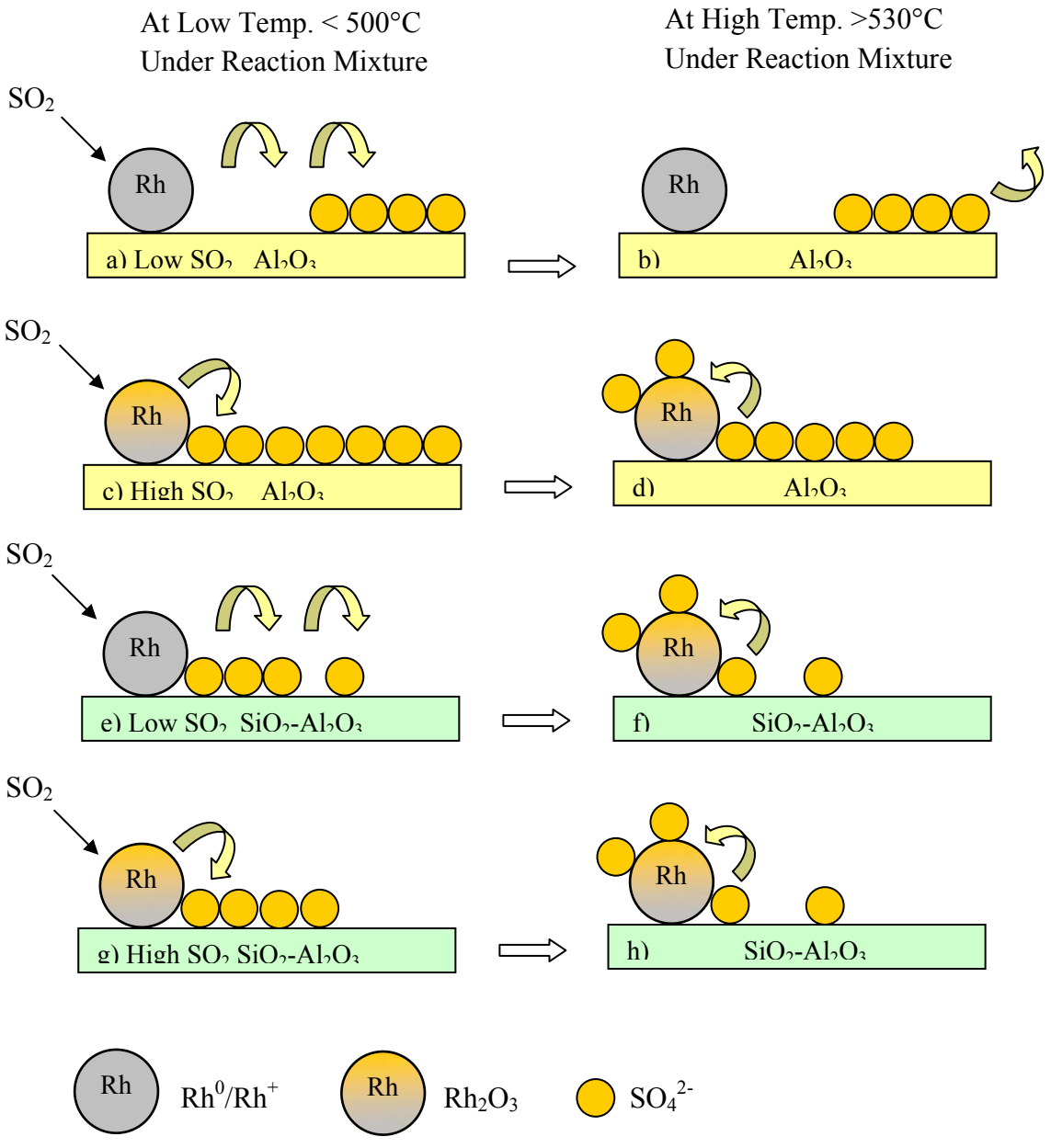

Figure 3.12: *Scheme of SO_2 poisoning and regeneration mechanism for Rh/La-Al_2O_3 and Rh/Siralox catalysts.*

3.4 Conclusions

1. The extent of catalyst sulphation was found to be highly dependant on the nature of the support material when the CPO of methane is carried out in the low to moderate temperature regime (300 to 800°C).

2. In the presence of a sulphating support such as La_2O_3-Al_2O_3 the partial oxidation reaction was much less inhibited than a less sulphating support such as SiO_2-Al_2O_3. The sulphating support acts as a sulphur storage reservoir, which minimises the poison from adsorbing on or near the active Rh sites where reactions take place.

3. TPR/TPD experiments illustrated that, although the SiO_2-Al_2O_3 supported Rh catalyst stores significantly less bulk aluminium sulphate species due to the presence of surface silica, the catalyst accumulates more S on or close to the precious metal.

4. During methane CPO reaction, sulphur poisoning appears to mostly affect the indirect reaction path to syn-gas involving steam reforming of residual methane thus shifting products distribution towards CO_2 and water.

5. Once sulphur is removed from the feed, Rh sites can be almost completely regenerated at relatively low temperatures. However, as temperature increases above a threshold level of 530°C, sulphur species stored on the support, as $Al_2(SO_4)_3$ surrounding the Rh sites, can spill back onto the metal thus re-oxidizing it and consequently inhibiting the CPO reaction in favour of the total oxidation of methane.

References

[1] H.C. Yao, S. Japar, M. Shelef, J. Catal. 50 (1977) 407.

[2] R. Burch, P.K. Loader, Appl. Catal. A: General 143 (1996) 317.

[3] S. Bernal, J. Calvino, G.A. Cifredo, V. Perrichon, A. Laachir, J. Catal. 137 (1992) 1.

[4] P. Hwang, C.T. Yeh, Q. Zhu, Catal. Today 51 (1999) 93.

[5] R.K Usmen, R.W. McCabe, L.P. Haack, G.W. Graham, J. Hepburn, W.L.H. Watkins, J. Catal. 134 (1992) 702.

[6] Y. Zhang-Steenwinkel, H.L. Castricum, J. Beckers, E. Eiser, A. Bliek: J. Catal. 221 (2004) 523.

[7] T. Wang, A. Vazquez, A. Kato, L.D. Schmidt, J. Catal. 78 (1982) 306.

[8] W. Daniell, U. Schubert, R. Glockler, A. Meyer, K. Noweck, H. Knozinger, Appl. Catal. A: General 196 (2000) 247.

[9] E. Finocchio, G. Busca, P. Forzatti, G. Groppi, A. Beretta, Langmuir 23 (2007) 10419.

[10] A. Erdohelyi, F. Solymosi, J. Catal. 84 (1983) 446.

[11] F. Solymosi, M. Pasztor, J. Catal. 104 (1987) 312.

[12] F.J. Gracia, S. Guerrero, E.E. Wolf, J.T. Miller, A.J. Krop, J. Catal. 233 (2005) 372.

[13] W.Z. Weng, C.R. Luo, Y.Y. Liao, H.L. Wan, Topics in Catal. 22 (2003) 87.

[14] E.P.J. Mallens, J.H.B.J. Hoebink, G.B. Marin, J. Catal. 167 (1997) 43.

[15] K. Heitnes, J. Hofstad, B. Hoebink, A. Holmen and G. Marin, Catal. Today 40 (1998) 157.

[16] O.V. Buyevskaya, K. Walter, D. Wolf, M. Baerns, Catal. Lett. 38 (1996) 81.

[17] R. Wang, H. Xu, X. Liu, Q. Ge, W. Li, Appl. Catal. A: Gen. 305 (2006) 204.

[18] J. Barbier, D. Duprez, Appl. Catal. B: Environ. 4 (1994) 105.

[19] A. Bitsch-Larsen, N.J. Degenstein, L.D. Schmidt, Appl. Catal. B: Environ. 78 (2008) 364.

4. Sulphur Inhibition on the Catalytic Partial Oxidation of Methane Over Rh-Based Monolith Catalysts

4.1 Introduction

The adverse impact of sulphur compounds on catalytic performance is well known [1,2] and is the subject of much current research, particularly in the case of (autothermal) steam reforming of liquid fuels [3-7] and automotive catalysts [8,9]. However, studies on the effect of sulphur during the CPO of methane over Rh based catalysts have so far remained scarce, as recently [10] pointed out by the group of L.D. Schmidt, who investigated the impact and features of poisoning by CH_3SH on Rh–Ce coated foam monoliths operated at short contact time. They found a marked negative effect on CH_4 conversion and H_2 selectivity by even small amounts of sulphur, mainly attributed to a partially reversible inhibition of the steam reforming reaction. In this chapter, we set out to investigate the effects of sulphur addition during the CPO of methane at short contact times and self sustained high temperatures over Rh catalysts supported on either La_2O_3-Al_2O_3 or SiO_2-Al_2O_3 coated monolith samples. Individual effects of feed ratio, nitrogen dilution and addition of two different sulphur surrogates such as SO_2 and H_2S will be discussed with regards to both steady state and transient operation of the CPO reactor during poisoning/regeneration cycles or low temperature light-off phase.

4.2 Experimental Procedure

The Rh/La_2O_3-Al_2O_3 (R-LA) and Rh/SiO_2-Al_2O_3 (R-SA) monolith samples were prepared according to the procedure described in Chapter 2.1.2. The catalytic tests were carried out on monolith samples as described in Chapter 2.2.2.

4.3 Results and Discussion

Table 4.1 illustrates catalysts denomination, metal loading, total surface areas and Rh dispersions measured by CO chemisorption after H_2 reduction at 800 °C. The commercial γ-aluminas stabilized either with La_2O_3 or SiO_2 are characterized by a specific surface area of 140 and 360 m^2/g respectively. The addition of alumina binder and calcination in air at 800

°C, used to obtain the final washcoat, caused a reduction in the specific surface area for the SA washcoat only (down to 270 m^2/g), which was still twice that of LA sample due to its smaller average pore size (98Å vs. 135Å for LA). The actual noble metal loading is close to the nominal one for both catalysts. BET values for the final monolith catalysts after deposition of Rh are in line with the corresponding washcoat layers, therefore the higher metal dispersion value obtained for R-SA sample is justified by the larger surface area of the silica stabilized alumina support.

Sample	Honeycomb[a] LxD (mm)	Washcoat material	B.E.T.[b] m^2/g	Pore diameter Å	Rh by ICP[b] wt %	Rh dispersion[c] %
LA	–	3% La_2O_3-γAl_2O_3	143	135	–	–
SA	–	10% SiO_2-γAl_2O_3	270	98	–	–
R-LA	10x17	LA	150	120	0.77	39.0
R-SA	10x17	SA	249	97	0.73	66.5

[a] cordierite, 600cpsi, channel side 0.96mm, wall thickness 76μm
[b] referred to total weight of active phase, monolith substrate excluded
[c] by CO chemisorptions after reduction in H_2 at 800°C; CO/Rh stoichiometry=1

Table 4.1: *ICP-MS, BET and CO chemisorptions for structured catalysts and their corresponding supports.*

4.3.1 Pseudo-adiabatic Catalytic Tests

The effect of addition and removal of 8, 18 and 37 ppm H_2S to and from the reaction feed under CPO conditions over R-LA monolith operated at a fixed CH_4/O_2 feed ratio is illustrated in Figure 4.1. The addition of H_2S resulted in a rapid decrease in CH_4 conversion and H_2 selectivity with a corresponding sharp increase in the catalyst temperature; moreover the extent of catalyst deactivation depended on sulphur concentration in the feed. On the other hand, the oxygen conversion was always 100% and was not affected by sulphur poisoning, in good agreement with results obtained by L.D. Schmidt [10]. This is most likely due to the kinetics of the oxidation reactions which remains much faster than the transport phenomena even in the presence of sulphur. The fast S-poisoning impacts adversely on the H_2 selectivity whereas the CO selectivity is almost unaffected also at the highest H_2S concentrations. At each H_2S level, CPO performance reach a steady state within roughly 10 minutes, with methane conversion and syngas selectivities passing through an initial minimum which

becomes more pronounced at higher S levels. However, upon removing the H_2S from the reaction feed (after ~ 25 min.), the activity of the catalyst was found to increase immediately and the initial CPO activity/selectivity was regained on a time scale that is comparable to that of the poisoning process.

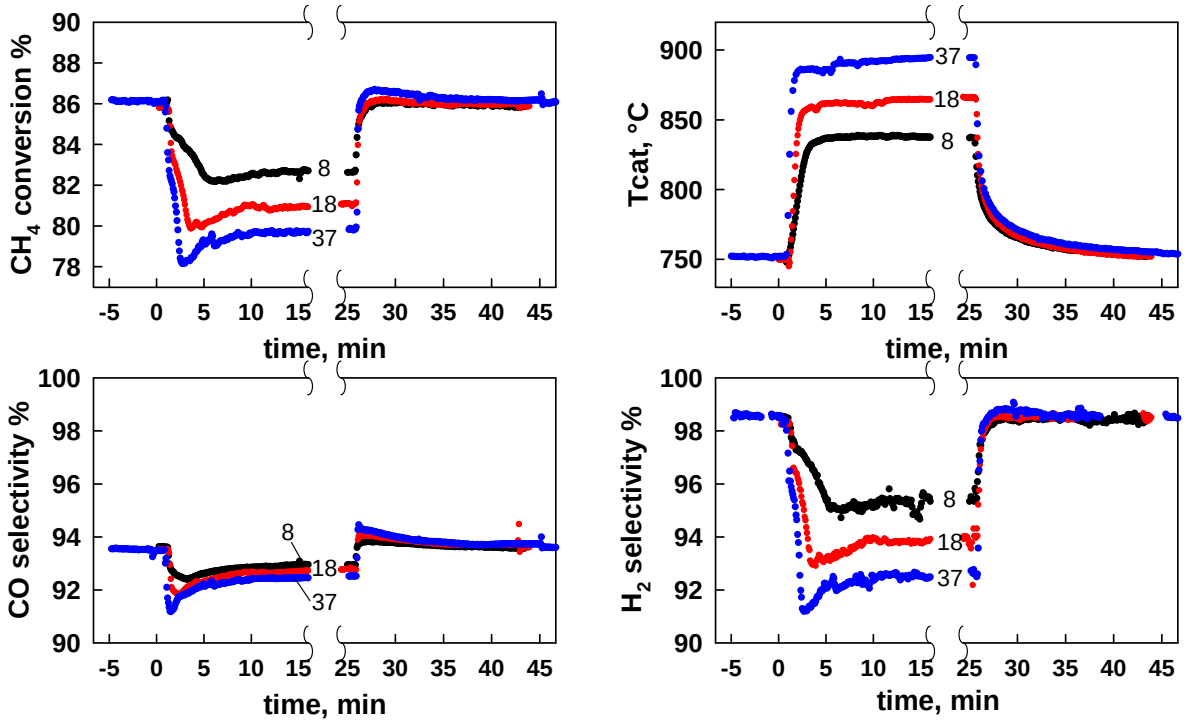

Figure 4.1: *Transient response to H_2S addition (8, 18 or 37 ppm) and removal on methane conversion, catalyst temperature, CO and H_2 selectivities during methane CPO on R-LA monolith. Feed CH_4/O_2=2, GHSV= 6.7·10^{4}h^{-1}, N_2=20% vol.*

The complete reversibility of the S-poisoning effect under the studied reaction condition was also confirmed by the identical values of the temperature measured in the catalyst before the addition and after the removal of sulphur from the reaction feed. This result partially contrasts with the long-lasting regeneration and not complete recovery of the initial activity observed by Bitsch-Larsen et al. [10] over their Rh/Ceria/γ-Al_2O_3 catalyst. This could be due to the strong adsorption of H_2S on ceria [5] even at high T and P_{H2}, which may retard catalyst regeneration due to a slow desorption of surface S-Ce species by a reverse spillover process onto Rh sites, an effect observed over our alumina based supports during CPO of methane at lower temperatures (530 °C–700 °C) [11]. Furthermore, the rapid response upon the introduction and removal of sulphur suggests that direct adsorption onto the active Rh sites is responsible for the adverse effects of sulphur. Table 4.2 summarises the differences in CPO performance of R-LA monolith at steady state due to increasing H_2S levels at a fixed CH_4/O_2 feed ratio of 2. It is

observed that the decrease in methane conversion measured at 8 ppm H_2S is accompanied by a corresponding increase in water production of the same magnitude (in terms of molar flow rates at reactor exit normalized to a CH_4 feed of 100) and at the same time less CO and H_2 is produced. Furthermore, the change on the H_2/CO ratio before and after the addition of H_2S is close to three.

		H_2S				Differences*		
CH_4/O_2=2		0 ppm	8ppm	18ppm	37ppm	Δ (8-0)	Δ (18-0)	Δ (37-0)
X_{CH4}	(%)	86.1	81.9	81.0	79.8	-4.2	-5.1	-6.3
Y_{H2}	(%)	84.7	78.1	76.4	73.9	-13.2	-16.5	-21.2
Y_{CO}	(%)	80.6	76.1	75.2	73.8	-4.5	-5.4	-6.8
Y_{H2O}	(%)	1.4	3.8	4.6	5.9	+ 4.8	+6.3	+8.9
Y_{CO2}	(%)	5.5	5.8	5.8	6.0	+ 0.3	+0.3	+0.5
H_2/CO	-	2.10	2.05	2.03	2.00			
T_{cat}	(°C)	752	839	865	895	+87	+103	+143
T_{out}	(°C)	655	683	701	718	+28	+56	+63

* Products molar flows per 100 CH_4 feed

Table 4.2: *Impact of H2S addition at various levels on the steady state methane CPO on R-LA monolith. Feed CH_4/O_2=2, GHSV= $6.7 \cdot 10^4 h^{-1}$, N_2=20% vol.*

These results strongly suggest that the poisoning effect of H_2S is related to its ability to inhibit the endothermic steam reforming reaction (4.1) which mainly occurs in the second region of the catalyst bed between the unconverted methane and water produced in the first oxidation zone of the reactor [10,11].

$$CH_4 + H_2O \leftrightarrow CO + 3H_2 \qquad \Delta H_r^{25°C} = +206 \text{ kJ/mol} \qquad (4.1)$$

This hypothesis is further supported by the lower reaction temperature measured both in the catalyst and in the outlet gas in the absence of sulphur in the feed where higher methane conversion is achieved. Indeed Rh is reported to be very active for steam reforming of methane even at extremely short contact time (< 1 ms) but not for dry reforming with CO_2 [12]. The slight increase in CO_2 yield seems to be caused by the shift in the equilibrium of the slightly exothermic water gas shift reaction (4.2), due to significant reduction of H_2 and rise of H_2O partial pressures. Any contribution to syngas formation under the selected process conditions from dry reforming has already been ruled out in several previous studies [12].

$$CO + H_2O \leftrightarrow CO_2 + H_2 \qquad \Delta H_r^{25°C} = -41 \text{ kJ/mol} \qquad (4.2)$$

A similar behaviour was also observed at higher H_2S levels (Table 4.2), where the larger reduction of methane conversion corresponds to a more pronounced kinetic inhibition of steam reforming, since the change on the H_2/CO ratio before and after the addition of sulphur follows the stoichiometry of reaction (4.1). Indeed the exit H_2/CO ratio progressively decreases from 2.1 down to 2.0 at 37 ppm H_2S as expected from the almost unaffected CO selectivity reported in Figure

It can also be noted from Figure and Table 4.2 that the inhibiting effect of sulphur doesn't reach a saturation level up to 37 ppm H_2S in the feed, which again partly contrasts to what was observed by Bitsch-Larsen et al. [10] comparing results at 0, 14 and 28 ppm of CH_3SH addition during methane CPO over a Rh/Ceria foam catalyst at a GHSV=$1.4 \cdot 10^5$ h^{-1}. In fact, regardless of the strongly enhanced mass and heat transfer characteristics of their 80 ppi foam catalyst with respect to a 600 cpsi honeycomb [13], the initial sulphur free CPO performance was slightly lower than the results obtained in this study. Moreover, the impact of sulphur inhibition was much stronger, with an observed drop in methane conversion and H_2 yield down to 65% and 49% respectively at 28 ppm of sulphur. Since sulphur appears to affect mainly the methane steam reforming and that this reaction largely proceeds under kinetic control, all the factors such as GHSV, Rh loading, dispersion, type of support and reactor temperature profile will directly influence the sensitivity of the process to sulphur poisoning.

In order to investigate if the extent of catalyst poisoning is affected by different sulphur bearing compounds, the experiments were repeated by substituting H_2S with SO_2 into the reaction feed. The CPO results are completely reproducible in terms of catalyst temperatures and methane conversions as shown in Figure 4.2a-b respectively, as well as H_2 and CO yields (not shown), being only affected by the total S concentration in the feed and not by the type of sulphur precursor. This is in good agreement with recently reported results for isooctane CPO on Rh-based catalysts in the presence of thiophene, sulphur dioxide, benzothiophene, dibenzothiophene [14], and is most probably due to the rapid and complete conversion of all the S species into H_2S, which is the thermodynamically stable specie under the typical CPO operating conditions i.e. high H_2 partial pressure and high temperatures (> 800 °C).

The study was further extended by considering feed conditions with either lower or higher N_2 dilution (10% vol. or 55.6% vol., the latter corresponding to using air as the oxidant) at fixed CH_4/O_2 feed ratio of 2, in order to examine the effect of initial catalyst temperature on the

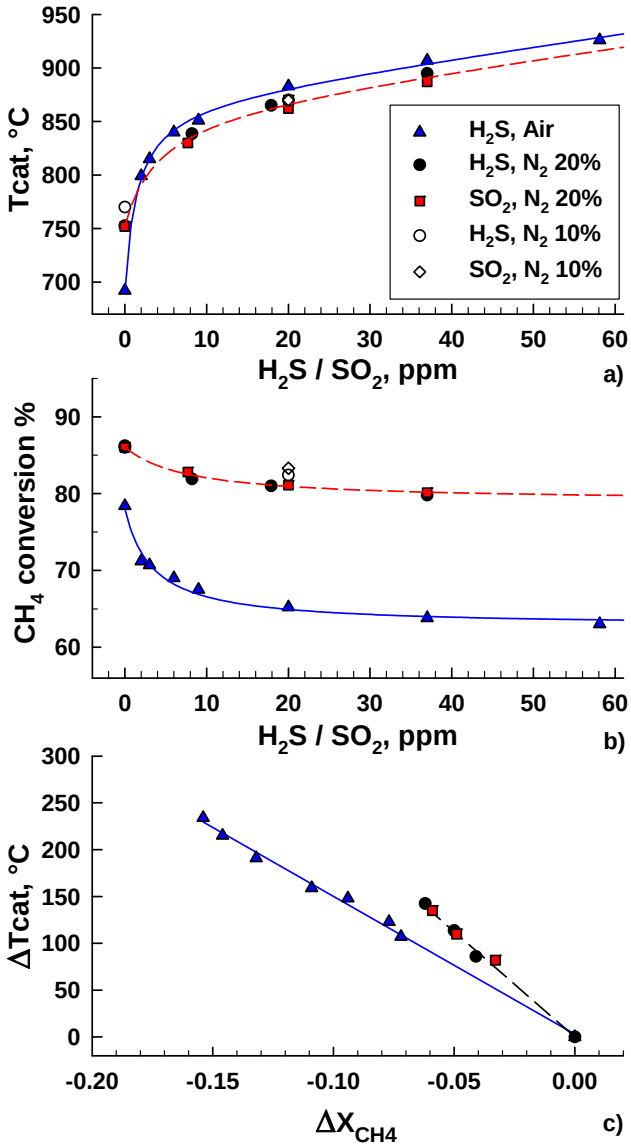

Figure 4.2: *Impact of H_2S or SO_2 addition on (a) the catalyst temperature and (b) CH_4 conversion during the CPO of methane over R-LA monolith at CH_4/O_2=2 at three different N_2 dilution levels of the feed (10% vol., 20% and 55.6%=air). c) Rise of catalyst temperature as a function of the variation of methane conversion measured upon the addition of increasing levels of H_2S. GHSV= $6.1 \cdot 10^4$, $6.7 \cdot 10^4$ and $8.1 \cdot 10^4$ h^{-1} respectively for feed mix containing N_2=10, 20, 55.6 %vol.*

extent of sulphur poisoning. The results are once again reported in Figure 4.2a and b in terms of catalyst temperature and methane conversion vs. sulphur concentration in the feed. Under sulphur-free conditions, catalyst temperature decreases significantly with N_2 dilution, passing from 766 °C at 10 % N_2 down to 690 °C when air is used as the oxidant. In spite of large variation in the initial conditions, the temperature profiles, while displaying the same increasing trend as sulphur is added, tend to merge in a single narrow band. Some minor differences are expected due to the occurrence of a slight shift in the temperature profiles

along the catalyst: increasing dilution was experimentally accompanied by an increase in the GHSV and both factors tend to move the temperature peak, normally placed close to the entrance [10,12], further ahead in the reactor and closer to the measuring position in the centre of the monolith. Indeed temperatures measured at each S concentration when using air are constantly higher than when using a less diluted feed - Figure 4.2a.

Figure 4.2b illustrates that although similar catalyst temperatures are reached upon addition of a fixed sulphur inlet concentration, a significantly lower methane conversion and syngas yields are obtained at higher feed dilution. This indicates that sulphur has a much stronger impact when the CPO is conducted in air, since even the addition of sulphur as low as 2 ppm causes a temperature rise of more than 100 °C and a methane conversion drop of ~7 points.

In Figure 4.2c the same results are plotted in terms of temperature rise measured on the catalyst upon S addition as a function of the corresponding change in methane conversion with respect to the sulphur free reaction feed. The data for reaction tests carried out in air and at 20% N_2 dilution follow single straight lines in the whole range explored (0-58 ppm S). By assuming a thermal equilibrium between gas and solid (i.e. exit gas temperature is equal to the measured catalyst temperature), a simple heat balance on the gas phase can be written:

$$\Delta H_r^{T_0} = -\frac{W \cdot C_p}{F_{CH4}} \cdot \left(\frac{\Delta T}{\Delta x_{CH4}} \right) \tag{4.3}$$

which relates the variation of temperature ΔT (°C) and methane fractional conversion Δx_{CH4} to a heat of reaction ΔH_r^{T0} (kJ/mol) at the initial temperature T_0 (700 °C) through the specific heat of the gas mixture *Cp* (0.0344 kJ/(mol·°C)), its total flow rate *W* (7.3 mol/h) and methane feed flow rate F_{CH4}(1.64 mol/h). By substituting the value of $\Delta T/\Delta x_{CH4}$ obtained from the slope of the line in Figure 4.2c (-1473°C, for CPO in air) into eq. 4.3, it results that $\Delta H_r^{700\ °C}$ = +225 kJ/mol, which perfectly corresponds to the heat of reaction of methane steam reforming at the temperature of 700 °C. Similar results are also obtained with the data set at 20% N_2 dilution: indeed the different slopes of the plots in Figure 4.2c are justified by the variation of gas composition (i.e. *Cp*) and overall reactor temperature. In this way it is ultimately confirmed that S poisoning during methane CPO on Rh catalysts is due to a selective severe inhibition of the steam reforming reaction, which mostly proceeds under kinetic control by

converting the residual methane from the first oxidation zone of the reactor with water therein produced. With regards to the extent of sulphur inhibition on the CPO process, this was found to be greater if the initial temperature of the catalyst was maintained lower, i.e. when using air as an oxidant: there is a higher chance of forming stable S-species which will then decompose much less readily than if the reaction had been carried out at higher temperatures [1,2]. However it is worth noting that the final operating temperature of the system in the presence of sulphur is largely unaffected by the dilution level but only depends on the sulphur concentration in the feed - Figure 4.2a. Moreover, the rather rapid response (either inhibition or recovery of catalytic performance) upon introduction and removal of sulphur from the feed (Figure 4.1), suggests a direct adsorption of sulphur onto active Rh sites that eventually reaches an equilibrium coverage that depends on the temperature and the ratio of partial pressures of H_2 and H_2S.

Figure 4.3 reports the sulphur activity, defined as the ratio of inlet H_2S to H_2, measured at steady state at the exit of the reactor, as a function of the inverse of the temperature recorded on the catalyst. Even if the system is not isothermal and the partial pressure of H_2 varies along the reactor, all the experimental data collected at $CH_4/O_2=2$ by varying the sulphur content of the mixture follow a single straight line, showing a similar behaviour to the previously reported chemisorption of S on alumina supported Ni catalysts at fixed coverage [1,2,15]. The thermodynamic equilibrium curve relevant to the bulk Rh_2S_3 formation [8] is also presented in Figure 4.3, which allows us to exclude the presence of metal sulphides under the studied CPO conditions, since much higher sulphur levels would be required. Nevertheless the relative high affinity of Rh for sulphur adsorption is projected to adversely affect catalytic performance of methane CPO in air (catalyst temperature of ≈700 °C) already at P_{H2S}/P_{H2} of $1.5 \cdot 10^{-7}$, corresponding to sulphur levels in the feed of approximately 350 ppbs by volume (Figure 4.3). In the range of operating conditions explored, sulphur does not shut down completely the steam reforming reaction as already observed in ref. [10] through the detailed H_2 and CO profiles along the reactor. This is confirmed here by the progressive detrimental effect on syngas yield observed with further S addition that leads to a rise in the catalyst bed temperature. This in turn causes restoration of some active sites and/or speeds up the reaction on Rh sites which are free from adsorbed sulphur species, producing more H_2 until the equilibrium condition is reached. Indeed saturation level on Rh (1 0 0) surface was reported to be 0.55 monolayers of H_2S [16].

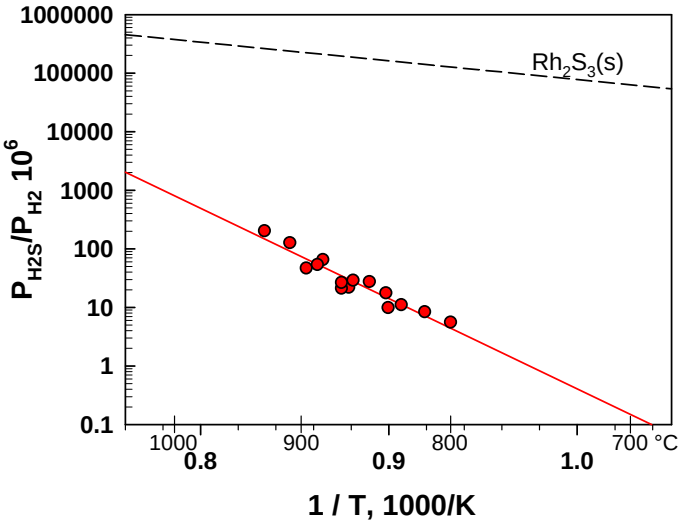

Figure 4.3: *Thermodynamic activity of sulphur chemisorbed on R-LA catalyst during methane CPO at CH_4/O_2=2 in the presence of H_2S.*

The role of the catalyst support was also investigated by comparing the CPO activities of R-LA and R-SA monolith samples under pseudo-adiabatic conditions as a function of CH_4/O_2 feed ratio, using 10% N_2 dilution, in the presence or absence of 20 ppm H_2S (Figure . In the absence of sulphur, R-LA catalyst outperforms the R-SA counterpart in the whole range of feed conditions. For both catalysts methane conversion and yields to CO and H_2 follow the same qualitative trend as predicted by equilibrium curves (constant pressure and enthalpy) calculated excluding the formation of solid C. Although there were no significant differences in the operating temperatures for the two catalytic systems, the products distributions indicate once again a larger contribution of steam reforming on R-LA sample rather than on R-SA, in spite of the higher dispersion of the noble metal measured by CO chemisorption on samples reduced in H_2 at 800 °C (Table 4.1). The differences in activity for the two systems tend to disappear at the lowest CH_4/O_2 feed ratio, since at higher O_2 concentrations methane conversion also reaches 100% on the R-SA sample, thus significantly reducing the amount of residual methane from the oxidation zone which can then react via the steam reforming.

The presence of a support material such as SiO_2-Al_2O_3 (SA), which has a lower affinity for sulphur than the La_2O_3-Al_2O_3 (LA) sample, did not help in preventing or limiting the extent of S-poisoning of Rh active sites which become the main target for sulphur adsorption. In the presence of 20 ppm H_2S in the reaction feed both catalysts showed (Figure 4.4) a drop in methane conversion which was accompanied by a decrease in CO yield of similar magnitude

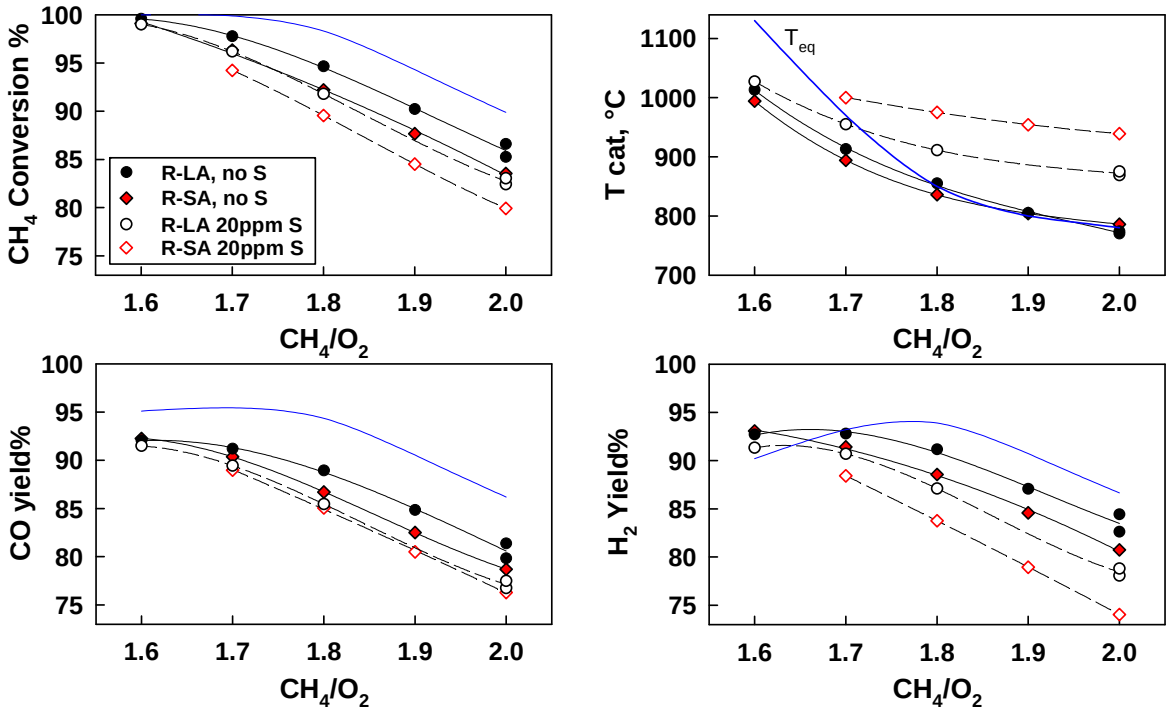

Figure 4.4: *CH_4 conversion, CO and H_2 yields and catalyst temperatures measured on R-LA and R-SA monoliths as a function of CH_4/O_2 ratio with sulphur free feed (full symbols) and with 20 ppm H_2S (empty symbols). GHSV= $6.1 \cdot 10^4 h^{-1}$,N_2=10%. Solid lines correspond to adiabatic equilibrium among gaseous species only.*

whereas the drop in H_2 was always larger in accordance with the steam reforming stoichiometry. Figure 4.4 also indicates that in the presence of sulphur the catalyst temperature on the R-SA catalyst is always greater than on the R-LA sample. The passive silica layer on the alumina support may force sulphur species to stay closer to the active Rh sites. Furthermore, the higher metal dispersion on the R-SA sample can result in an increase in the sulphur saturation level of Rh sites [1-2], thus enhancing the inhibition effect due to a lower number of S-free active sites available for SR.

It is also clear that by progressively increasing the amount of oxygen in the feed, the catalytic activities for the two systems become very similar. In particular the inhibition effect of sulphur becomes less pronounced at lower CH_4/O_2 ratio, since the contribution of steam reforming to the overall conversion becomes limited and also the higher operating temperature on the catalyst reduces the extent of S adsorption on active metal sites. This contrasts with the results reported by Bitch-Larsen et al. [10] who observed a severe sulphur inhibition effect at C/O = 0.73 (CH_4/O_2 = 1.46) and higher GHSV=7.5 x 10^5 h^{-1} (dilution not specified). In fact, apart from the possibility of some loss in the catalytic activity caused by

overheating of their Rh/Ce foam catalyst as recognized by the authors, the rather low operating temperature of the catalyst (800 °C) under sulphur free reaction conditions could also explain the higher inhibition effect of sulphur on the catalytic reaction, as shown in the present work by our results at different dilution levels (Figure).

4.3.2 CPO Light-Off

A low light-off temperature is a key parameter in most combustion applications that invariably require easy ignition procedures with fast response and should avoid auxiliary devices such as pre-burners in order to get rid of their additional contribution to pollutants formation [17,18]. Fresh R-LA and R-SA catalysts showed similar values of the minimum preheating temperature required to ignite a S-free CH_4-air reaction mixture (268-270 °C, Figure 4.5a and b). Moreover, the light-off temperature did not change for catalysts exposed to sulphur and regenerated under reaction mixtures at high temperatures (>800 °C). This is in agreement with the rapid and reversible inhibiting effect of S observed on the CPO reaction and suggests that, independently from the type of support, sulphur is not accumulated or stored on the catalyst in significant quantities upon exposure to H_2S or SO_2 under self sustained operation at high temperature and P_{H2}.

However the addition of sulphur in the reaction mixture shifted the catalyst light-off to progressively higher temperatures (Figure 4.5a and b). The effect is not evident at low H_2S concentrations, but starts to become more significant above 10 ppm, with both catalysts showing a delay of approximately 35 °C at 20 ppm of S, regardless of the type of support. The slight increase in the ignition temperature following sulphur poisoning is an indication that also the oxidation activity is affected by the presence of the S in the feed. As shown in Figure 4.5a by the transient CO_2 and CO profiles, either with or without 20 ppm H_2S in the reaction mixture, ignition proceeds through the initial formation of total oxidation products, whereas CO (and H_2) are only formed when a sufficiently large depletion of molecular and Rh-surface oxygen species is obtained. Therefore it seems that sulphur inhibition under pre-ignition conditions is directly due to a lower availability of Rh active sites which in turn are more difficult to reduce. However, it should be noted that before light-off is achieved, the catalyst is exposed to oxidising conditions at low to moderate temperature since the feed mixture is characterised by high oxygen partial pressure and the reducing capability of methane is quite

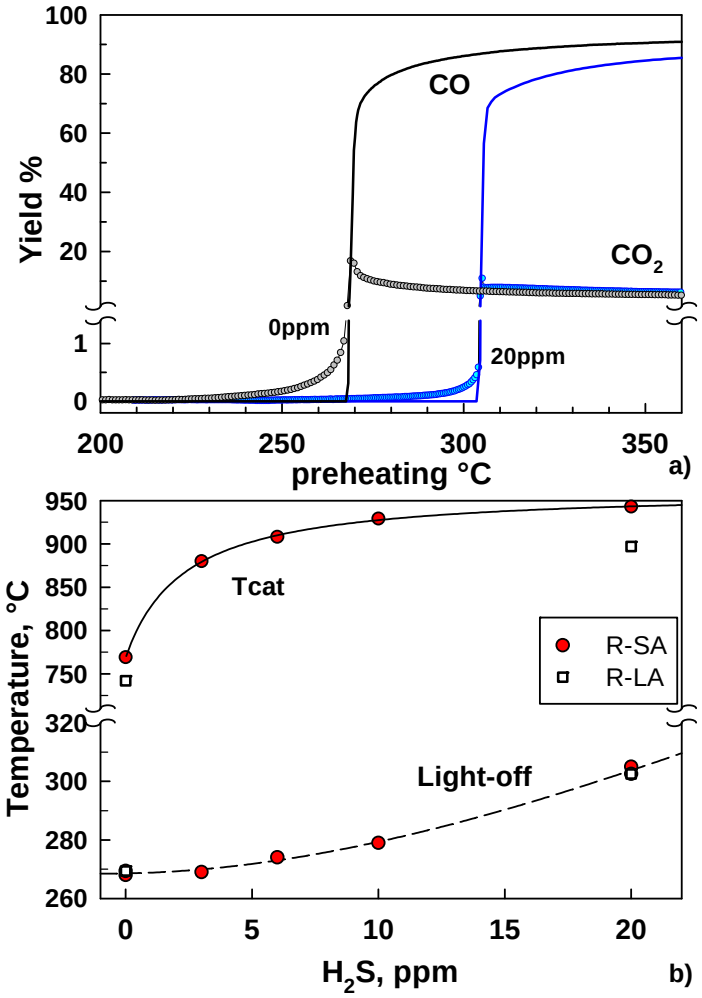

Figure 4.5: *Light-off of CPO at CH_4/O_2=1.8 in air, GHSV=$8 \cdot 10^4$ h^{-1}. a) CO and CO_2 yields as a function of preheating temperature over R-LA monolith with 0 or 20 ppm H_2S; b) Effect of H_2S concentration on the light-off temperature and on the final catalyst temperature $T_{cat.}$ under self-sustained operation at preheating temperature of 350 °C.*

low. The eventual negative impact of sulphur poisoning on the kinetics of the oxidation reactions at high temperature with low or zero partial pressure of oxygen (under self-sustained operation) could not be verified since catalytic oxidation on Rh is very fast and oxygen diffusion from the bulk of the gas to the surface remains the rate-limiting step. Under pre-ignition conditions sulphur tolerance is strongly influenced by the catalyst support, since S-species can be readily oxidised to SO_3 on the noble metal sites and stored on the catalyst support mainly in the form of aluminium sulphates. In fact, the higher sulphating LA support (rather than the silica enriched SA) was found to prolong S-tolerance by acting as a scavenger that keeps the sulphur away from the active Rh sites [11].

In this case we were not able to observe any significant differences between the two supports, most probably because of the limited time during which the catalysts were exposed to sulphur before the CPO ignition occurred. This corresponded to the time required to heat up the system from roughly 200 °C to the light-off temperature at a rate of ≈5 °C/min. Due to both this limited range of time and the sulphur concentrations explored, the complete sulphur saturation of the supports was prevented thus avoiding accumulation of S directly on the Rh active sites. In fact, even at the highest S concentration tested (20 ppm H_2S) we observed a light-off temperature which was only 3 °C lower on R-LA than the R-SA sample.

In addition to increasing the catalyst light off temperature, the presence of sulphur in the reaction feed caused an increase in the catalyst operating temperature following ignition (Figure 4.5b), due to the inhibition of the endothermic steam reforming reaction. However, although there were no significant differences in the catalyst light-off temperatures between the two samples, the final operating temperatures were quite different, with the R-SA monolith running significantly hotter than the R-LA sample at the same S concentration. As already pointed out, this is probably due to the higher Rh dispersion and higher S saturation level on the R-SA monolith sample.

4.4 Conclusions

1. During the CPO of methane under self-sustained conditions at high temperatures (>800 °C), the presence of sulphur in the feed mainly inhibits the steam-reforming reaction by directly poisoning the active Rh sites. As a result, the sulphur storage capacity of the support gets much less important under these conditions and therefore the poisoning of the Rh sites becomes the sole factor in catalyst deactivation.

2. Even addition of very low sulphur concentration (2 ppm) caused a significant increase in the operating temperature accompanied by a proportional drop in methane conversion and hydrogen selectivity, due to selective inhibition of the SR reaction.

3. The effect of sulphur poisoning was found to be completely reversible and the catalyst immediately regained its initial activity when the sulphur was removed from the feed. The extent of sulphur poisoning was also found to be independent from the type of sulphur precursor i.e. H_2S or SO_2.

4. The extent of SR inhibition and temperature increase was found to be greater when operating in air (i.e. at lower starting temperatures) and seems to be controlled by the thermodynamic adsorption-desorption equilibrium which controls the extent of surface coverage of Rh by sulphur species.

5. The detrimental effect of sulphur tends to diminish at lower CH_4/O_2 feed ratios due to the simultaneous increase in the catalyst temperature and to the reduction in the contribution of steam reforming to the overall syn-gas production.

6. Although the sulphur storage capacity of the support did not show any beneficial effect on the S-tolerance, it did however effect the metal dispersion which, at higher levels, appears to increase the sulphur saturation coverage and therefore adversely affecting the SR activity.

7. The presence of sulphur in the reaction mixture shifted the catalyst light-off to progressively higher temperatures indicating a decrease in the rate of methane oxidation at low temperature and high P_{O2} due to a lower availability of Rh active sites.

References

[1] C. Bartholomew, Appl. Catal. A: General 212 (2001) 17.

[2] J. Oudar, Catal. Rev. Sci. Eng. 22-2 (1980) 171.

[3] C. Brinkmeier, PhD Dissertation, University of Stuttgard, 2006.

[4] R. Kalia, A. Gutierrez, O. Krause, App. Catal. B: Environmental 84 (2008) 324.

[5] M. Mundschau, C. burk, D. Gribble Jr., Catal Today 136 (2008) 190.

[6] M. Ferrandon, J. Mawdsley, T. Krause, App. Catal. A: General 342 (2008) 69.

[7] V. Choudhary, K. Mondal, T. Choudhary Catal. Comm. 8 (2007) 561.

[8] C. Brinkmeier, PhD Dissertation, University of Stuttgard, 2006.

[9] T.J. Truex, SAE paper n. 01-1543 (1999).

[10] A. Bitsch-Larsen, N.J. Degenstein and L.D. Schmidt, Appl. Catal. B: Environmental 78 (2008) 364-370.

[11] R. Torbati, S. Cimino, L. Lisi, G. Russo, Catal. Lett. 127 (2009) 260.

[12] R. Horn, K.A. Williams, N.J. Degenstein, A. Bitsch-Larsen, D. Dalle Nogare, S.A. Tupy, L.D. Schmidt, J. Catal. 249 (2007) 380.

[13] F. Donsì, S. Cimino, A. Di Benedetto, R. Pirone, G. Russo, Catal. Today 105 (2005) 551.

[14] G.B. Fisher, K.M. Rahmoeller, C.L. DiMaggio, K. Wadu-Mesthrige, J.G. Weissman, E.C. Tan, L. Chen and J.E. Kirwan, North American Catalyst Society 20th North American Meeting, Huston TX June17-22, 2007.

[15] J. Hepola, J. McCarty, G. Krishnanc, V. Wong, Appl. Catal. B: Environnmental 20 (1999) 191.

[16] R. Hegde, J. White, J. Phys. Chem. 90 (1986) 296-300.

[17] L. Smith, H. Karim, M. Castaldi, K. Lyle, S. Etemad, W. Pfefferle, V. Khanna, K. Smith, J. Eng. Gas Turbines Power 127 (2005) 27.

[18] S. Cimino, G. Landi, L. Lisi, G. Russo, Catal. Today 117 (2006) 454.

5. Effect of Partial Substitution of Rh Catalysts with Pt or Pd During the Catalytic Partial Oxidation of Methane in the Presence of Sulphur

5.1 Introduction

Many studies have been published on the partial oxidation of methane over noble metals but only few studies have been done very recently in the presence of sulphur compounds [1,2]. Although there has been no direct study on the improvement on the sulphur tolerance of Rh based catalysts conducted under CPO conditions, it has been reported that the addition of Pt [3] or Pd [4] to Rh improves the activity of the catalyst during the steam reforming of sulphur containing fuels. In addition partial substitution of Rh with Pt or Pd will be highly economical due to high cost of Rh metal. Accordingly, the purpose of this work is to investigate the enhancement in sulphur tolerance of Rh-based catalyst by partially substituting Rh with either Pt or Pd under self-sustained steady state operation at high temperatures and short contact times as well as during low temperature light-off phase. In this chapter the use of in-situ diffuse reflectance infrared Fourier transform spectroscopy (DRIFTS) of adsorbed CO at room temperature has been used to investigate changes on the surface state of rhodium before and after exposures to sulphur species at temperatures and conditions close to those expected under actual CPO of methane. Furthermore, an attempt is made to identify sites responsible for the loss in the catalytic activity by comparing the results with the activity data.

5.2 Experimental Procedure

The La_2O_3-Al_2O_3 supported monometallic Rh (Rh/LA) and bimetallic Rh-Pt (Rh-Pt/LA) and Rh-Pd (Rh-Pd/LA) monolith samples were prepared according to the procedure described in Chapter 2.1.2. The catalytic tests were carried out on monolith samples as described in Chapter 2.2.2. Catalysts were characterised by techniques described in Chapter 2.3.

5.3 Results and Discussion

5.3.1 Characterisation

Table 5.1 illustrates catalyst denomination, total surface areas and their total CO uptake after H_2 reduction at 800 °C. The commercial γ-alumina stabilized with La_2O_3 (Sasol) is

characterized by a specific surface area of ~140 m^2/g in contrast to 8 m^2/g of the α-alumina employed to prepare reference Rh catalyst for DRIFTS experiments, as a result the Rh/AA sample has a much lower dispersion with respect to the Rh/LA sample. The metal dispersions were calculated by assuming the stoichiometric factor between the CO and metal atoms to be 1:1. However, since the stoichiometric ratio depends on the precious metal and several possible forms of adsorbed CO may coexist, caution should be exercised when comparing the dispersion values of different catalysts. As a result, only dispersion values for the monometallic Rh catalysts are presented in Table 5.1. Furthermore, assumption of a unique stoichiometry should also be carefully considered for catalysts containing only Rh, as the CO adsorption changes from predominantly linear to gem-dicarbonyl form for catalysts with low and high rhodium dispersion, respectively [5,6] (see DRIFTS experiments). In addition, since CO can adsorb on Rh, Pt and Pd, it is not possible to measure the number of each metal sites independently, consequently the chemisorptions data are also reported in terms of the total amount of CO consumed per gram of precious metal. The Rh/LA sample has the highest CO uptake, due to its high Rh content and large surface area of the support material. The bimetallic catalysts have similar CO uptake due to substitution of half of Rh for Pt or Pd.

The actual loadings of noble metals are close to the nominal one for both catalysts: in particular it can be noted that Rh content is halved in bimetallic samples and substituted by a corresponding weight of Pt or Pd. BET values for the final monolith catalysts after deposition of precious metals are in line with the corresponding support washcoat layer (~150 m^2/g), which was obtained with addition of alumina binder and calcination in air at 800 °C.

Sample	Honeycomb[a] LxD (mm)	Washcoat material	B.E.T.[b] m^2/g	ICP[b] wt % Rh	Pt	Pd	CO Uptake (mmol/g pgm)	Dispersion[c] %
AA	–	α-Al_2O_3	7.8					
LA	–	3% La_2O_3-γAl_2O_3	143	–	-	-	–	-
Rh/AA	–	-	8.0	0.92	-	-	0.90	6.7
Rh/LA	10x17	LA	150	0.95	-	-	5.54	42
Rh-Pt/LA	10x17	LA	151	0.50	0.48	-	3.53	-
Rh-Pd/LA	10x17	LA	153	0.51	-	0.60	3.60	-

[a] cordierite, 600cpsi, channel side 0.96mm, wall thickness 76μm
[b] referred to total weight of active phase, monolith substrate excluded
[c] by CO chemisorptions after reduction in H_2 at 800°C; CO/Metal stoichiometry=1

Table 5.1: *ICP-MS, BET and CO chemisorptions for structured catalysts and their corresponding supports.*

SEM inspection of all monoliths showed a good adhesion of the washcoat whose accumulation in the corners causes the typical roundening of the originally squared channels of the cordierite substrate. SEM/EDS mapping on both longitudinal and transverse sections of the monoliths indicated that the sequential impregnation procedure employed for the preparation of bimetallic systems ensured a uniform dispersion of precious metals elements throughout the washcoat layer (but not in the cordierite support): this is shown in Figure 5.1 by the EDS maps in false colours for Rh and Pt.

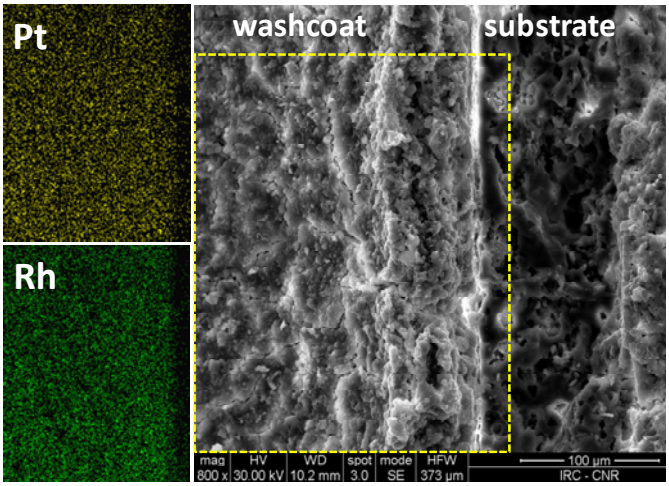

Figure 5.1: *SEM image of a longitudinal section of the Rh-Pt bimetallic monolith catalyst with corresponding false colours EDS maps showing Pt and Rh distribution in the stabilized alumina washcoat layer (LA).*

DRIFTS spectra of adsorbed CO on pre-reduced catalysts provides information on the state and morphology of the rhodium component as the adsorption mode of CO is sensitive to different rhodium structures [5]. In order to gain insight into the nature of the Rh active sites during the CPO of methane in the absence and presence of sulphur under self-sustained reaction conditions at high temperatures, DRIFTS experiments were carried out at room temperature before and after sulphation of the sample at 800 °C under H_2S/H_2 reaction mixture. The reducing nature of the sulphur-containing mixture was chosen in order to carry out the experiments under conditions close to those prevailing during actual autothermal operation, since both short contact time and high reactants concentration used in the catalytic tests could not be reproduced in the DRIFT cell. Furthermore, preliminary tests indicated that the effect of sulphur poisoning was independent from the type of sulphur precursor (SO_2 or H_2S) in the presence of high concentrations of H_2.

The DRIFTS spectrum of CO adsorbed at room temperature over reduced Rh/LA is shown in Figure 5.2a. The dominant features of the spectrum are the doublet bands at 2090 and 2016 cm^{-1} corresponding to gem-dicarbonyl species on isolated Rh atoms. The presence of these bands is related to highly dispersed Rh metal particles on the catalyst surface [6]. However, there is also a presence of a very weak band at around 2060 cm^{-1} which can be assigned to the linearly adsorbed CO on Rh crystallites or clusters in the zero oxidation state, the identification of which is impeded by the overlap with the twin dicarbonyl bands. The presence of linear and dicarbonyl features in the spectrum indicates the existence of two different adsorption sites on the surface of the catalyst. Following the sulphation of the sample at 800 °C and cooling down under H_2S/H_2 reaction mixture, the band at 2060 cm^{-1} becomes the only distinct band in the CO spectrum indicating the presence of only linearly adsorbed CO – Figure 5.2b. These results suggest that only the dispersed Rh species (responsible for Rh-$(CO)_2$ formation) are affected by S-poisoning whilst the Rh-CO species are not modified by sulphur. Thus, sulphur appears to act as a selective poison which preferentially adsorbs on smaller crystallites i.e. sulphur adsorption is structure-sensitive [7]. Figures 5.2c-e illustrate the effect of catalyst regeneration by reduction at progressively higher temperatures (500 °C to 700 °C) which results in an increase in the intensity of the doublet bands. Reduction at 800 °C results in the complete reappearance of the gem-dicarbonyl bands illustrating that the sulphur poisoning is reversible- Figure 5.2f.

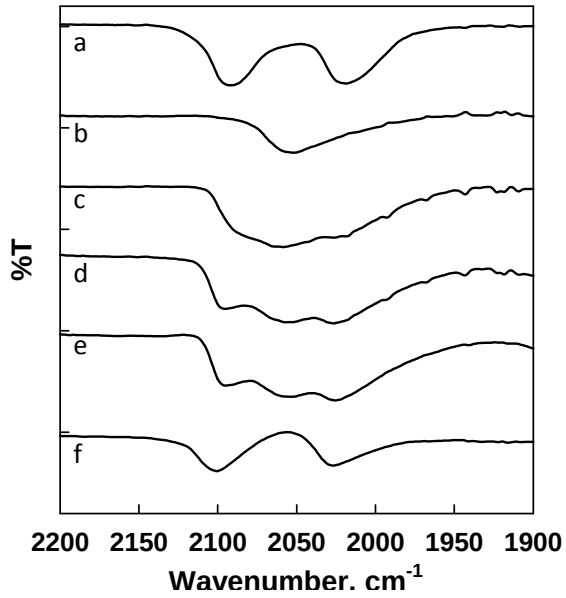

Figure 5.2: *DRIFT spectra of CO adsorption at room temperature over Rh/LA catalyst following: a) reduction of fresh catalyst at 800 °C for 1 h, b) H_2S/H_2 reaction at 800 °C for 30 min., c) regeneration under 2%H_2-N_2 reaction mixture for 1 h at c) 500 °C, d) 600 °C, e) 700 °C and f) 800 °C. Spectra are offset for clarity.*

The adsorption of CO at room temperature before and after S poisoning is schematically represented in Figure 5.3.

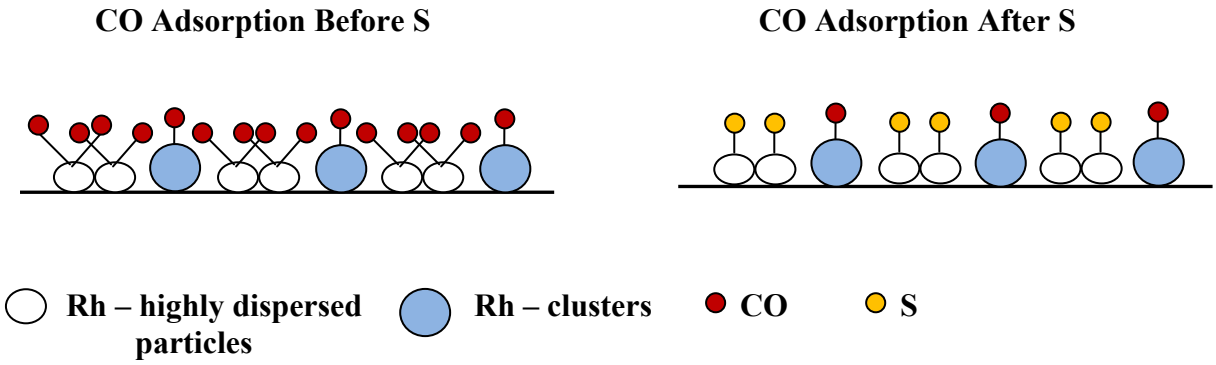

Figure 5.3: *Schematic representation of CO adsorption at room temperature before and after sulphur poisoning on Rh catalyst.*

In order to confirm the selective adsorption of sulphur on highly dispersed Rh sites, the same experiments were repeated on Rh/AA catalyst with a lower precious metal dispersion (Table 5.1), due to the much lower surface area of α-Al_2O_3 support. Accordingly, the DRIFTS spectrum of the CO adsorbed at room temperature over reduced Rh/AA sample reveals a strong band at 2070 cm^{-1} and two shoulders at 2098 and 2025 cm^{-1} as shown in Figure 5.4a. The fact that absorption bands of the dicarbonyl species were poorly developed and the band ascribable to linear CO was much more intense confirms a higher fraction of larger metallic Rh particles with respect to the highly dispersed Rh^+ phase. This result is in agreement with the latest findings on Rh/α-Al_2O_3 where increasing Rh concentration in the sample resulted in an increase in the intensity of the linear CO band due to growth in metal particle size [8]. The difference in the position of the linear CO bands on freshly reduced rhodium sites on La-γAl_2O_3 (2060 cm^{-1}) and α-Al_2O_3 (2070 cm^{-1}) is a consequence of different particle size. This result agrees with the observation that frequencies of CO species shift to higher wavenumbers for bigger metal particles [9]. Figure 5.4b shows the spectrum of the adsorbed CO after H_2S/H_2 reaction mixture at 800 °C for 30 min. The band at 2070 cm^{-1} becomes the only distinct band in the CO spectrum with the gem-dicarbonyl species being completely removed from the rhodium surface, exemplifying the preferential adsorption of S on isolated Rh^+ sites. However, the IR band due to adsorbed linear CO is found to shift slightly to higher wavenumbers (from 2070 to 2080 cm^{-1}) following sulphation. The upward shift in the vibrational frequency is likely to be due to the increase in the dipole-dipole coupling as a result of a higher coverage of adsorbed CO. A similar behaviour is also reported by Anderson

et al. [10] who observed that evacuation of CO at room temperature and at higher temperatures caused the strong band at 2071 cm^{-1}, attributed to linearly adsorbed CO shift to 2058 cm^{-1}, due to a decrease in dipole coupling between adjacent CO molecules. In an attempt to reactivate the sulphur poisoned catalyst, the sample was treated with hydrogen at 800 °C for 1 h. The relative intensity of the peak at 2080 cm^{-1} decreased and at the same time returned back to its initial wavenumber (2070 cm^{-1}), while the intensities of the gem-dicarbonyl bands increased, indicating that the catalyst can be regenerated by hydrogen treatment.

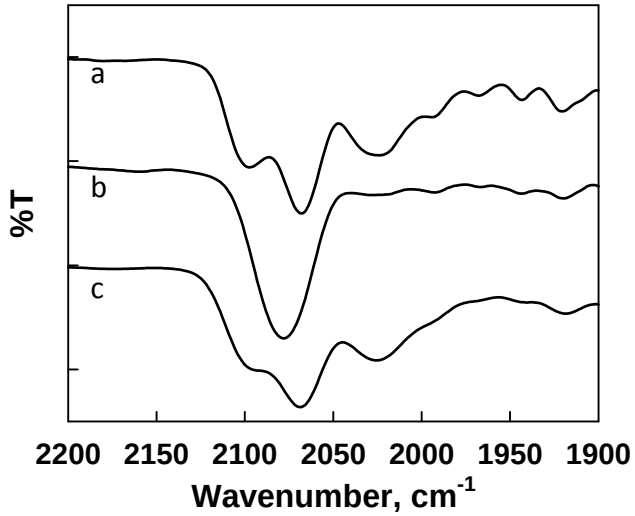

Figure 5.4: *IR spectra of CO adsorption at room temperature over Rh/α-Al_2O_3 following: a) reduction of fresh catalyst at 800 °C for 1 h; b) H_2S/H_2 reaction at 800 °C for 30 min. and c) after hydrogen reactivation at 800 °C for 1 h.*

In conclusion, the above IR measurements confirm that sulphur preferentially adsorbs on smaller Rh crystallites which are much less abundant on Rh/AA catalyst where the formation of large metallic particles (Rh^0) is favoured.

Figure 5.5 shows the IR spectra of CO adsorbed at room temperature on the reduced, sulphur poisoned and hydrogen reactivated Rh-Pt/LA catalyst. Once again the spectrum is dominated by bands at 2095 and 2025 cm^{-1} due to a rhodium gem-dicarbonyl species following sample reduction at 800 °C, as shown in Figure 5.5a. However, the presence of a shoulder at 2060 cm^{-1} which was masked by the intense dicarbonyl bands for supported rhodium only, is clearly visible for the bi-metallic catalyst. It has been stated by many authors [11-13] that CO adsorption on Pt gives two bands attributed to linear (2050-2070 cm^{-1}) and bridge forms

(1840-1860 cm^{-1}) although Chang et al. [14] observed only one peak at 2060 cm^{-1} following CO adsorption over fresh Pt/γ-Al_2O_3 catalyst. In our experiments the band at 1845 cm^{-1} was very weak and in some cases it was not detected. The band at 2060 cm^{-1} can be assigned to CO adsorption on Pt clusters which also includes to a lesser extent the contribution of CO bonded to metallic Rh particles. The infrared absorption bands of the CO adsorbed at room temperature following exposure to H_2S is shown in Figure 5.5b. Once again the linearly adsorbed CO band becomes the only distinct band in the CO spectrum following sulphation accompanied by a shift to higher wavenumbers, from 2060 cm^{-1} for a freshly reduced sample to 2075 cm^{-1} following sulphation. The shift to higher frequency is consistent with the IR spectra characterizing CO adsorbed on sulphur-poisoned Pt catalysts, reported by Hoyos *et al*. [15] and is suggested to be a consequence of partial deposition of sulphur on Pt clusters, and/or the formation of PtS. Following hydrogen treatment (Figure 5.5c) the spectrum of the hydrogen reactivated sample, although the bands are less intense compared to the freshly reduced sample, the profile of the spectra are very similar, suggesting that also the bi-metallic Rh-Pt catalyst can be reactivated following sulphur poisoning.

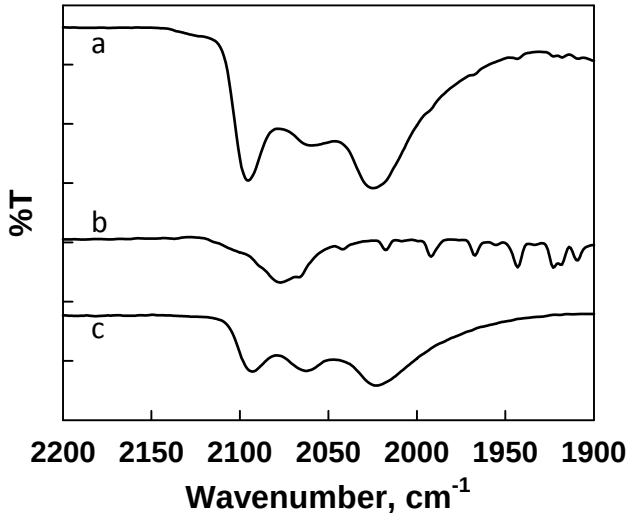

Figure 5.5: *IR spectra of CO adsorption at room temperature over Rh-Pt/La-Al_2O_3 catalyst following: a) reduction of fresh catalyst at 800 °C for 1 h; b) H_2S/H_2 reaction at 800 °C for 30 min. and c) hydrogen reactivation at 800 °C for 1 h.*

Figure 5.6 illustrates the infrared spectra of CO adsorbed at room temperature on Rh-Pd/LA catalyst. Following sample reduction (Figure 5.6a), the only bands observed (2090 and 2017 cm^{-1}) are due to the gem-dicarbonyl CO species formed on well dispersed rhodium particles. Theses bands are overlapped with the very weak IR band of the linear species (~2060 cm^{-1}). It

has to be noted, however, that unlike the bimetallic Rh-Pt catalyst (Figure 5.5a), which clearly exhibited the band corresponding to linear adsorbed CO (at 2060 cm^{-1}) on metallic Pt particles, the band typically attributed to linear adsorbed CO on Pd (at 2060-2070 cm^{-1}) [16,17] in the Rh-Pd sample is absent. It has also been reported that the intensity of bands related to linear CO adsorbed on rhodium is more intense than the corresponding bands on palladium [17]. Moreover, the linear CO band on palladium is strongly affected by reduction cycles [16] or even by evacuation treatment at room temperature [17], thus in these spectra the contribution of the Pd^0-CO species can be tentatively neglected. Furthermore, it has been shown that under oxidising conditions, the Pd-Rh alloys were enriched in palladium, whereas under reducing condition, palladium particles tend to segregate while rhodium could diffuse through the Pd layer without any phase separation of the alloy particles [18,19]. The reason that the spectrum of CO adsorbed on freshly reduced Rh-Pd sample is characteristic of well dispersed Rh particles, could be due to the presence of palladium which promotes the formation of Rh gem-dicarbonyl species. Similar conclusion was also reached by Maillet et al. [17] following the reduction treatment of various alumina supported Pd-Rh catalysts at high temperatures. After treatment in the H_2S/H_2 reaction mixture at 800 °C, the spectrum of CO adsorbed at room temperature (Figure 5.6b) is characteristic of linear CO-Rh^0 species (band at 2060 cm^{-1}) as observed on Rh only catalyst, with the complete removal of the gem-dicarbonyl species. Regeneration at 800 °C in the reducing atmosphere results in the reappearance of the gem-dicarbonyl bands illustrating that the sulphur poisoning is reversible- Figure 5.6c.

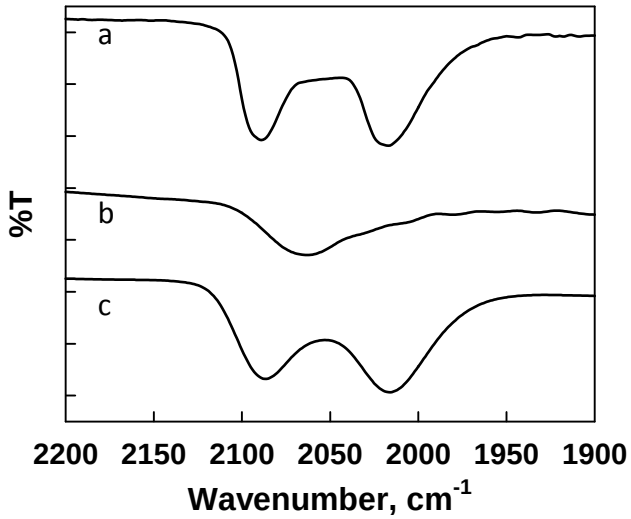

Figure 5.6: *DRIFTS spectra of adsorbed CO on Rh-Pd/La-Al_2O_3 catalyst at room temperature after: a) reduction of fresh catalyst at 800 °C for 1 h; b) H_2S/H_2 reaction at 800 °C for 30 min. and c) hydrogen regeneration at 800 °C for 1 h.*

Overall, the above DRIFTS studies indicate that the addition of another noble metal such as Pt or Pd does not influence directly the way sulphur adsorbs and interacts on the highly dispersed Rh sites.

5.3.2 CPO Light-Off

It has already been demonstrated that the presence of sulphur in the reaction feed on Rh based catalysts shifts the minimum catalyst light-off for CPO to higher temperatures [20]. The shift in the catalyst light-off temperature is due to sulphur poisoning which reduces the availability of active metal sites. During the transient pre-ignition period the catalyst is exposed to a large partial pressure of oxygen. Table 5.2 illustrates the effect of addition of 20 ppm H_2S in the reaction feed on the ignition of methane-air mixtures at fixed feed ratio (CH_4/O_2 = 1.8) over LA supported Rh, Rh-Pt and Rh-Pd monolith samples pre-reduced under reaction conditions: the results are presented in terms of both minimum light-off temperatures and final operating temperature under self sustained operation at fixed preheating. It can be seen that both in the absence and presence of sulphur, the monometallic Rh sample which has the highest Rh content shows the lowest light-off temperature (270 °C and 302 °C, respectively), indicating that dissociation of methane occurs more readily over Rh active sites under the studied reaction condition. In fact the substitution of half of the Rh loading with either Pt or Pd causes a rise of the minimum light-off temperature to about 290 °C regardless of the nature of the second precious metal. It should be noted however that, the increase in the catalyst light-off temperature and in the catalyst operating temperature, observed for all the catalysts before and after the addition of H_2S in the feed, is smallest over the bimetallic Rh-Pt catalyst and largest over the Rh-Pd sample (Table 5.2). Therefore, Pt appears to be able to limit the poisoning effect of S towards Rh sites, whereas the opposite trend is observed in the presence of Pd.

Catalyst	**H_2S = 0 ppm**		**H_2S = 20 ppm**		**Δ T Light-off**	**$\Delta T_{cat.}$**
	Light-off	**$T_{cat.}$**	**Light-off**	**$T_{cat.}$**		
	°C		°C		°C	
Rh	270	750	302	909	32	159
Rh-Pt	290	816	309	900	19	84
Rh-Pd	289	770	333	942	44	172

Table 5.2: *Effect of H_2S addition on light-off and on the final catalyst temperature during CPO of methane under self-sustained operation at pre-heating temperature of 350 °C over La-Al_2O_3 supported Rh, Rh-Pt and Rh-Pd monoliths. CH_4/O_2 = 1.8 in air, GHSV = 8 x 10^4 h^{-1}.*

In order to get further insights on the reason for such protecting effect, TPD experiments were carried out following S ageing of the three supported Rh, Rh-Pt and Rh-Pd catalysts at 300 °C with 100 ppm SO_2 in air for 2 h. Results are shown in Figure 5.7 comparing desorption profiles of SO_2 which was the only detected S-specie. All the catalysts show a broad desorption peak centered at 750-780 °C which appears to be mostly due to the decomposition of very stable aluminum sulphate species [21]. The possible contribution of other S-species is masked by the main signal. From the peak areas the amount of sulphur taken up by the catalysts decreases in the order Rh-Pt > Rh > Rh-Pd (0.95, 0.79 and 0.60 mg of S/g cat, respectively). The higher amount of S uptake on the bimetallic Rh-Pt catalysts corresponds to the to higher oxidation activity of Pt which more readily oxidises SO_2 to SO_3 rather than Rh and Pd [22]. Once oxidized to SO_3 the sulphur species can be readily stored on the catalyst support as $Al_2(SO_4)_3$ thus minimising the build-up of S on or close to the active Rh sites where methane activation reactions take place. On the other hand the detrimental effect of Pd in the bimetallic Rh-Pd system is due to its higher sensitivity to sulphur poisoning and formation of stable $PdSO_4$ species [23]. This reduces the rate of SO_3 formation and SO_3 migration on to the support which in turn decreases sulphation of the support material whilst leading to higher accumulation of sulphate species around the precious metal which inhibits the catalytic activity. In analogy to the current results, it was already reported that the use of a less sulphating support for Rh such as a SiO_2-Al_2O_3 does not enhance the sulphur tolerance of the catalyst with regards to light-off delay, since more sulphur tends to stick close to the Rh active sites [21].

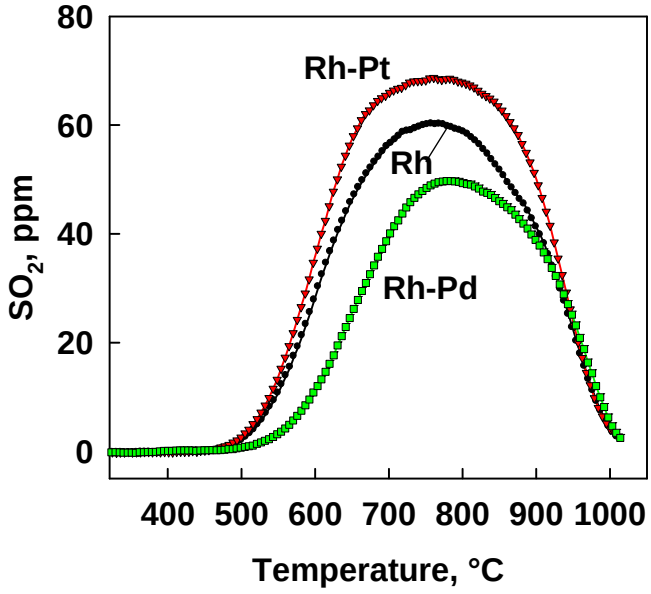

Figure 5.7: *TPD profiles of SO_2 from S-aged Rh, Rh-Pt and Rh-Pd supported (LA) catalysts (300 °C 100 ppm SO_2 in air, 2 h ~14 mgS/ g_{Cat}).*

5.3.3 CPO Activity measurement

Figure 5.8 compares the catalytic activities of LA supported Rh, Rh-Pt and Rh-Pd catalysts during the CPO of methane, under pseudo-adiabatic conditions at a fixed CH_4/O_2 feed ratio, using 10% N_2 dilution, in the absence or presence of 20 ppm H_2S. In the absence of sulphur monometallic Rh catalyst showed the best performance in terms of methane conversion and CO and H_2 yields. Substitution of half of the Rh loading with same weight amount of Pt and even more with Pd entails a reduction in fuel conversion and yield to syn-gas. This is accompanied by a significant increase in the operating temperatures measured on bimetallic monoliths. Among bimetallic catalysts, Rh-Pt performs better than Rh-Pd. Such results confirm that Rh is the most active and selective metal for methane CPO, whereas on both Pt and Pd reactions leading to total oxidation products become more important. In fact it was reported that the higher syngas yield on Rh is strictly associated to its higher methane steam reforming activity whose contribution is significant even at very short contact times [24].

The presence of 20 ppm H_2S in the reaction feed resulted in a loss in the activities and an increase in the surface temperature by $\geq$ 100 °C of all the catalysts, the effect being more pronounced over the Rh-Pd system. The decrease in methane conversions in the presence of sulphur was accompanied by a decrease in CO yield of similar magnitude (except for Rh-Pt) while in comparison the drop in H_2 yield was always larger. The decrease in the catalytic performances and the rise in the catalyst temperature in the presence of H_2S is an indication of the inhibition of the steam reforming reaction, as shown in previous studies [20,25,26]. The significant loss in activity observed over the Rh-Pd catalyst could be caused by the formation of stable palladium sulphide or due to the migration of sulphur into bulk Pd which can then adversely affect the Rh-Pd interaction. An alternative explanation may be due to the presence of highly dispersed Rh particles on the surface of the Pd particles, which are more readily poisoned by the sulphur in the reaction feed, since it was shown in section 5.3.1 (Figure 5.6) that the presence of palladium promotes the formation of Rh gem-dicarbonyl species. These results also support our previous findings [21] where the inhibition effect of S was found to be greater over a sample which had higher Rh dispersion. Unlike the Rh-Pd system, however, the bimetallic Rh-Pt catalyst with only half the amount of rhodium content by weight (2:1 Rh:Pt molar ratio) showed a better specific tolerance to sulphur inhibition since the overall catalytic performance are close to the monometallic Rh catalyst.

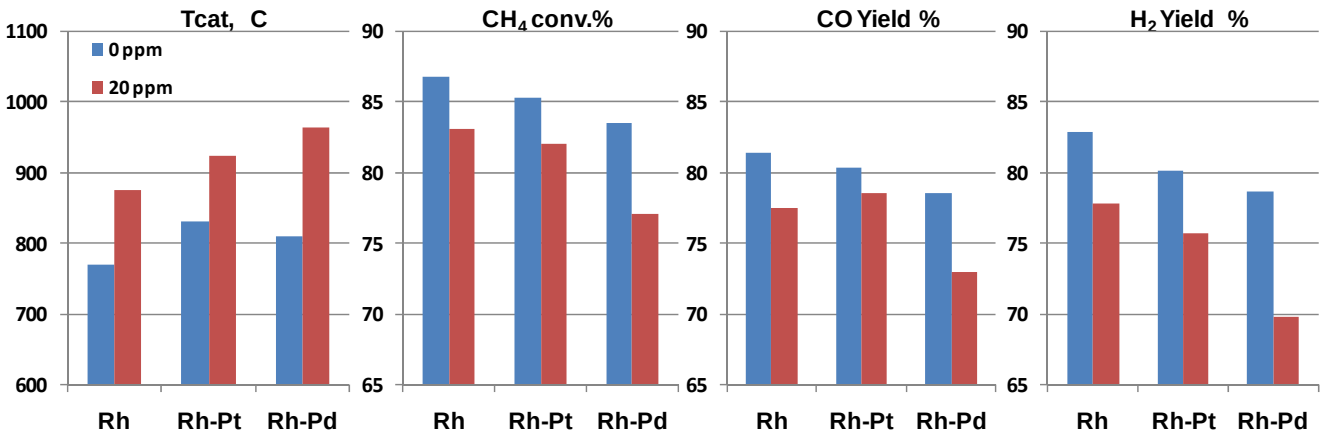

Figure 5.8: *Comparison of CH_4 conversion, CO and H_2 yield and catalyst temperature on Rh, Rh-Pt and Rh-Pd supported on La-Al_2O_3 catalysts in the absence and presence of 20 ppm H_2S. CH_4/O_2 = 2, GHSV = 6.1 x 10^4 h^{-1} and N_2 = 10%.*

As a result, further studies were carried out over the bimetallic Rh-Pt catalyst in order to gain better understanding of its improved performance.

Figure 5.9 illustrates the transient effect of addition and removal of 8, 18 and 37 ppm H_2S to and from the reaction mixture under CPO conditions over Rh-Pt/LA monolith operated at a fixed CH_4/O_2 feed ratio, using 20% N_2 dilution. The addition of H_2S resulted in a sharp decrease in CH_4 conversion and H_2 selectivity with a corresponding rapid increase in the catalyst temperature following a similar trend to that observed in our previous study over the monometallic Rh/LA monolith [20]. However, unlike the monometallic Rh sample where the CO selectivity was almost unaffected, even at the highest sulphur concentrations [20], there is a slight increase in the CO selectivity over the bimetallic Rh-Pt which increases with H_2S concentration in the feed. The extent of reaction inhibition by S was also found to be greater at lower H_2S concentration. However, the inhibition effect of sulphur did not reach a saturation level even at H_2S concentrations of 37 ppm.

Upon removing the H_2S from the reaction feed, the initial conversion and product distribution were regained immediately. The recovery in the catalytic activity was also accompanied by a sharp decrease in the catalyst temperature to its initial value before the H_2S addition, indicating that the sulphur poisoning effect was completely reversible under the studied reaction condition, in accordance with the above IR studies. Furthermore, the rapid response upon the introduction and removal of sulphur suggests that the inhibition was caused by

selective reversible sulphur adsorption onto the metal active sites. However, as seen in Figure 5.9 the catalyst performance continues stable in the presence of H_2S indicating that there is a steady state between S adsorbing on the surface of the active sites and S desorbing into the gas phase, which is governed by the catalyst temperature and sulphur concentration.

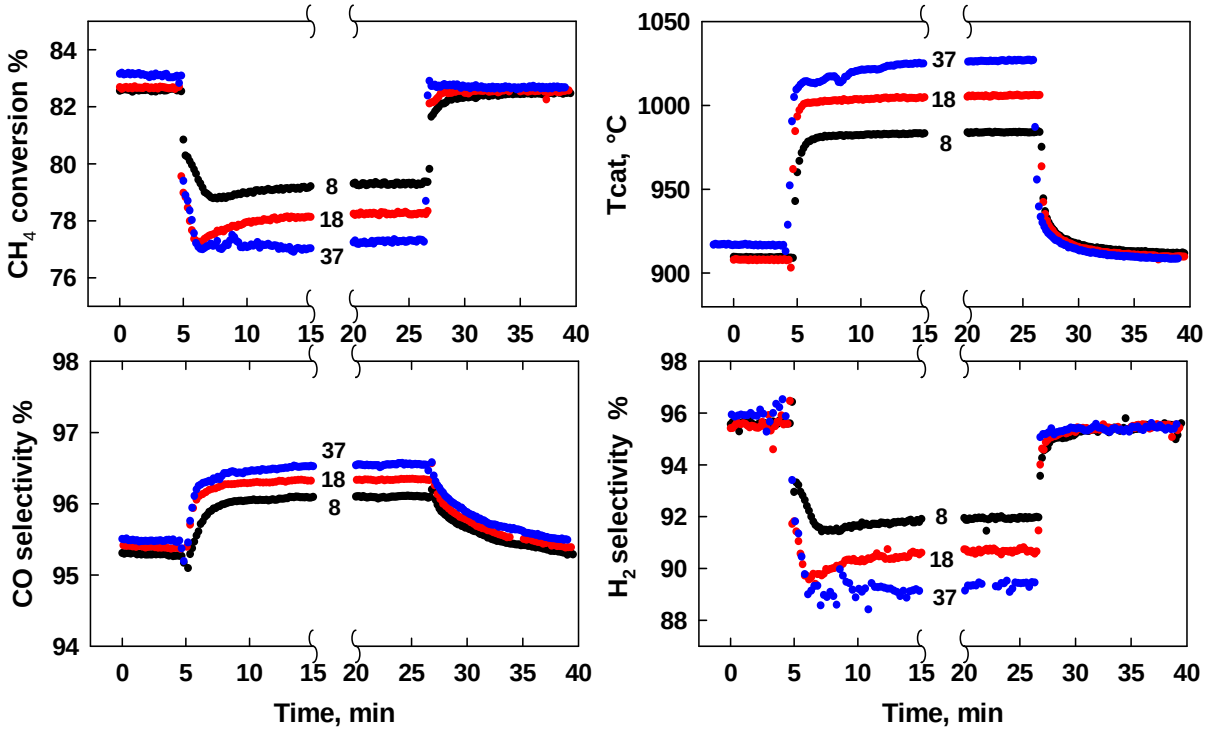

Figure 5.9: *Transient response to H_2S addition (8, 18 or 37 ppm) and removal on methane conversion, catalyst temperature, CO and H_2 selectivities during methane CPO on Rh-Pt/LA monolith. Feed CH_4/O_2=2, GHSV= 6.7·10^{4}h^{-1}, N_2=20% vol.*

The differences in the catalytic CPO performance of Rh-Pt/LA monolith at steady state due to increasing H_2S concentrations at a fixed CH_4/O_2 feed ratio are summarized in Table 5.3. It can be seen that the reduction in methane conversion following sulphur addition is accompanied by a larger reduction in hydrogen production, with a molar ratio of approximately 3.6-3.8. These values are higher than those reported previously for the monometallic Rh catalyst [20], which were close to 3, indicating that the poisoning effect of H_2S is related to its ability to inhibit the endothermic steam reforming reaction (5.1) which mainly occurs in the second region of the catalyst bed, after oxygen has been consumed, between the unconverted methane and water produced in the first oxidation zone of the reactor [20,26].

$$CH_4 + H_2O \leftrightarrow CO + 3H_2 \qquad \Delta H_r^{25°C} = +206 \text{ kJ/mol} \qquad (5.1)$$

		H_2S				Difference*		
CH_4/O_2=2		0 ppm	8ppm	18ppm	37ppm	Δ (8-0)	Δ (18-0)	Δ (37-0)
X_{CH4}	(%)	82.7	79.3	78.2	77.1	-3.4	-4.5	-5.6
Y_{H2}	(%)	79.0	72.5	71.0	68.8	-13.0	-16.0	-20.4
Y_{CO}	(%)	79.0	76.2	75.3	74.4	-2.8	-3.7	-4.6
Y_{H2O}	(%)	3.7	6.8	7.2	8.3	+6.2	+7.0	+9.2
Y_{CO2}	(%)	3.7	3.1	2.9	2.7	-0.6	-0.8	-1.0
H_2/CO	-	2.00	1.90	1.89	1.85			
T_{cat}	(°C)	909	984	1005	1025	+75	+96	+116
T_{out}	(°C)	696	721	733	744	+25	+37	+48

* Products molar flows per 100 CH_4 feed

Table 5.3: *Effect of H_2S addition at various concentrations on the steady state methane CPO on Rh-Pt/LA monolith. Feed CH_4/O_2=2, GHSV= $6.7 \cdot 10^4 h^{-1}$, N_2=20% vol.*

In addition, unlike the monometallic Rh catalyst where the decrease in methane conversion in the presence of sulphur was accompanied by a decrease in CO yield of similar magnitude (Figure 5.8), over the bimetallic Rh-Pt catalyst CO selectivity rises upon sulphur addition (Figure 5.9), and the decrease in CO yield is slightly less than the corresponding reduction in methane conversion. At the same time, unlike the only Rh catalyst, the ΔCH_4 does not correspond to the ΔH_2O i.e. the additional amount of water formed in the products is more than what is expected by its consumption in methane steam reforming (5.1).

To sum up, products redistribution from the bimetallic Rh-Pt catalyst in the presence of S appears to be the result of two superimposed effects: i) inhibition of steam reforming path on Rh sites and ii) improved process selectivity towards oxidation of H_2 to H_2O, probably due to the nature of the Pt active sites, which display a higher intrinsic selectivity towards CO and H_2O during methane CPO in comparison to Rh sites [24]. Both effects are compatible with the selective adsorption of S on isolated (well dispersed) Rh sites only. In agreement with DRIFTS results the formation of surface Rh sulphide species does not appear to be directly affected by the simultaneous presence of Pt on the surface of the catalyst. However the equilibrium coverage of Rh by sulphur depends on temperature and partial pressure of H_2 and H_2S, therefore it is indirectly affected by the presence of Pt in the catalyst formulation, since the presence of Pt causes an increase in the catalyst operating temperature during the self sustained CPO of methane, due to its higher oxidation activity.

In order to examine the effect of initial catalyst temperature on the extent of sulphur poisoning over the Rh and Rh-Pt catalysts, the CPO reactions were carried out by using N_2 dilutions of either 20 or 55.6 %vol. with the latter corresponding to using air as an oxidant at a fixed CH_4/O_2 feed ratio of 2. The results are illustrated in Figure 5.10 in terms of catalyst temperature, methane conversion, yields to CO and H_2, vs sulphur concentration in the feed. The temperature profiles for both catalysts display the same increasing trend as sulphur is added, but some major differences can be noted when comparing their behaviours at different dilutions. When using feed conditions with lower N_2 dilution, the bimetallic Rh-Pt system always operates at higher temperatures (~100 °C) than the Rh only sample regardless of the sulphur content in the reaction mixture. Figure 5.10 indicates that resulting methane conversions are similar and progressively decrease with S content approaching a plateau above 30 ppm of H_2S.

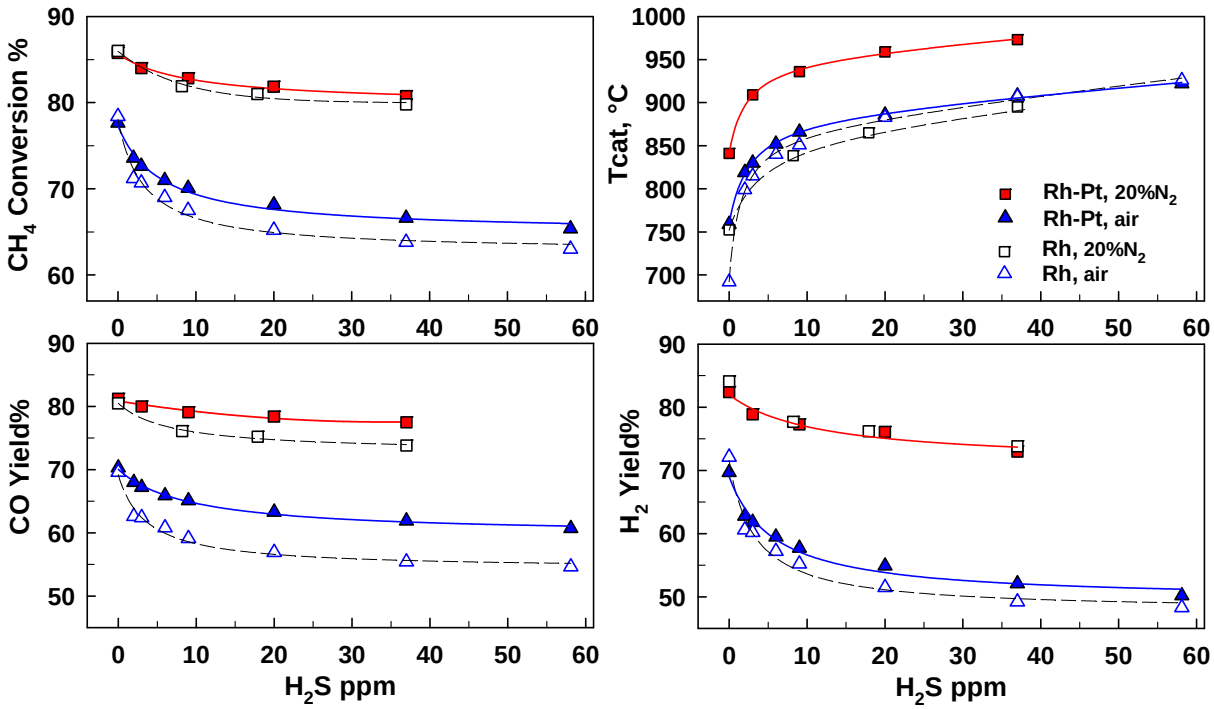

Figure 5.10: *Effect of H_2S addition on CH_4 conversion yields to CO and H_2 and the catalyst temperature during the CPO of methane over Rh-LA and Rh-Pt/LA monolith at CH_4/O_2 = 2 at two different N_2 dilution levels of the feed (20% and 55.6% = air). GHSV = 6.7 x 10^4 and 8.1 x 10^4 h^{-1}, for feed mixture containing N_2 = 20% and 55.6% vol.%, respectively.*

It can be seen that in the presence of S there is a significant advantage in terms of yield to CO and CH_4 conversion over the Rh-Pt catalyst, whose higher operating temperature appears to be induced by its lower Rh content, thus reducing the impact of S inhibition. It was already

shown in Figure 5.8 that even at lower dilution (N_2=10%), corresponding to higher operating temperature, Rh only catalyst is still able to outperform the bimetallic Rh-Pt counterpart with regards to H_2 yield and methane conversion in the presence of 20 ppm H_2S.

When CPO experiments are carried out in air (i.e. at higher dilution), significantly lower methane conversions are achieved over the two catalytic systems, due to the lower operating temperature and shorter contact times. In the absence of sulphur both samples show similar activities in methane conversion and yields to CO and H_2. However, upon addition of sulphur the rate of deactivation of Rh-Pt catalyst is slower than its monometallic counterpart, showing higher methane conversions and yields to CO and H_2. Furthermore, in the absence of sulphur in the reaction feed, the bimetallic system operates at approximately 70 ºC higher than its monometallic counterpart whilst the difference diminishes when adding small amounts of sulphur (2 ppm) in to the reaction feed. In the presence of sulphur, the Rh only catalyst shows a bigger jump in the catalyst temperature and a greater loss in CH_4 conversion compared to the Rh-Pt system, thus indicating a higher sensitivity to sulphur poisoning when operating at lower initial reaction temperatures. This was already shown to be related to the equilibrium between formation-decomposition of surface Rh-sulphides species [20].

Therefore the higher sulphur tolerance of the bimetallic catalyst, in particular when operating under dilute reaction environment appears to be strictly connected to both the higher self sustained catalyst temperature, which tends to reduce the impact of S on Rh sites favouring surface sulphide decomposition [20], and to the simultaneous presence of Pt sites, whose activity are almost unaffected by S-poisoning. In fact the substitution of some Rh for the less expensive Pt has a similar qualitative effect to the lowering of the feed dilution. Indeed significant improvement in the sulphur tolerance of the catalyst with increasing reaction temperature has been observed when steam reforming sulphur containing fuels [25] as the stable S species decompose more readily at higher reaction temperatures, thus reducing the sulphur coverage on the catalyst surface. This is a further indication that the presence of Pt in bimetallic Rh-Pt catalyst improves the thermal stability and intrinsic activity of Rh particles for the steam reforming reaction. Similar synergistic effects were also observed by Kaila et al. [27,28] during the autothermal reforming of simulated and commercial low sulphur diesel fuels on bimetallic Rh-Pt catalysts supported on ZrO_2.

Figure 5.11 compares the temperature rise measured on the two catalysts upon S addition as a function of the corresponding change in methane conversion with respect to the sulphur free reaction feed. The data for CPO reaction tests carried out over both catalysts in air follow single straight lines in the whole range explored (0-58 ppm S). By assuming a thermal equilibrium between gas and solid (i.e. exit gas temperature is equal to the measured catalyst temperature), a simple heat balance on the gas phase can be written [20]:

$$\Delta H_r^{T_0} = -\frac{W \cdot C_p}{F_{CH4}} \cdot \left(\frac{\Delta T}{\Delta x_{CH4}} \right) \tag{5.2}$$

which relates the variation of temperature ΔT (°C) and methane fractional conversion Δx_{CH4} to a heat of reaction ΔH_r^{T0} (kJ/mol) at the initial temperature T_0 (760 °C, for CPO in air over Rh-Pt) through the specific heat of the gas mixture *Cp* (0.03501 kJ/(mol·°C)), its total flow rate *W* (7.2 mol/h) and methane feed flow rate F_{CH4}(1.636 mol/h). By substituting the value of $\Delta T/\Delta x_{CH4}$ obtained from the slope of the line in Figure 9 (-1329°C, over Rh-Pt) into eq. 5.2, it results that $\Delta H_r^{760°C}$ = +205 kJ/mol, which corresponds reasonably well to the heat of reaction of methane steam reforming at the temperature of 760 °C. This value however, is lightly less than that calculated for Rh only sample ($\Delta H_r^{700°C}$ = +225 kJ/mol, from CPO data in air [20]) which corresponds perfectly to the heat of reaction of methane steam reforming at 700 °C.

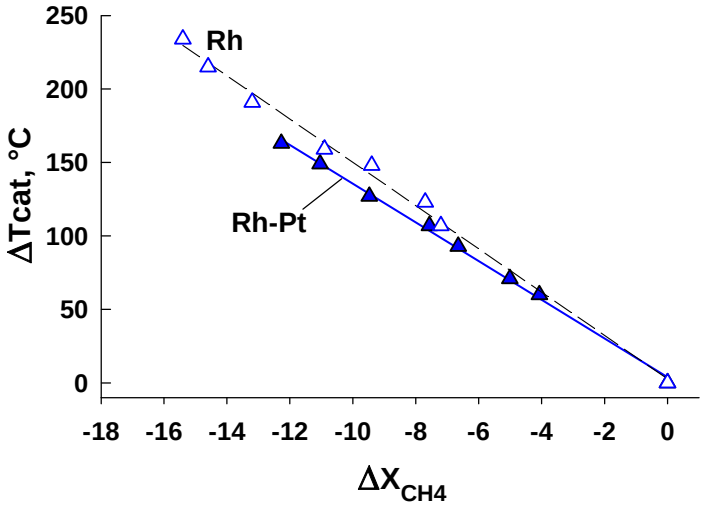

Figure 5.11: *Increase in catalyst temperature as a function of the variation of methane conversion measured upon the addition of increasing levels of H_2S over Rh/LA and Rh-Pt/LA monolith. CH_4/O_2 = 2, air as oxidant, GHSV = 8.1 x 10^4 h^{-1}.*

These findings confirm that the presence of sulphur in the feed mainly inhibits the steam reforming reaction by selectively poisoning the isolated Rh sites in both catalysts. The small differences in the values of ΔH_r^{T0} obtained are in agreement with the larger increase in H_2O production (i.e. lower H_2 selectivity) observed over bimetallic Rh-Pt catalyst. Under S-free feed Rh is more active than Pt in activating CH_4 molecules [26]; thus the final product distribution is largely affected by the intrinsic high and unmatched selectivity of Rh to H_2 rather than that of Pt. However the selective S adsorption on well dispersed Rh sites which has been demonstrated to strongly inhibit the steam reforming reaction, is also likely to slow down the oxidation reactions occurring in the first part of the reactor on those Rh sites. In the monometallic Rh catalyst this is hardly detected from final product of CPO, since it might only shift downstream the monolith the point at which molecular oxygen is completely consumed. On the other hand the activity of Pt sites are almost unaffected by S, therefore in the presence of sulphur they can contribute to a larger extent to methane conversion with the consequence of higher selectivity to H_2O (and CO).

5.4 Conclusions

1. Results of CPO light-off, steady state and transient operation under self-sustained, pseudo-adiabatic conditions at short contact time, demonstrated that Rh is always the most active and selective element for syn-gas production from methane in sulphur free conditions, due to its unique ability to catalyze the steam reforming reaction.

2. DRIFTS experiments of adsorbed CO before and after sulphur poisoning showed that sulphur acts as a selective poison by preferentially adsorbing on smaller well dispersed Rh crystallites (Rh^{+}) characterised by Rh-$(CO)_2$ bands whilst the metallic Rh sites (Rh^{0} in larger aggregates) are mostly unaffected.

3. Experiments on Rh catalysts supported on γ or α alumina with a large difference in metal dispersion confirmed that S-poisoning of Rh sites is structure sensitive and is completely reversible under high temperature reductive conditions. DRIFTS experiments indicated that the presence of Pt or Pd does not influence the way S adsorbs on highly dispersed Rh sites.

4. Partial substitution of Rh with Pt was shown to be effective at reducing and limiting the detrimental effect of S on monometallic Rh catalyst. In the presence of sulphur, the methane conversion is equal or higher on Rh-Pt than on monometallic Rh catalyst, the benefit being more significant when operating in air, i.e. at higher dilution. The improved performance of the bimetallic Rh-Pt catalyst is due to its higher operating temperature which facilitates sulphur desorption from the catalyst and reduces its accumulation thus resulting in higher catalytic activity and better tolerance against sulphur.

5. Partial substitution of Rh with Pd, however, was found to have a detrimental effect on the overall catalytic activity and to be ineffective at improving the S-tolerance probably due to its higher sensitivity to S-poisoning than Rh.

References

[1] A. Shamsi, Catal. Today 139 (2009) 268.

[2] A. Bitsch-Larsen, N.J. Degenstein and L.D. Schmidt, Appl. Catal. B: Environmental 78(2008) 364.

[3] R.K. Kaila, A. Gutiérrez, A.I. Krause, Appl. Catal. B: Environmental 84 (2008) 324.

[4] A.C. McCoy, M.J. Duran, A.M. Azad, S. Chattopadhyay and M.A. Abraham, Energy and Fuels, 21 (2007) 3513.

[5] J.J. Benitez, I. Carrizosa, J.A. Odrizola, Appl. Surf. Sci. 84 (1995) 391.

[6] E. Finocchio, G. Busca, P. Forzatti, G. Groppi and A. Beretta, Langmuir 23 (2007) 10419.

[7] R. Maurel, G. Leclercq, J. Barbier, J. Catal. 37 (1975) 324.

[8] A. Donazzi, A. Beretta, G. Groppi, P. Forzatti, V. Dal santo, L. Sordelli, V. De grandi, 6WCOC, 2009.

[9] C. Cao, A. Bourane, J.R. Schlup, K.L. Hohn, App. Catal. A: General 344 (2008) 78.

[10] J. Anderson, C. Rochester, Z. Wang, J. Mol. Catal. A 139 (1999) 285.

[11] J.B. Peri, J . Catal. 52 (1978) 144.

[12] J. A. Anderson and C.H. Rochester, J. Chem. Soc. Faraday Trans. 87(9) (1991) 1479.

[13] C.R. Apesteguia, C.E. Brema, T.F. Garetto, A. Borgna, J.M. Parera, J. Catal. 89 (1984) 52.

[14] J.R. Chang and S.L. Chang. J. Catal. 176 (1998) 42.

[15] L.J. Hoyos, M. Primet, H. Praliaud. J. Chem. Soc. Faraday Trans. 88 (1992) 3367.

[16] O. Dulaurent, K. Chandes, C. Bouly, D. Bianchi, J. Catal. 188 (1999) 237.

[17] T. Maillet, J. Barbier, P. Gelin, H. Praliaud, D. Duprez, J. Catal. 202 (2001) 367.

[18] M. Chen and L.D. Schmidt, J. Catal. 56 (1979) 198.

[19] B.M. Joshi, H.S. Gandhi and M. Shelef, Surf. Coatings Technol. 29 (1986) 131.

[20] S. Cimino, R. Torbati, L. Lisi, G. Russo, App. Catal. A: General 360 (2009) 43.

[21] R. Torbati, S. Cimino, L. Lisi, G. Russo, Catal. Lett. 127 (2009) 260.

[22] T.J. Truex, Interaction of Sulfur with Automotive Catalysts and the Impact on Vehicle Emissions, SAE paper 011543 (1999).

[23] P. Gélin and M. Primet, Appl. Catal. B: Environmental 39 (2002) 1.

[24] R. Horn, K.A. Williams, N.J. Degenstein, A. Bitsch-Larsen, D. Dalle Nogare, S.A. Tupy, L.D. Schmidt, J. Catal. 249 (2007) 380.

[25] M. Ferrandon, J. Mawdsley, T. Krause, App. Catal. A: General 342 (2008) 69.

[26] A. Bitsch-Larsen, N.J. Degenstein and L.D. Schmidt, Appl. Catal. B: Environmental 78(2008) 364.

[27] R.K. Kalia, A. Gutierrez, S.T. Korhonen and A.O. Krause, Catal. Lett. 115 (2007) 70.

[28] R.K. Kalia, A. Gutierrez, O. Krause, App. Catal. B: Environmental 84 (2008) 324.

6.1 Overall Conclusions

The effect of sulphur addition on the CPO of methane was investigated over Rh catalysts supported on commercial γ-Al_2O_3 stabilized by either La_2O_3 or SiO_2. At low to moderate temperature regime (300 to 800°C) over powder samples, the extent of catalyst sulphation was found to be highly dependant on the nature of the support material. In the presence of a sulphating support such as La_2O_3-Al_2O_3, the partial oxidation reaction was much less inhibited than a less sulphating support such as SiO_2-Al_2O_3. The sulphating support acts as a sulphur getter and keeps the sulphur away from the active metal sites and this minimises the build-up of S on or close to the active Rh sites where reactions take place. TPR/TPD experiments illustrated that, although the SiO_2-Al_2O_3 supported Rh catalyst stores significantly less bulk aluminium sulphate species due to the presence of surface silica, the catalyst accumulates more S on or close to the precious metal. During methane CPO reaction, sulphur poisoning appears to mostly affect the indirect reaction path to syn-gas involving steam reforming of residual methane thus shifting products distribution towards CO_2 and water. Once sulphur is removed from the feed, Rh sites can be almost completely regenerated at relatively low temperatures. However, as temperature increases above a threshold level of 530°C, sulphur species stored on the support, as $Al_2(SO_4)_3$ surrounding the Rh sites, can spill back onto the metal thus re-oxidizing it and consequently inhibiting the CPO reaction in favour of the total oxidation of methane. The drop in methane conversion was not accompanied by a decrease in oxygen conversion which remained complete following ignition.

The presence of sulphur in the feed during the CPO of methane under self-sustained conditions at high temperatures (>800 °C) and short contact times over Rh based monolith samples mainly inhibits the steam reforming reaction by directly poisoning the active Rh sites. The sulphur poisoning is rapid, completely reversible and is dependent on sulphur concentration in the feed but not on the type of S-bearing compound. It was found that even addition of very low sulphur concentration (2 ppm) causes a significant increase in the operating temperature accompanied by a proportional drop in methane conversion and hydrogen selectivity, due to selective inhibition of the SR reaction involving residual methane from the first oxidation zone in the reactor. The adverse effect of sulphur is proportionally larger at lower S concentrations and its threshold level in the reaction feed is calculated to be in the ppb level. The extent of SR inhibition and temperature increase was found to be greater

when operating in air (i.e. at lower starting temperatures) and seems to be controlled by the thermodynamic adsorption-desorption equilibrium which controls the extent of surface coverage of Rh by sulphur species. The detrimental effect of sulphur tends to diminish at lower CH_4/O_2 feed ratios due to the simultaneous increase in the catalyst temperature and to the reduction in the contribution of steam reforming to the overall syn-gas production. Under the typical operating conditions of methane CPO, sulphur in the feed inhibits the SR reaction by directly poisoning the active Rh sites thus preventing the sulphur storage capacity of the support from showing any beneficial effect on the S-tolerance. However the type of support did effect the metal dispersion which, at higher levels, appears to increase the sulphur saturation coverage and therefore more adversely affecting the SR activity. Light-off performances of the Rh based catalysts were found to be much less affected by the presence of sulphur, as long as the transient exposure to sulphur species under pre-ignition oxidizing conditions is limited enough as not to cause significant sulphation of the catalyst support.

The effect of partial substitution of $Rh/La\text{-}Al_2O_3$ monolith catalysts with either Pt or Pd during the CPO of methane in the presence of H_2S under self-sustained high temperature conditions was also investigated, with the aim of improving the sulphur tolerance of the catalyst whilst reducing its cost by decreasing the Rh content. Results of CPO light-off, steady state and transient operation under self-sustained, pseudo-adiabatic conditions at short contact time demonstrated that Rh is always the most active and selective element for syn-gas production from methane in sulphur free conditions, due to its unique ability to catalyze the steam reforming reaction. However it was shown by DRIFT spectra of adsorbed CO before and after sulphur poisoning that sulphur acts as a selective poison by preferentially adsorbing on smaller well dispersed Rh crystallites (Rh^+) characterised by $Rh\text{-}(CO)_2$ bands whilst the metallic Rh sites (Rh^0 in larger aggregates) are mostly unaffected. Experiments on Rh catalysts supported on γ or α alumina with a large difference in metal dispersion confirmed that S-poisoning of Rh sites is structure sensitive and is completely reversible under high temperature reductive conditions. DRIFT experiments indicated that the presence of Pt or Pd does not modify the way S interacts and adsorbs on well dispersed Rh sites. This result was in good agreement with CPO activity data on monometallic Rh catalyst, which showed a rapid and reversible inhibition of the methane steam reforming reaction and a consequent increase in the operating temperature of the system. The impact of S inhibition on Rh was larger at lower temperatures (i.e higher dilution). With regards to the bimetallic catalyst formulations, Pd was found to have a detrimental effect on the overall catalytic activity and to be ineffective

in improving the S-tolerance probably due to its higher sensitivity to S-poisoning than Rh. On the other hand the partial substitution of Rh with Pt showed to be effective in reducing and limiting the detrimental impact of S on monometallic Rh catalyst. In the presence of sulphur the methane conversion is equal or higher on Rh-Pt than on monometallic Rh catalyst, the benefit being more significant when operating in air, i.e. at higher dilution. The improved performance of the bimetallic Rh-Pt catalyst is due to its higher operating temperature which facilitates sulphur desorption from the catalyst and reduces its accumulation thus resulting in higher catalytic activity and better tolerance against sulphur. The correlation between the loss in the CPO activity in the presence of sulphur and the identification of metal sites most affected by sulphur gives a new insight for designing more efficient and resistant catalysts for the CPO of methane.